1990

The Analysis of 3-Channel "Vector" Visual Evoked Potentials and Possible Neuroanatomical Correlates

Lance Mitchell Siegel

School of Basic Health Sciences
Virginia Commonwealth University

This is to certify that the thesis prepared by Lance Mitchell Siegel entitled: The Analysis of 3-Channel "Vector" Visual Evoked Potentials and Possible Neuroanatomical Correlates has been approved by his committee as satisfactory completion of the thesis requirement for the degree of Masters of Science.

[redacted]

Juan Astruc M.D., PhD., Department of Anatomy, Department of Neurology

[redacted]

Alfred L. Ochs PhD., Department of Neurology

[redacted]

George R. Leichnetz PhD., Department of Anatomy

[redacted]

Hugo R. Seibel PhD., Department of Anatomy

[redacted]

Department Chair's Name or Representative's Name

[redacted]

School or College Dean's Name

24 April 1990

Date

The Analysis of 3-Channel "Vector" Visual Evoked Potentials and Possible Neuroanatomical Correlates

A thesis submitted in partial fulfillment of the requirements for the degree of masters of science, at the Virginia Commonwealth University

By
Lance Mitchell Siegel
B.S. - University of California, Los Angeles, 1985

Director: Juan Astruc, MD, PhD.
Professor of Anatomy and Neurology.

Virginia Commonwealth University
Richmond, Virginia
May, 1990

ACKNOWLEDGEMENTS

Since my childhood, I have always been interested with vision and the ability to see. Perhaps, it was as a child, watching my grandpa's and my uncle's eye sight fade to the point where they could no longer see life around them, that inspired me. Perhaps, it was my own fascination of the intricate properties of the eye and brain. I had always told my parents, that someday I would work with people to help save their vision. And through these past four years of work, and the countless hours of support and advice of my family and colleagues, I believe I have come one step closer to this goal. It is with this note that I thank those who have stood by me and supported me, in this endeavor.

First, I give my thanks and admiration to Dr. Alfred Ochs, who has encouraged me and supported me in this project for four years. From our early work with auditory evoked potentials, Dr. Ochs saw my interest in vision, and encouraged me and guided me towards completion of this project. I am indebted to him for his advice and help, especially during late night hours, weekends and even while at his home. Through my hyperactivity and my impatience, Dr. Ochs patiently provided me with the direction and the skills needed to conduct my own visual evoked potential project.

While much attention was given to the research aspect of this project, I must express my extreme appreciation to Dr. Juan Astruc for serving as my advisor to this project. Dr. Astruc stood behind my work, helping me get approval for the phases of my project, and overcoming the academic hassles and countless obstructions, thereby allowing me to proceed with my research. In addition, I am grateful for his technical advice, and tremendous insights, which allowed this project to reach the full potential that it did.

I must also thank Dr. George Leichnetz and Dr. Hugo Seibel, for serving as members of my committee. Their support and participation, not only in the final, often frantic, preparation of my thesis, but as well as through my whole medical and graduate school career was immensely appreciated. Numerous times I turned to both of these individuals for help and guidance, always receiving their utmost patience and attention.

Conducting a project of such magnitude requires the assistance and time of many individuals. In particular, I must recognize and thank Janet Thompson, and Sandy Lee who spent many hours assisting with the technical details of my study. Likewise, I am indebted to my classmates and colleagues who volunteered their time to serve as controls for my study. In addition, I am grateful to Dr. Robert De Lorenzo of the Department of Neurology, who was willing to support my project, and allow my use of the

necessary equipment and facilities at the Medical College of Virginia and the McGuire Veterans Administration.

Finally, and most important, I must thank my parents and family. I am indeed fortunate to have such a loving and supportive family. They have stood by me through my numerous endeavors, always wondering "what project I was taking on this week". I'm sure it is as exciting to them as to myself, that I am finally completing a project based on the desire I had since 5th grade. Well , Mom and Dad, Stacie and Dan, I've finally finished school, with a contribution to vision in my back pocket and an M.D. to my future.

Thank you to everyone, for all your help.

TABLE OF CONTENTS

Page

ABBREVIATIONS vi

SUMMARY OF TABLES vii

SUMMARY OF FIGURES ix

ABSTRACT xii

INTRODUCTION

History of Evoked Potentials 1
Evolution of the Three Channel Evoked Potential 3
The Study 4

MATERIALS AND METHODS 7

RESULTS

Existence of Pre and Post P100 Activity 13
Identification and Evaluation of Pre and Post P100 Activity (Early and Late Waves) 13
Reliability 15
Further Description of Activity 18
The Use of the Vector Potential to Identify a Lateral Geniculate Potential 20

DISCUSSION

Technology 21
Data Analysis
The identification of activity 25
The identification of discrete Pre and Post P100 activity 27
Numerical studies 29
Peaks can be expressed by direction 29
Reliability : Test - Retest
Right versus left eye comparison 31
Test - retest of an individual 31
Hemi-fields 32
The Lateral Geniculate Potential 35

General Summary
History of physiology. 36
Conclusion 37

TABLES 42

FIGURES 73

REFERENCES 159

VITA 165

ABBREVIATIONS

CLT - Lissajous' on Three Channel Recording
e.e. - ear lobe to ear lobe distance
EEG - ElectroEncephaloGram
EKG - ElectroCardioGram
ERG - ElectroRetinoGram
FERG - Flash ElectroRetinoGram
Fl - Foot lamberts
hc - head circumference
hrs. - hours
Hz - Hertz
LGB - Lateral Geniculate Body
m - meters
μv - microvolts
min - minutes
ms - milliseconds
OD - Right eye
OS - Left eye
ODn - Right eye, nasal retina
ODt - Right eye, temporal retina
OSn - Left eye, nasal retina
OSt - Left eye, temporal retina
PERG - Pattern ElectroRetinoGram
s - seconds
S.D. - Standard Deviation
sec - seconds
VEP - Visual Evoked Potential
VVEP - Vector Visual Evoked Potential
vs. - versus

SUMMARY OF TABLES

Page

Table 1 A-D : Intersubject Comparison of Peak Times, Identified by Graphical Observation for 30 and 60 min. of Arc (OS and OD). 43

Table 1 E : Table of Peak Averages for Left and Right Eyes at 30 and 60 min. of Arc. 48

Table 2 : Numerical Versus Graphical Comparison of the Identification of Peaks, (OS, 30 min of Arc). 50

Table 3 : Latitude and Longitudes for Peaks Identified Graphically by Visual Inspection. 52

Table 4 A,B : Intrasubject Comparison of Peak Latencies of a Subject's Right Versus Left Eye for 30 and 60 min of Arc. 54

Table 5 : Graphical Analysis of 2 Selected Closed Door (null) Studies. 58

Table 6 : Table of Subject Test-Retest. 60

Table 7 : Graphically Identified Peaks in Subject G's VVEP's Recorded at 60 minutes of arc for, Left and Right Eye, Full Field and Hemi-Fields (6 studies). 62

Table 8 A-D : Intersubject Comparisons of Peak Activity Identified from Graphical Observation of Hemi-field Stimulation for OS and OD Nasal and Temporal Retinal Fields. 64

Table 9 : Intrasubject Comparison of the Graphically Identified Peak Latencies of the 4 Hemi-fields in Three Subjects. 69

Table 10 : The Pattern ERG Values for Left and Right Eyes of Three Subjects. 71

SUMMARY OF FIGURES

Page

Figure 1 : Conventional (Queen's Square) VEP Electrode Montage. 74

Figure 2 : "Vector" (3-Channel) VEP Electrode Montage. 74

Figure 3 : 10-20 System of Electrode Placement. 76

Figure 4 : Conventional Plot of Visual Evoked Potential of Left Eye (OS). 78

Figure 5 : Plot of visual vector evoked potential. (Vertex View Point). 80

Figure 6 : Left and Right Eye Full Field VVEP Progression Plot. 82

Figure 7 : Full Field Stimulation Comparison of OS and OD VVEP's. 92

Figure 8 : Full Field Stimulation Comparison of OS and OD VVEP's. 96

Figure 9 : VVEP Hemi-field Graph of OD Temporal and OS Nasal Retina Stimulation in Subject C. 100

Figure 10 : A 0ms - 58ms Epoch of a Left and Right Full Field VVEP at 60 min of Arc, in Subject G, Compared to the VVEP Generated by a "Closed Door" (null) Study in Subject H. 102

Figure 11 : Graphic Comparisons of the Same Visual Field (ODn) at Separate Test Times. 104

Figure 12 A-L : Graphic Comparison of Given Time Segments of the VVEP's of the Four Hemi-fields in Subject E 106

Figure 13 : Comparison of Nasal Versus Temporal Hemi-field VVEP of the Left Eye of Subject C. 119

Figure 14 A, B, C : Hemi-field Symmetries in Three Subjects 123

Figure 15 : VVEP Hemi-Field Responses of Five Subjects Are Hand Drawn as Smooth Curves of the Approximately 40 - 135ms Range. 127

Figure 16 : Vector Addition of the P100 Wave of Two VVEP Hemi-field Generated Waves. 129

Figure 17 : Sample of a Pattern ERG Plot. 131

Figure 18 : Comparison of Peak Latency of 50ms Pattern ERG and the 55ms Peak. 133

Figure 19 : Comparison of the 55ms Wave of the Right Eye, Nasal and Temporal Field with a Full Field 55ms Wave of the Same Eye, at Identical Scaling. (60 min of Arc.). 136

Figure 20 : Identification of Occult Peaks Through Rotation of a Group of Data Points of a VVEP. 138

Figure 21 : Assigning Peaks to Variations in Displayed (graphic) Data. 140

Figure 22 : "Lighthouse Effect". 142

Figure 23 : The Best Way to Describe a Peak. 146

Figure 24 : Side by Side Comparison of Full Field VVEP of the Left and Right Eye at 60 min of Arc. 148

Figure 25 : The Neuroanatomical Correlates of the PERG and VVEP 157

The Analysis of 3-Channel "Vector" Visual Evoked Potentials and Possible Neuroanatomical Correlates

ABSTRACT

A thesis submitted in partial fulfillment of the requirements for the degree of masters of science, at the Virginia Commonwealth University

Lance Mitchell Siegel

Virginia Commonwealth University

Advisor: Juan Astruc, MD, PhD

The use of evoked potentials to evaluate the functional integrity of neuronal pathways has become a useful and accepted practice in clinical medicine. The use of visual evoked potentials for assisting in the diagnosis of such diseases as optic neuritis and multiple sclerosis is also well recognized. However, the visual evoked potential, unlike the auditory evoked potentials, lacks a well defined electrophysiological to neuro-anatomical correlation; especially that of a significant non-cortical component. Currently, visual evoked potentials rely principally on the measurement of a cortical (occipital) positive peak of activity at 100ms (P100), recorded with a single channel electrode system, to evaluate pathway integrity. In this study, visual evoked potentials were recorded

using a three-channel, orthogonal co-ordinate system which we have designated "vector" visual evoked potentials (VVEP). This method allows the generated evoked response to be plotted on a three dimensional co-ordinate system with respect to time. Through the use of pattern reversal of a checkerboard pattern, in full and hemi retinal field stimulation, reproducible activity both prior to and after the P100 wave was demonstrated. In particular, activity found at approximately 55ms is believed to be generated from the Lateral Geniculate Body. Furthermore, because this method summarizes the activity of the entire brain for a given time, as opposed to the single channel recording, a great deal of information about the entire visual pathway can be suggested. Finally, anatomical correlates to discrete activities identified by this method can be made.

INTRODUCTION

History of Evoked Potentials

Nerve fibers have long been known to conduct electrical activity when stimulated. Likewise, a pathological alteration of these fibers, such as through lesions or trauma, has been known to alter time and efficiency of conductivity. The stimulation of a neural pathway by the appropriate stimulus (i.e. sound for auditory, light for visual) induces a recordable electrical discharge response generated from areas along the conduction pathway. This recordable response is known as an evoked potential. The first evoked stimulation studies were conducted by Herna'ndez-Peo'n, (1956). These early studies to determine if there a characteristic response had difficulty overcoming background EEG activity which blocks out the evoked response. Through the use of stimulating and evoking a response over a large number of repetitive times, Herna'ndez-Peo'n was able to average out these background EEG waves, revealing the electrical response evoked by the olfactory stimulation. This process, done by hand, was long, tedious, and laborious. With the availability of a computer system it was possible to average out the background EEG, while preserving and enhancing the evoked response, which greatly facilitated evoked potential recording. Based on the applications of olfactory evoked potentials, visual evoked potentials were conducted. These first studies used a flashing light

to evoke a response. While this method did generate a characteristic wave form in an individual, there was a large variation across the population (Ciga'nek, 1968). Halladay introduced a method of a pattern reversal stimulus to evoke a response. This method generated a well reproducible peak of electrical activity over the occipital cortex 100ms following stimulation referred to as the P100 wave. The principal advantage of this stimulation method is that the latency of the P100 wave is constant across the population. The stability of this peak latency in normal subjects and the finding in multiple sclerosis patients that this activity was delayed (Halliday et al., 1973), allowed the first clinical applications of the evoked potential in detection of demyelination in the visual pathway (Halliday et al., 1972; Halliday et al., 1976).

Around the time the visual evoked potential's applications became apparent, short latency brain stem auditory evoked potentials were discovered (Jewett and Williston, 1971). By averaging responses from several thousand clicks, a characteristic plot consisting of seven wave forms was identified in the first 10ms following stimulation. Jewett proposed that these wave forms originate in the auditory nerve and progress through auditory pathways in the brain stem to the cortex. In 1977 Stockard et al., used lesion studies to confirm anatomical correlates along the auditory ascending pathway. Jeffreys attempted to assign anatomical correlates to the visually generated responses by stimulating various fields and altering electrode positions. The activity he identified was determined to be generated in the cortex (Jeffreys and *Axford*, 1971a,b).

The ability to identify pre-cortical (geniculate) activity remained elusive. In 1988, Ducati used depth electrodes in awake subjects to try and identify a geniculate potential, again without success.

Evolution of the Three Channel Evoked Potential

As early as 1916 researchers were looking for ways to characterize the electrical activity of the heart. Mann, in particular, was using a method termed vectorcardiography to record and display his data (Rautaharju, 1988). This method involved recording activity using a three dimensional recording axis arranged orthogonally. The activity was then plotted in three dimensions projected on the principal body planes for analysis. While the method showed promise in diagnosing conduction defects, the process was thought cumbersome, time consuming, and difficult to do outside the research center. In 1965 with the use of the EKG, controlled studies found this vector method no more sensitive or specific in diagnosing cardiac abnormalities, and the vector method fell into disuse (Rautaharju, 1988).

In the early 1980's, Jewett and his colleagues began to experiment with a three channel recording model of auditory evoked potentials (Williston et al., 1981; Pratt et al., 1985; Jewett et al., 1987). This method of three channel recording (CLT's) suggested some advantage over conventional one channel recording. In particular, this method summated the activity of the entire brain, and plotted this event per given time as a dipole moment in three dimensional space. These studies also demonstrated the problems

of recording, plotting and analyzing the data in this format (Martin et al., 1987; Sininger et al., 1987; Jewett et al., 1987).

Pratt and his co-workers followed Jewett's work with three channel visual evoked potentials (Pratt et al., 1982; Pratt et al., 1986; Towle et al., 1986). While these studies were able to identify activity found on conventional plots, it was very difficult to plot, describe and quantitate any new activity they recognized. Pratt et al., 1986, also introduced the name Lissajous' figures for these plots.

In 1988, through the use of advanced computer technology, the ability to plot, rotate, edit and quantify data in a 3-dimensional array on a standard desk top computer became possible. It is with this new enhanced computer capability that this study was proposed to better characterize the visual evoked potential.

The Study

The use of evoked potentials to evaluate integrity of neuronal pathways has become a useful and accepted practice in clinical medicine. The use of visual evoked potentials for assisting in the diagnosis of such diseases as optic neuritis and multiple sclerosis is also well recognized. However, the visual evoked potential, unlike the auditory evoked potentials, lacks a well defined electrophysiological to neuroanatomical correlation especially of pre-cortical sites along the visual pathway which may generate a potential (pre-cortical generators). Currently, clinical visual evoked potentials rely on the generation of a cortical (occipital) positive peak of activity at 100ms (P100), following the pattern reversal stimulation, *to*

evaluate pathway integrity. The conventional recording can be performed with a single channel electrode system, although multiple independent channels are now recommended (Jeffreys and Axford, 1971a,b; AEEGS Evoked Potential Guidelines, 1984). In this study, visual evoked potentials will be recorded using a three-channel orthogonal co-ordinate system which we have designated "vector" visual evoked potentials (VVEPs), based on the early vectorcardiogram studies. Earlier work by Jewett et al. (1987) and Pratt et al. (1986) has suggested the ability of the vector method to detect reliable activity other than the P100 wave. Through the use of commercially available 3-dimensional graphics computer software (D^2 Software, Austin, Texas), and a flexible data recording and editing system (Macintosh® personal computer), this study will identify and analyze visually evoked electrical activity over the entire 0-250ms recording epoch.

The present study is to evaluate normal VVEPS recorded from control subjects using a pattern reversal stimulus over a range of stimulus conditions. The goals of this study are as follows:

1) To prove the uniform presence of peak electrical (activity) other than the P100 wave in a group of subjects. In addition, particular attention will be paid to activity that may correspond with a lateral geniculate potential.

2) To prove that this induced electrical activity is not artifact by using different test conditions such as test-retest, null recordings, and hemi-field and inter-ocular consistencies.

3) To express data by numerical analysis as well as graphical techniques.

4) To conduct Pattern ERG studies to evaluate how retinal electrical activity contributes to the overall VVEP.

5) To propose possible anatomical correlations to the information obtained.

MATERIALS AND METHODS

Subjects:

The study was conducted in normal, healthy subjects 18 years or older. Exclusive criteria required that the patient have no known history of neurological abnormalities including seizures, head trauma, stroke, psychological impairment, loss of consciousness from minor trauma, or visual abnormalities uncorrected by lenses. The subjects were on no medications. The study was conducted under guidelines by the research ethics committee, with informed consent obtained for all subjects. Subjects were compensated $25-$40 depending on the number of testing parameters done, for an average of 2-4 hrs. sitting time. Each subject was designated by a letter in the alphabet which was constant to that individual throughout this report.

Electrode Placement:

The Conventional Electrode Placement:

The electrode placement for the conventional VEP is based on the international EEG 10-20 system (Standard EEG Montages, 1980). Inion to nasion distance is measured. An electrode is placed 10% of this total distance above the inion, in the occipital region, and is designated Oz. The second electrode of the recording pair is placed in the frontal region 30% of

the distance above the nasion (Fz). Conventionally, occipital positivity is up in these plots, (Figure 1).

The Vector Electrode Placement:

The electrode placement for the vector system relies on the avoidance of air sinuses, and awkward placement (i.e., nasopharyngeal). The three electrode pairs (three channel recording) is as follows (see figure 2):

positive electrode	negative electrode
P3	right tragus
P4	left tragus
Fz	inion

The location of the inion and Fz electrodes were described above. The tragus is defined as the area in the ear just anterior to the superior lobe of the pinna. The P3 and P4 electrodes are placed according to the 10-20 international system in the left and right parietal region, respectively. The inion to nasion (i.n.) distance is measured. The head circumference (hc) distance is measured. And the ear lobe to ear lobe (e.e) distance is measured. The P3 electrode is placed as follows: O1 in the left occipital region is marked on the scalp by moving 10% of the i.n. distance above the inion and 10% to the left of the hc distance. Pz is marked in the parietal region by measuring 30% of the i.n. distance up from the inion. T5 in the left temporal region is measured and marked on the scalp by measuring 10% of the e.e. distance up from the left earlobe and 20% of the hc distance towards the back of the head. C3 in the central region is measured and marked at 30% of the e.e. distance above the left earlobe. P3 is defined as

the intersection of a line drawn from C3 to O1 and T5 to Pz. The P4 electrode is placed as follows: O2 in the right occipital region is marked on the scalp by moving 10% of the i.n. distance above the inion and 10% to the right of the hc distance. Pz is marked in the parietal region by measuring 30% of the i.n. distance up from the inion. T4 in the right temporal region is measured and marked on the scalp by measuring 10% of the e.e. distance up from the right earlobe and 20% of the hc distance towards the back of the head. C4 in the central region is measured and marked at 30% of the e.e. distance above the right earlobe. P4 is defined as the intersection of a line drawn from C4 to O2 and T4 to Pz. (See figure 3).

The Pattern Electroretinogram (ERG) Electrode Placement:

The Pattern ERG electrode is placed on the lower eyelid of the recording eye and connected to the positive input. The negative electrode is placed on the ipsilateral tragus. While corneal electrodes are used to record Pattern ERG's clinically. The use of infraorbital skin electrodes were proved to be adequate to determine the peak latency needed for this study.

Stimulus Generation:

The stimulus was generated on an optical screen via projection of photographic slides for 30' and 60' of arc check size, with the subject 56cm from the screen. The subject was told to fixate at the center of the screen. The black and white squares were interchanged (pattern reversal) by reflecting the projector image off an electrically movable mirror. The alternation rate was 1.1 times/second. The data was recorded and

averaged on the Nicolet Pathfinder II®. The collection epoch was 250ms, from the time of initial stimulation, with an artifact rejection enabled , and a band width of 1-100Hz Two-hundred responses were generated, two times for each study, for a grand average of 400 responses. Hemi-field studies were conducted by stimulating only the nasal or temporal retinas for each eye by masking one half of the screen, in which the recording parameters were unchanged. The designation of hemi-fields refers to retinal (not visual) fields, and is as follows:

Right eye nasal retinal field stimulated: ODn

Right eye temporal retinal field stimulated: ODt

Left eye nasal retinal field stimulated: OSn

Left eye temporal retinal field stimulated: OSt

This required the subject to fixate the center of the screen, while the side of the screen which was not stimulating was covered, by closing a door. Null Studies required the subject to either stare at a dark blank screen (closed both doors over checkerboard screen), or at a non-flashing checkerboard pattern. In all cases, the non stimulated eye was covered with a gauze eye patch. Pattern ERGs were recorded simultaneously in selected subjects, generating a pattern-reversal ERG recording.

Recording Environment:

Subjects were seated on a firm chair, in a dimly lit room, with comfortable temperature, and a non-constant background noise. The patient was kept alert by turning on the lights after each collection of a 200 response study. For 30 and 60 min of arc, the brightness for *bright checks*

was 70fL (foot Lamberts) , while the dark checks were 5 fL. The contrast was 87%. The contrast (C) was defined by:

$$C = (\text{Bright} - \text{Dark}) / (\text{Bright} + \text{Dark}) \times 100\%$$

Talking to the patient was kept to a minimum, mainly to keep them alert and abreast of their progress.

Data Collection:

The data was recorded and averaged on the Nicolet Pathfinder II®. The data was stored on an internal hard disc and later transferred to the Macintosh® personal computer using a customized version of Nicolet software.

Data Analysis:

The data was analyzed on the Macintosh® personal computer using the MacSpin® program from D^2 software, Austin, Texas. Data was viewed with the origin at zero millivolts, and spatially uniform scaling. The use of uniform spatial scaling assures the points are plotted at an equal scale with all the other points in the epoch, regardless of angle of view or the amount of enlargement. Figure 5 shows an example of this scaling. (The vector tracing is a tracing of positivity of the three electrodes P3, P4, Fz). Figure 5A shows the 50ms wave in scale to the rest of the plot. Although enlarged (close up) views of this 50ms event are seen in Figures 5B and 5D, proportional scaling is maintained. Peaks were defined as the apices of change of direction at a perpendicular view point. At least 3 view points of an entire epoch were displayed at mutual right angles. Since

there is no way to determine peaks from troughs in three dimensional plots, both were considered significant and tabulated. A detailed analysis of peak activity can be found in Figure 21. In the sense of vector recordings, in this study a peak is synonymous with an apex, wave or trough. For the determination of magnitude at a given point the following formula was used.

$$Mag_i = \{(P3)_i^2 + (P4)_i^2 + (Fz)_i^2\}^{1/2}$$

Where Mag_i, $P3_i$, $P4_i$, Fz_i, are the i^{th} component of the time series and $P3_i$, $P4_i$, Fz_i, is the projection of the vector magnitude (Mag_i) along the three principal axes.

Latitude and longitude were defined by the following operations in Mac-Spin®:

Latitude	Longitude
$Tan^{-1}\ \{P4/(Mag^2 - P4^2)^{1/2}\}$	$Tan^{-1}\ \{P3/Fz\}$

This polar coordinate determination is made by the vector from the origin to the peak. The validity and usefulness of this as well as the co-ordinate system on an anatomical basis is discussed in conjunction with Figure 23.

RESULTS

Existence of Pre and Post P100 Activity:

The use of the visual evoked potential to evaluate visual pathway integrity is usually determined by the evaluation of the latency of the P100 wave in a conventional plot. A sample conventional plot is shown in Figure 4. While the P100 is prominent in this type of plot, the presence of early and late activity (pre and post P100) are variable among normal subjects. The use of the Vector Visual Evoked Potential (VVEP), of which a plot is shown in Figure 5 (a-f), allows increased capability to discern earlier and later events. While investigating this method it became apparent that both pre and post P100 events could be routinely defined and evaluated. Figure 5 demonstrates the analysis of the VVEP in discrete segments. After examining a number of initial studies, the presence of early and late activity in all subjects, prompted the further study and evaluation of this phenomena.

Identification and Evaluation of Pre and Post P100 Activity (Early and Late Waves):

The initial studies involved the stimulation of the entire retinal field of one eye with either 30 or 60 min of arc checks with a pattern reversal stimulus presentation. The VVEP's for these subjects were displayed on

the Macintosh® personal computer, using MacSpin® software. The identification of discrete activities (waves) with respect to time as demonstrated in Figure 5 was conducted by visual observation from optimum view points and recorded in table form for each eye at each check size. In all studies both pre and post P100 activity could be identified. In the 100 ms prior to the P100, between 5 and 15 waves were seen, with about 10 being the most frequent. In the post P100 epoch (100-250ms), 3-8 waves were seen with 5 being the average. The time required for a trained observer to assign the peak latency of each P100 wave using the vector method was similar to the time required with conventional recordings, as was the ability to assign times to the preceding and succeeding wave forms (N 70 and N 130). In addition, it was possible to identify a wave prior to the N70 in all subjects tested. An average latency was determined for the nominal peaks (50, 70, 100 and 130ms) at both 30 and 60 min of arc, (table 1 E), for both the left and right eyes, being 58ms, 72ms, 99ms, and 129ms, respectively. The individual components are shown in Tables 1 A-D. While the trends tended to suggest early waves at approximately 12.5ms, 22.5ms, 40ms no reproducible times could be ascertained. Trends of the later activity, post P100, demonstrated reproducible peaks of activity at approximately 160ms, 190ms, 210ms.

Through the use of maximum and minimum magnitudes of the numeric data set, an attempt was made to use automatic recognition procedures, i.e. to identify peaks of activity from the numeric data set alone. As seen in Table 2, as described in the table legend, the use of *100 pts*

(arbitrary units) between subsequent maximum and minima generated a far greater number of peaks than by visual observation alone. Using a selection criteria of 10%, i.e. a subsequent maxima or minima was 10% greater or less then the preceding event did little to change the number of peaks. Using a 25% selection criteria was probably the best at comparing with a visual observation as a standard, but even this threshold yields additional events. The use of a larger threshold criteria tended to exclude important events.

Because the vector method relies on a 3-dimensional method of plotting, the ability to assign direction to an activity is possible. Table 3 shows the direction of post 50ms wave activity in 3 subjects. Except for the P100 no similarity in direction could be seen either in the same subject or in different subjects. As commented on in the discussion section, these differences may be due more to the inherent definitions of the display itself than to the anatomical differences of the activity generated.

Reliability:

With the identification activity across the entire 250ms recording epoch, the question of reproducibility was addressed. Using a subject as its own control, the visual graphic evaluation of the potential evoked by stimulation of the left eye (OS) was compared with that of the right eye (OD) under the same recording parameters. As seen in Table 4A and 4B side by side comparisons show similarities of the entire epoch within a subject. This is particularly true of the events occurring after the 50ms peak. While the earlier events (prior to the 50ms), show only minimal similarity within

a subject (intrasubject), they show even less similarity between subjects (intersubject). However, the trends tend to suggest activity across the population at approximately 12.5ms, 22.5ms and 40ms.

Although the data tables suggest reproducibility, the graphic representations of the VVEP plot firmly support it. Figure 6 a-q and 7 a-g, (along with Figure 24 a-q) show how initial activity prior to 50ms tend to show similar numbers and times of direction changes, but no definable symmetry. Post 50 ms however, all subjects studied demonstrated, on full field stimulation, nearly superimposable images for the left and right eye. Because the plot represents the composite of two pathways, due to the nasal and temporal retina fibers diverging to opposite sides of the brain, a hemi-field stimulation study was performed (Figure 9). The symmetry of this study from 50ms on is readily apparent, the further utility of hemi-field stimulation is shown in the next section.

To further demonstrate reproducibility, two other studies were conducted. The first study required the subject to stare at a either a non-alternating screen or a blank screen (closed door), both of which are designated as a null study. Table 5 shows the peaks of activity identified by visual observation for the first 65ms. This occurrence of peaks every 2-5ms occurred throughout the recording epoch, thus an average of >20 events occurred in the pre P100 range due to "noise" in a null study. This is in contrast to the 8-10 larger events that typically occur in that range on a regular recording. Thus although some of the early waves recorded in a regular VVEP study may be noise, it is unlikely that they are *all* artifact.

This is further supported by Figure 10, in which a recording of a standard VVEP is shown in comparison with a closed door study. Furthermore when the closed door study is scaled with a point equivalent in magnitude to the P100, the closed door study coalesces to a tight clustering of points, while the standard study has a much higher degree of order. This is because, the software package automatically scales the entire data set to the value of the largest point in order to provide maximum visibility.

The second study required that a subject be tested on two separate occasions. The data obtained by graphic observation is listed in Table 6. There appears to be a great deal of similarity in the values, except perhaps for the retest of subject H- left eye, particularly among the later waves. This could arise from an assignment bias of peak times (as covered in the discussion). The graphic plot of test-retest data also demonstrates reproduciblility (Figure 11), in which the differences are discussed below.

Perhaps the best method of demonstrating reproducibility is testing the same phenomena under different conditions and getting similar results. Table 7 demonstrates the peak times obtained from six different studies, at 60'of arc study, [left and right eye as well as all four hemi-field stimulations, (left and right, nasal and temporal)]. The identification of almost the exact same number of peaks at almost the exact same times beginning with the 50ms wave demonstrates a high degree on internal consistency and emphasizes the physiological basis for these wave activities.

Further Description of Activity:

The vector method is an excellent method to display the evoked potential data in a spatial orientation. This value can be used to further define activity of the visual pathway on the basis of lateralization of the visual field by stimulating different sides (nasal vs. temporal) of the retina. Note that in this thesis, nasal and temporal refer to the stimulated retina and not to the stimulated visual field, which would have the opposite designation. The consistency of hemi-field stimulation was demonstrated in the reliability section above. The true magnitude of its power to evaluate the visual pathway is demonstrated here. The visual graphic identification of peaks is shown in Tables 8 A-D, these tables compare a given hemi-field across a subject set. As with full field stimulation, a 50ms, 70ms, 100ms and 130ms wave occur uniformly across the subjects. The suggestion of activity at 12.5ms, 22.5ms and 40ms, along with late activity at 160ms, 190ms and 230ms can also be made. Table 9 compares intrasubject data, although similarities can be drawn like those of Tables 8 A-D, there is really only minimal similarity among the corresponding fields (eg.left nasal (OSn) and right temporal (ODt)) when the data is viewed in table form by an arbitrary assignment of time to a suggested peak of activity. This however, is quite different from the outstanding symmetry seen when comparing hemi-field VVEP plots graphically. As Figures 12 a-l, 13 a-l, 14 A-C show, from approximately 40ms on there is remarkable mirror symmetry of the two different pathway plots, (i.e. left nasal (OSn) vs. left temporal (OSt)), while the same pathway plots, (i.e. left nasal (OSn) vs.

right temporal (ODt)) appear almost identical. In addition, the progression of the plot from 40ms to 150ms appears to be uniform across the subject population for a given hemi-field. This is demonstrated by Figure 15. Thus the electrical progression of the plot begins at 45ms on the side opposite (contralateral) to the stimulation, makes a peak on that contralateral side at approximately 55ms (50ms wave), crosses the midline to peak on the same side (ipsilateral) of stimulation at 70ms, then crosses the midline again to peak at a 100ms on the side opposite (contralateral) to the stimulation. Thus, ODn and OSt have a P100 oriented along the P4 axis , while the ODt and OSn have the P100 oriented along the P3 axis. The electrical plot then proceeds towards Fz , giving the 130ms peak. This trend is followed for all the subjects tested, with only subject D having some questionable variation at 50ms in the nasal stimulations. In addition some subjects have an additional wave form coming off the p100 wave before progressing to Fz,(i.e., subject K- OSn, ODt).

The use of hemi-fields poses the question of whether such a potential generated by a half field stimulation is half of a full field stimulation. To test this hypothesis, the P100 waves of a number of subjects (two of which are shown in Figure 16) from two hemi-field stimulation studies were added by vector addition and plotted. As seen by the figures, the addition of two hemi-field plots correspond to the full field stimulation. The principle of the full field plot actually being a composite of two independent pathways, support the value of individual hemi-field testing. Likewise, the individual 50ms wave appears to be oriented perpendicular to the conventional

recording axis with the peak pointing contralateral to the stimulated retinal field. Thus the recording with full field stimulation may actually average these events and tend to cancel the potential. This is exceedingly important in considering why the 50ms peak has not been well described conventionally.

The Use of the Vector Potential to Identify a Lateral Geniculate Potential:

The recording of a reproducible event at approximately 50 ms raised the possibility of recording a lateral geniculate potential To determine the contribution of the retinal ERG potential which occurs at approximately the same time, pattern reversal ERG's were conducted. A sample plot is shown in Figure 17. The average time for the second peak of the pattern ERG was also found to be around 50ms, (Table 10). To determine whether the 55ms peak was a pattern ERG potential, both were plotted together, (Figure 18 a-f). This figure shows the labeling in two subjects of the point in the VVEP electrical progression of where the ERG occurs, this event is at a discretely different time from the "50ms" wave. This hypothesized geniculate wave which is said to occur at about 50ms is postulated to be the wave that occurs here at 57ms, and thus this thesis, will refer to this presumptive geniculate wave as the 55ms wave. As previously shown in the hemi-field data, a reproducible generation of this 55ms wave occurs contralateral to the stimulated hemi-field. The full field would expect to average these two lateral components the resultant summated potential would be directed along the midline. This phenomena is shown in Figure 19.

DISCUSSION

Technology

The use of the evoked potential to evaluate neurological pathway integrity has become an accepted and useful neurological testing tool. Using the vector method, this thesis has demonstrated the presence of reproducible activity prior to and after the P100 wave. Secondly, an event occurring at 55ms has been identified which is believed to be the lateral geniculate potential. Finally, through hemi-field VVEP symmetry, a reliable method for evaluating the individual visual pathways was obtained. This activity from the initial PERG retinal potential up to the end of the 250ms recording epoch, allowed anatomical correlates for the proposed generators to be assigned. These findings are a major contribution to the study of visual evoked potentials.

The visual evoked potential has been used to assist in the diagnosis of such diseases as multiple sclerosis, optic neuropathies, tumors, and stroke (Halliday et al., 1973; Halliday et al., 1972; Halliday et al., 1976). Further work has suggested that the visual evoked potential may assist in the diagnosis of migraine headaches, and seizure disorders (Rudino, 1988; Marsters et al., 1988; Watanbe et al., 1986). The "conventional" visual evoked potential is recorded with a single electrode pair, in an anterior to

posterior orientation. While this method does reveal a significant P100 wave, other activity is not always present. The inherent nature of this anterior to posterior recording pair does not allow adequate recording of any other electrical dipole activity that may occur in another direction, i.e. dipole activity perpendicular to a recording pair is not recognized. Likewise, conventional methods have an inherent bias by assigning a peak to an isoelectric event when it passes an electrode recording pair. This present study refers to this phenomena as "the lighthouse effect" and is described in Figure 22. Since the evoked potential actually induces an array of entire brain activity, a summation of dipole activity at any given time would give a more realistic idea of the electrical activity generated by the evoking stimulus. This can be done by using a vector based three dimensional orthogonal recording system. Although Pratt et al., 1984, have subsequently used the name 3-channel recordings or Lissajous' trajectories for such an electrode placement, the present study uses the original term vector visual evoked potential, following Jewett's and Williston's original pioneering efforts in this field (Williston et al., 1981). While numerous methods of electrode placement arrangements have been made (Jeffreys and Axford, 1972a,b; AEEGS Evoked Potential Guidelines, 1984; Martin et al., 1987), the present study uses a method to increase symmetry while maintaining an optimal recording environment. In further contrast to previous studies, the electrodes in this present study are orthogonally placed, unlike Pratt et al. (1984), who needed to apply a mathematic correction to their data to generate a true orthogonal representation.

The overall goal of this project was to evaluate a normal population to establish a normative VVEP (Vector Visual Evoked Potential) data set. This was accomplished by using a number of criteria. Only adult subjects with no history of visual or neurological impairment were used. The recording environment was designed to maintain an optimal recording environment. Arousal was maintained by room temperature control, posturing and turning the room lights on after each individual recording. Visual attention has been shown to be very important in visual evoked potentials, with the P100 (and probably other waves) being markedly diminished and delayed by the lack of attention (Bertram and Lee, 1986). The use of an alternating pattern reversal stimulus was employed, which has been shown to be far superior in generating a reproducible evoked response within the normal population than over a flash stimulus (Ciga'nek, 1968; Cobb et al., 1967).

Although the benefits of using an evoked potential method that evaluates the entire brain activity is obvious, putting such a method into practice has been more difficult. Both Jewett and his colleagues, who recorded mainly auditory 3-channel evoked potentials, and Pratt and his co-workers, who recorded mainly visual 3-channel evoked potentials, have had difficulty analyzing and expressing their data. They have reported their analysis as being tedious, and the ability to define the activity has been cumbersome (Martin et al., 1987; Sininger et al., 1987; Towle et al., 1986; Pratt et al., 1987; Epstein and Reznick, 1986). Both Pratt and Jewett's analysis have suggested a model using a best fit plane for a peak of activity.

While this thesis will not deal with the mathematics of such a method, it appears that this method is neither reliable nor reproducible. Because an electrical peak is composed of an apical portion, and ascending and descending limbs to preceding and following apices , any change in the electrical potential from any of the three apical portions involved in the plane will significantly change the orientation of the best fit plane while doing little to change the occurrence of an event at a particular time. Thus, identifying and describing the time of occurrence of an event seems much more important than describing it in terms of a spatially designated plane. The physiological significance of some of the events described by Pratt come into question. Closed door studies show an average of 15-20 events prior to the P100 wave, all accounted for by noise. A well recorded study usually has 8-10 events in this time period. Pratt reported 15-20 events in this time period, which suggest that the data he described may noise.

Some problems inherent in those early studies have been the lack of an adequate way to record, view and analyze the data of 3-channel recordings. Through the use of more sophisticated recording equipment as well as the advent of new commercially available computer software, most of these problems were obviated. The present study demonstrated the ability to generate reproducible results as well as quantitate and evaluate the data in a manageable way. This was accomplished by the recording of the evoked response with a Nicolet Pathfinder II®, and transferring the data to a Macintosh® personal computer to be analyzed by the MacSpin® program. This program allowed the plotting of continuous activity with

respect to time in a 3-dimensional co-ordinate system. Further applications of the program allowed a continuous rotation of the data set, and spatial scaling of the data. This thereby allowed arbitrary view points to be used to identify all peaks of activity.

Data Analysis

The identification of activity:

Peaks of activity were identified. Although the decision as to the time of a peak was arbitrary, some consistencies in defining a peak were employed. (See Figure 21). Re-analysis of the same data set at a later time demonstrated the consistency of identifying peaks (data not shown). It was important to note that although discrete peaks could be identified, (and re-identified at a later time), the assignment of an unequivocal time for the event was not always possible, and thus the occurrence of an event is as important as the exact time that its peak occurs. This is already a well known phenomena for the P100 wave in conventional recordings. Identifying the exact time of the evènt in the individual may vary whether the same or different person evaluates the data of a VEP (Visual Evoked Potential) at a another time.

As demonstrated in Figure 5, the initial studies showed the ability to identify peaks of activity not readily discernable in conventional methods. It also became apparent that the notation of conventional recording had little meaning in vector recording. Conventional visual evoked potentials define the 100ms wave as a Positive occipital wave at 100ms, thus P100. Likewise, the preceding trough and succeeding trough on the conventional

recording are designated N70 and N130 for Negative wave at 70 and 130ms. The occasional appearance of a occipital positive wave prior to the 70 has been designated a P50 wave based on conventional nomenclature. The assignment of a positive wave as being a peak and a negative wave as a trough has an even more historical perspective. Through the use of the auditory evoked response (Stockard et al., 1977; Jewett et al., 1971), the positive peaks are said to anatomically correlate to the active generators of the electrical potential. While there is some support for peaks corresponding to active generators in auditory evoked potentials (Stockard et al., 1977; Pratt et al., 1987; Radtke et al., 1986; Gardi et al., 1987), there is little support for peaks being assigned to anatomical generators in visual evoked potential. This positive-negative assignment of an activity is in fact an inherent function of where the electrodes are placed, as demonstrated by Jeffreys (1977). The significance of this point is not whether an activity is positive or negative at a recording site, but simply that it exists. The vector method locates peaks of activity without this assignment bias. Thus in the vector method there is only the identification of a discrete time of maximal activity. This wave, with its associated apex latency is what is important, and thus the use of the term peak, wave, trough, apex are synonymous in the vector method and make no reference to positive or negative direction, as is done with conventional evoked potentials.

Because of the extreme magnitude of the P100 wave (greater than 10X that of the largest wave prior to the 70ms wave), the data was analyzed in discrete subsets, as was suggested by Pratt et al. (1986). The subset from 0-

65ms was evaluated for any discrete activity and recorded. The subset of 65-140ms was evaluated with respect to the P100 wave, with all peaks being of comparable magnitude. The final subset from 140 - 250ms, tended to have a more "flowing" progression of activity with more rounded less discrete peaks. In addition many small peaks of 3-4 times less magnitude were seen that were consistent with noise. Here the general trends of the peaks were noted using the midpoint of the rounded peak and ignoring background noise.

The identification and evaluation of discrete Pre and Post P100 activity.

Discrete Activities:

After examining more than 50 studies in more than 10 individuals using the vector method, the ability to identify waves not readily seen in convention plots was supported in every case. In Tables 1 A-D, a identification of peak activity other than the P100 is shown a selected group on subjects. A summary Table 1-E shows the VVEP values of the nominal activities found on the conventional plot as well as a highly reproducible wave occurring at approximately 55ms. This wave, which is a presumptive candidate for the long-sought-after lateral geniculate wave at about 50ms, is hereby referred to as the 55ms wave, and is discussed in some detail later in the text. As seen by this table, no significant difference is found between the left or right eyes, or between the 30' or 60' check size, which is supported by other studies as well (Novak et al., 1988). The presence of activity prior to the 55ms wave is seen in every case. As discussed in the results section, and as is seen in table 5 and figure 10, these events cannot be *accounted* for

by noise alone. Because of the variability of the numbers and latencies of the early waves (prior to 45ms), it is impossible to say that a 40ms wave in one subject is the same 40ms wave as in another. Likewise, the absence of a wave in one subject does not mean it was noise, or not physiologically significant in the other. Thus, although no exact times could be assigned to early waves, trends did suggest waves at approximately 12.5, 22.5, and 40ms. In addition, peak activity was suggested in the post 130ms period at 160, 190, and 220 ms. These potentials, as well as the N70, P100 and N130 are most likely generated along the visual pathway. This pathway progresses from the retina along the optic tracts, synapsing primarily at the LGB. From the LGB the pathway progresses along the optic radiations to synapse at the occipital cortex. At the occipital cortex, numerous pathways are believed to branch out throughout the cortex. While it is generally accepted that most potentials are generated by sites of synapses (Jewett et al., 1971), Chimento et al. (1987), showed curved neural pathways can generate a potential as well. In addition, while the VEP has been described in terms of evaluating the aforementioned visual pathway, the retina is known to project (albeit to a lesser extent) to the superior colliculus, pretectum, and the hypothalamus. The contribution of these pathways provide an alternate explanation for the source of the 55ms potential. However, all these pathways contribute to the evaluation of the midbrain. The support or dismissal of these individual contributions would require future experimentation, for example, depth electrodes or lesion studies, since clinical lesions involving these alternate pathways are very

rare. How these pathways might contribute to later events is unknown and any discussion would be speculative.

Numerical studies:

Because the smooth curve is generated from individual data points, a numeric data sheet can be made. Likewise, the magnitude of a point on the curve can be calculated. It was thought that an automated method of peak identification might be feasible by using the maxima and minima generated. As seen in Table 2, this resulted in a tremendous number of peaks. It became apparent that noise and even small changes would be identified as a peak. In addition, every time the graph crossed an axis a minima would be generated that had no corresponding peak. The implementation of inclusion/exclusion percentages was employed with only modest benefits. A method of using first and second derivatives to find maximal areas of change to find peaks and inflection points might further enhance peak selection in an automated method, but was not explored in this study. It is important to note that all conventional evoked potential recordings are analyzed visually in the graphic form. It is much more compelling to see trends graphically, than from numerical printouts. Such appears to be the case with vector evoked potentials as well.

Peaks can be expressed by direction:

Because the vector method plots data in a 3-dimensional setting, the peaks can be assigned a direction. It appears that the general direction of the peak is in fact significant. It also appears that intrasubject graphic comparisons are far more similar in space and time than *intersubject*

comparisons, (as is seen in the next section discussing symmetry). Assigning a best fit plane to an event, however, does not seem, in this study, to adequately describe an event, and saying that a peak occurs in a plane is simply an epiphenomena of a peaks occurring serially in free time. Table 3 assigned orientation to the peaks occurring at the nominal times listed. As can be seen only the P100 showed any similarities across the population, or within an individual. Perhaps the biggest problem of this program is the defining of the coordinates of a peak. A program we wrote computes the polar coordinates of a vector from the origin to the point in question. As seen in Figure 23, three completely different peaks would have the same polar coordinates (Figure 23 a,b,c). Likewise, two very similar peaks, that occur on different sides of an axis have very different co-ordinate (Figure 23 d,e). A suggested method to circumvent this problem using inflection points and peak bisection is given in Figure 23 f,g.

An additional note concerning direction is the assignment of latitude and longitude based on the axis representation. That is to say the 0 degree longitude runs through the P3 axis. A rotation matrix such that the axis are aligned to the principal body planes might be useful, but was not derived in this present study.

A final problem in comparing peaks by direction is the identification that two peaks described in different individuals are actually the same physiological event. Because of peak latency differences across a normal population, comparing directions of an individuals VVEP at an exact time would be meaningless. The use of a mathematical cross correlation study

to find the peaks in a group of subjects might prove worthwhile. However, such a study was not done in this thesis.

Reliability : Test-Retest

Right verses left eye comparison:

It might be expected that within an individual, a potential evoked with stimulation on the left side should be similar to the right side. This is especially important with visual evoked potentials for full field stimulation, which involves two retinal neural pathways which conduct to both sides of the brain for each eye. A comparison of peaks identified is seen in the intrasubject comparison Table 4 A,B for 30' and 60' of arc. As discussed in the results section there is some striking similarity within a subject in table form, in which some of the differences can be accounted for by peak time assignment error. However, the most profound implications of a left versus right eye comparison can be seen in the Figures 6,7,8 and Figure 24. The figures demonstrate the lack of symmetry from 0-40ms, however suggest that wave forms that cannot be accounted for by noise alone. From 40ms until the end of the recording epoch (approximately 250ms), both the left and the right eye seem to follow the same course in time and space, this symmetry is superimposable, and strongly support that the events post 40ms are reproducible and physiologically significant.

Test - retest of an individual:

The testing of an individual under set conditions was repeated at a later time (five hours in 1 subject and 1 month in the other). Table 6 shows the comparisons, a degree of similarity is apparent, again however the

graphic representation is even more impressive, Figure 11. Perhaps the most supportive of the epoch post 40ms as being significant and reproducible can be seen in Table 7. In this study 6 different testing fields were studied all at 60' of arc in the same individual.

The use of a null study (closed door) or a non-flashing checkerboard screen yielded similar results. Both generated a graph of highly random noise with numerous small peaks. These peaks were of approximately one half to full size of the peaks in the 0-40ms range. Thus, discerning peaks from noise in the early epoch is difficult. As already described, the peak activity in the 0-40 range in this study had too few events to be generated strictly by noise. While noise is constant (same across all studies), the presence of an evoked potential influences the appearance of this noise. As seen in Figure 10a, there appears to be far less peaks than in the closed door, Figure 10c. The noise in 10a is the same as in 10c, it is the greater magnitude of the evoked potential, however, that makes the noise difficult to see.

Hemi-fields:

The visual system is unique in that half of the retinal field tract (the nasal field) diverges to the other side of the brain to converge with the temporal field tract on that side. Thus by stimulating retina hemi-fields the four pre-chiasmal pathways can be studied. This in turn, should give a truer representation of the electrical progression along the visual pathway (Blumhardt et al., 1978; Blumhardt and Halliday , 1979). The strength of this approach was supported by a recent work of Novak et. al (1988) who

showed the advantages of a hemi-field evoked potential study in the diagnosis of multiple sclerosis patients. Again tables were compiled comparing the peaks identified of a given hemi-field across the test population, as well as an intrasubject comparison table of the four hemi-fields. Although the similarity could be seen within a subject, as well as the continued suggestion of the 12.5, 22.5, 40, 160, 190, and 220ms waves, the tables again were not very informative. Perhaps, the most significant point in the compilation of the tables was a very prominent 55ms wave in these hemi-field studies. It was not until the graphic printouts of the individual hemi-fields were compared that the strength of this approach became evident. Again from 0-40ms no symmetry or logical progression could be seen, yet again, there were too few activities for the events in this period to be just noise. From 40ms until 250ms, however, there was a remarkable display of symmetry. As seen in Figures 12-15, the progression of the evoked potential elicited from each temporal retina is a striking mirror image of the nasally elicited evoked potential of the same eye. And as equally exciting, the temporal evoked potential of one eye was almost identical (superimposable) with the nasal evoked potential of the other eye. This corresponds exactly with what is predicted from the anatomical pathways of the retinal field tracts. In fact, it is remarkable how symmetrical these plots are when one considers that the brain and the electrodes are never precisely symmetrical, and electrical noise and physiological test-retest variability unavoidably occur.

The progression of a given hemi-field plot appears to be uniform across the population from the 50-150ms time period. Smoothed curves of each of the four hemi-fields of five different subjects is shown in figure 15. The degree of similarity within an individual as well as across the population, in terms of general shape, progression of plot, and location of the major peaks (55, 70, 100, 130) in time and space, show great promise for clinical applications of this vector hemi-field method.

In addition, to show that the full field potential was, in fact, the summation of two hemi-fields, the P100's of a temporal and nasal retina stimulation were added vectorially and plotted. In comparison with a full field study, the summated hemi-fields equaled a full field response. This concept has particular importance in respect to some of the other waves, i.e. especially the 55ms wave which is organized contralaterally to the stimulated hemi-retina. A full field stimulus would produce two opposing hemi-field potentials which would be expected to average out or diminish this potential. We propose that these considerations explain why the 55ms potential is only sporadically seen and not well described in the literature. Figure 19 illustrates this phenomenon.

In addition, the extreme laterality of a hemi-field VVEP in comparison with a midline generation of a full field VVEP for the 40ms to 140ms epoch supports the stimulation of one pathway for the hemifield stimulation and the summation of two pathways for the full field stimulation (both sides of the brain). The appearance that after 140ms the hemi-field plots tend to be organized along the midline and similar to the

full field potential, suggest an activation of both sides of the cerebral cortex at this point.

The Lateral Geniculate Potential:

Researchers have long sought to identify an event which corresponds with a lateral geniculate potential. The identification of such a potential would allow a complete analysis of the visual pathway by including the lateral geniculate component to the cortical activity and the Pattern ERG currently obtained. This study has identified a discrete event at approximately 55ms which corresponds with the time predicted for a geniculate potential (Ducati et al., 1988; Wiggins et al.,1982). Because the activity has an identifiable time and direction, is repeatable within and across subjects, does not occur with null stimulation, and occurs at the predicted time after the pattern ERG (Figure 16) (Mc Donald,1976), it is not likely to be noise. This event is of very small magnitude and thus is rarely identified on a conventional visual evoked potential recording. In addition, as previously mentioned, full field stimulation will produce the individual left and right lateral geniculate dipole moments which cancel each other out (Figure 19). The argument of this 55ms wave being a retinal potential cannot be overlooked, but in those studies in which the Pattern ERG was recorded simultaneously with the VVEP, the 55ms wave was always a discrete event occurring between the Pattern ERG event and the 70ms wave. Furthermore, the likelihood of an ERG potential radiating to the electrodes in the montage used in this study in such a reproducible manner is unlikely. The Lateral Geniculate Body (LGB) is a highly organized

structure, both receiving and projecting fibers in a topographical manner. The LGB is composed of both X-related and Y-related cells, in which the generation of this LGB potential could be caused by the X-related cells, Y-related cells or both. The X-related cells (parvocellular, layers 4-6) tend to have a more central retinal distribution and better spatial resolution. The Y-related cells (magnocellular, layers 1 and 2) on the other hand, tend to be better stimulated by peripheral stimulation of the retina with increase sensitivity to contrast. However, how these properties could contribute to the 55ms activity is beyond the scope of this study.

As to what the activities in the 0-40ms portray, it is possible that the trend for a 22.5ms and a 40ms wave may actually be the retinal potentials recorded at distant electrode pairs. The lack of symmetry of these events would support this, however no confirmation exists.

General Summary :

History of physiology:

The attempts to use the visual evoked potential to evaluate the entire visual pathway has been marked with only limited success. While a characteristic P100 wave is generated as a cortical potential, it says little about the pathway leading up to it, other than it is conducting visual impulses from the retina. It does not allow localization of pathology, or a method for evaluating the midbrain (geniculate) component. Unlike the auditory evoked potential, no reproducible intermediate generators have been found. While both Jeffreys and Axford (1972a,b), and Pratt et al. (1986, 1982), have tried to define anatomical correlates to the visual evoked

potential, neither have met with great success. Likewise, use of scalp surface electrodes to define early activity has had little success (Zahn and Matthews, 1983; Whittaker and Siegfried, 1983). Ducati et al. (1988), tried to further define the early potentials, i.e. geniculate potentials with depth electrodes but was also unsuccessful. It has been suggested that the reason for this failure is that the LGB may be a closed system (Lorente de No', 1947), i.e., electrical fields anatomically cancel out. Another reason suggested here is that approaching from the posterior angle, Ducati may have been recording perpendicular to the LGB dipole and thus not recorded any geniculate activity. Full field stimulation may have contributed to a cancelling out of the activity.

In search of an LGB potential, major attention has been paid to the early VEP activity. Almost no attention has been given to the late activities (post 130ms), which are believed to be cortically derived (Jeffreys and Axford, 1971a,b; Celesia, 1984). The use of the vector study shows these waves to be reliable and reproducible in an individual. These late waves may have implications in the diagnosis of strokes, association tasks, and other neurological pathology, but until now there poor reproducibility made their use limited.

Conclusion:

1. Perhaps the most profound implication of this study is the identification of a reproducible event at approximately 55ms, which has fulfilled many characteristics required of a LGB potential. In addition, the reproducibility of the late waves (160, 190, and 220ms), as well as the

characterization of the waves recorded in the conventional evoked potential (70, 100, 130ms), make this study and excellent characterization of the visual pathway. It appears that the data arranged in a table or analyzed by a automated computer printout is not the best method for evaluation. It also appears that the intrasubject comparison of pathway progression is far more useful in making these points than intersubject comparison. It is the plot of the VVEP progression that demonstrates the high degree of symmetry in these normal subjects that make this study important. Through the use of a VVEP study with hemi-fields, along with a simultaneous Pattern ERG, the entire visual pathway can be evaluated. This strong degree of symmetry in normal subjects suggests very strong clinical applications in pathological subjects. One might expect, in pathological subjects, not only a delay in peak latencies, but also a change in the progression and presentation of the vector plot. The advantage of the hemi-fields use has already been shown (Novak et al., 1988), in which the following statement was made:

> "Our study showed that many patients with retrochiasmatic lesions may be identified with hemifield testing. The actual sensitivity of this method is difficult to estimate and awaits comparison with more sensitive methods for the clinical assessment of the visual fields in these patients."

The vector method with hemifield testing offers this sensitivity. Likewise the potential of the vector method to evaluate discrete regions of the visual system will further aid in helping in the diagnosis of such *diseases as*

migraine headaches, early multiple sclerosis, optic neuritis, epilepsy, stroke, ischemia, tumors and other disorders. (Halliday et al., 1976; Halliday et al., 1972; Halliday et al., 1973 ; Novak et al., 1988; Marsters et al., 1988; Raudino, 1988).

2. The concerns of the vector method as being more time consuming, is a real concern that can easily be rectified. The most time consuming step is the transfer of data from the Nicolet Pathfinder II® into the working MacSpin® program, while most of this is partially automated, taking about 15 min. per data set to transfer, a fully automated program would take minutes. The set up takes no longer than the application of five extra electrodes. With a testing time increased by doing the hemi-fields the VVEP can be done in two hrs. A whole test with transfer and analysis can be completed in less than four hours at present. Thus, the major problems of the vector method are simply data transfer, and getting used to the MacSpin® program. Once the data is in the MacSpin® program, an experienced user could evaluate the data by graphic comparison in all 6 tests (left, right, and four hemi-fields) in about 30 min.

3. Finally, the extreme reproducibility and symmetry of this study lends the conclusion that the wave forms identified can be tied to anatomical correlates, while lesions studies would be necessary to confirm these correlates, the progression of events and proposed anatomical correlations are as follows (Figure 25):

The retina is stimulated by the evoking stimulus with an associated discharge at 12.5ms of still as of yet unknown origin. At approximately

22.5ms an initial Pattern ERG peak is formed (Holder, 1989). These two events are seen as sporadic events on the VVEP, with the 22.5ms event being prominent on the pattern ERG as the initial negative wave, and at 45ms the ganglion cells of the retina discharge giving the second Pattern ERG peak (Maffei and Fiorentini, 1981; Arden et al., 1982). This ERG discharge is visualized as a peak or a cluster of points occurring on the VVEP. It takes from 5-10ms to travel from the retina to the LGB (Mc Donald, 1976), at this time interval, a straight line veers off from the pattern ERG point on the VVEP and forms the ascending loop of the 55ms wave. The peak that occurs consistent with the LGB at 55ms. This descending limb of the 55ms peak courses directly to the 70ms peak, which has been proposed to arise from the optic radiations (Pratt et al., 1986). From this point the activity of the VVEP forms the P100 wave which is the positive occipital wave. This activity then gives rise to a group of cortically generated waves, the 130, 160, 190, and 220, of which the later are believed to be generated from both sides of the cortex in a hemifield study (Blumenhardt and Halliday, 1979; Bodis-Wollner, 1977; Celesia, 1980; Celesia et al., 1984).

TABLES

Table 1 A-D : Intersubject Comparison of Peak Times, Identified by Graphical Observation for 30 and 60 min. of Arc (OS and OD). These tables list the activity (peaks) identified by visual graphical analysis of given subjects at the given check size (minute of arc). I. the nominal 50ms wave, II. the 70ms wave (N70), III. the P100 wave, and IV. the 130ms (N130) wave. The other numbers are lined up by time, but as explained in the text may not be the same physiological events. Peak times are given in ms.

Table 1 A : Intersubject Comparison of Peak Times, Identified by Graphical Observation for 60 min. of Arc (OD).

	SUBJECT:						
	A	**B**	**C**	**D**	**E**	**F**	**G**
	.5/3	3		1.5	1/2.5	2.5	
	6.5	6.5		5	6	3.5/5.	4.5
	9	9	9	8.5	9.5	11	
	14/17·	11.5/(14)		(14.5)	(16)	(15)	13
		18.5					
	22.5	22	22.5	21	21.5	22	20.5
	27.5	26					
	30.5	28.5		(30)		27	29
	36	33.5	36	(36.5)	32.5		
	40/45	38.5			38.5		42.5
		46	47		45	44	(46)
I.	53/59	55.5	55	54.5	58.5	56.5	53.5
II.	69.5	72	72	65.5	76.5	74.5	72
III.	100	103	104	92.5	100	95	104
IV.	(133)	136	137.5	130.5	132	129.5/138.5	128
		(156.5)	163	172.5	168		163
	182					183	
	213	189/200.5	200.5	194	216		198
		226	231	225		228.5	230.5
	(252)	(245.5)					

Table 1 B : Intersubject Comparison of Peak Times, Identified by Graphical Observation for 60 min. of Arc (OS).

SUBJECT :

	A	B	C	D	E	F	G
	1.5	.5/2.5	.5	1.5	2.5		2.5
	5	5.5	4	5.5		4.5	
	7.5		9		8.5	8	
	11.5	11		10.5		10.5	
	14	13.5	13.5		13		13.5
	16.5	16.5/(18)	(15.5)	(17)	19	16	
	21.5	22.5		19.5	21.5	20.5	
	25.5		23.5	23	25.5	27	24
	28		29	28			
	35	31.5/35.5	35	32	33/37		34.5
	40.5	41.5	43.5	39.5	40.5	43.5	(42.5)
	47				49.5/56.5		44.5
	51.5		51				(51.5)
I.	54	58.5	59.5	55.5	62	53	55.5
II.	71.5	73	74	67	72.5	73.5	70
III.	94.5	104	100	86	104.5	98.5	108
IV.	118	132	137	114	123.5	136	130.5
	138	145		137	150.5		147.5
		156		151.5/159.5			
	176	172	169	176	175.5	182.5	167.5
	204	210	195	195.5		219.5	201
	243.5	219	227.5	230	226.5		230

Table 1 C : Intersubject Comparison of Peak Times, Identified by Graphical Observation for 30 min. of Arc (OS).

SUBJECT :

	A	B	C	D	E	F	G
					(.5)		1.0
	2.5	2.5	4.0		4.0		4.0
	5.5	(6.0)		7.5	7.5	6.0	6.5
	9.0	8.0	9.5		9.5	8.5	
	13	11	13.5	13.5		12	11.5
	17	15	15.5		15		14.5
							17.5
	19.5	19.5	18	19	20	21	19.5
	26	23/26	23	23	22.5	24.5	23.5
	30.5	31.5		30.5	28	29.5	(27)
		36		37	35.5	38.5	(36)
	41.5	39.5	41.5	43	42.5		
	47	43.5		46			47
		54/59	51	52.5			56.5
I.	56.5	69	59	60	62	50.5	60
II.	72.0	72/76	71.0	65.5	76.0	72.0	78.5
III.	90.0	98.5	100.5	88.0	101.0	89.0	109.0
IV.	121.5	125.5	136.5	119.5	130.0	127.0	139.5
				(135)		134	
				140	147.5	141/148	
	170	168	158.5	160	170	169.5	(175.5)
				184	179.5	178	
	217.5		193.5	208.5	199		
		224.5	234	230	223	219	234

Table 1 D : Intersubject Comparison of Peak Times, Identified by Graphical Observation for 30 min. of Arc (OD).

	SUBJECT:					
	E	D	C	B	A	F
	3	5	5.5	2/6.5	1.5/6	.5/3/5
	(8)	8.5	9.5	8.5		8.5
		13	12.5		12.5	
	15			16.5		16
		17	17.5	19/20.5	17	19.5
	24	22.5	23	24	21.5	
	(31)	(28)	27	29.5	25.5	26.5
		(39)	32/36	35.5	31.5	
			47	40.5/42.5	40/45	38.5
				51.5/54	48.5	49.5
I.	55	58	54.5	63.5	58.5	62
II.	75	69	72	78	71.5	76
III.	104	91	103.5	102	91.5	96
IV.	127.5	126.5	138	132.5	122.5	124
	133.5					
	(148)	148			150.5	153.5
	165.5	171	168.5	182	182.5	186
	188.5	207.5	200			
	224.5	231	238.5	237	237.5	217

Table 1 E : Table of Peak Averages for Left and Right Eyes at 30 and 60 min. of Arc. No statistically significant difference is found between 30 or 60 min. of arc or between each eye for a given wave time. Bold numbers represent nominal peak time given in the literature for that peak. Peak times are given in ms, with standard deviations.

Table 1 E : Table of Peak Averages for Left and Right Eyes at 30 and 60 min. of Arc.

nominal peak time	check size	OD	OS
50	60' of Arc	56.1ms +/- 2.0	56.9ms +/- 3.2
	30' of Arc	58.5ms +/- 3.6	59.6ms +/- 5.6
70	60' of Arc	71.7ms +/- 3.5	71.6ms +/- 2.4
	30' of Arc	73.6ms +/- 3.3	72.4ms +/- 4.1
100	60' of Arc	99.8ms +/- 4.5	99.4ms +/- 7.4
	30' of Arc	98.0ms +/- 6.0	96.6ms +/- 7.8
125	60' of Arc	132.4ms +/- 3.4	127.2ms +/- 8.9
	30' of Arc	128.5ms +/- 5.8	128.5ms +/- 7.4

Table 2 : Numerical Versus Graphical Comparison of the Identification of Peaks, (OS, 30 min of Arc). The first three criteria attempt to use an automated recognition procedure which identifies maximal and minimal activity by numerical magnitude difference. The 100 pts. column requires that a subsequent maximum or minimum must be at least 100 μv greater/lesser in magnitude. The 10/25% columns require that a subsequent maximum or minimum must be at least 10% or 25% greater or lesser than that maximum or minimum point. The column labeled graph. is those activities identified by visual graphical analysis using the MacSpin® program as described in the text. Peak time is in ms.

Table 2 : Numerical Versus Graphical Comparison of the Identification of Peaks, (OS, 30 min of Arc).

Subject : C				Subject : A			
100pts	10%	25%	graph.	100pts	10%	25%	graph.
3.0	3.0	-	4.0				2.5
9.0	9.0	9.0	9.5	5.0	5.0	5.0	5.5
14.0	-	-	13.5	9.5	9.5	9.5	9.0
15.5	15.5	-	15.5	12.5	12.5	12.5	13.0
18.0	18.0	18.0	18.0	17.0	17.0	17.0	17.0
23.0	23.0	23.0	23.0	23.0	23.0	23.0	19.5
27.5	27.5	-		26.5	26.5	26.5	26.0
29.0	29.0	-		30.0	30.0	30.0	30.5
33.0	-	33.0		32.0	32.0	32.0	
37.5	37.5	37.5	41.5	38.0	38.0	38.0	36.0
49.5	49.5	49.5		40.5	40.5	40.5	41.5
51.5	51.5	51.5	51.0	46.0	46.0	46.0	(47.5)
57.0	57.0	57.0	59.0	50.0	50.0	50.0	
74.0	74.0	74.0	71.0	57.5	57.5	57.5	56.5
80.0	80.0	80.0		60.5	60.5	-	
81.5	81.5	-		68.0	68.0	68.0	
83.5	-	-		70.0	70.0	-	72.5
101.0	101.0	101.0	100.5	74.5	74.5	-	
128.5	128.5	128.5		76.5	-	-	
137.5	137.5	137.5	136.5	90.5	90.5	90.5	90.0
142.5	142.5	142.5		111.5	111.5	111.5	
145.0	145.0	-		121.5	121.5	121.5	121.5
151.5	151.5	151.5		134.5	134.5	134.5	
155.5	155.5	155.5		161.0	161.0	161.0	
159.0	159.0	-	158.5	165.0	165.0	-	
161.0	161.0	-		171.0	171.0	-	170.0
166.5	166.5	166.5		180.5	180.5	-	
193.5	193.5	193.5	193.5	183.0	183.0	-	
200.5	200.5	-		195.5	195.5	195.5	
203.5	203.5	-		197.5	-	-	
208.0	208.0	208.0		201.5	201.5	201.5	
210.0	-	-		203.5	203.5	203.5	
222.0	222.0	222.0		211.0	211.0	211.0	
224.5	224.5	224.5		218.0	218.0	218.0	217.5
226.5	226.5	-		223.5	223.5	223.5	
235.0	235.0	235.0	234.0	225.5	225.5	225.5	
239.0	239.0	239.0		231.0	231.0	231.0	
				253.0	253.0	253.0	

Table 3 : Latitude and Longitudes for Peaks Identified Graphically by Visual Inspection. Latitude and longitude are derived by the MacSpin® program (see materials and methods). 3 subjects (D,G,E) are shown. The (epoch) 1-512 corresponds with the left eye and the 513-1024 corresponds to the right eye at 60' of arc. Latitude and longitude are in degrees. The bold numbers 50, 70... correspond to the nominal peak activity time +/- 10ms for the 50 and 70ms, and +/- 15ms for the 100-220ms events. When two events fell within a criteria, both are listed. Blank squares are where no well defined direction could be assigned to the activity.

Table 3 : Latitude and Longitudes for Peaks Identified Graphically by Visual Inspection.

Subject:	Epoch	Nominal Peak Time: 50 LAT	50 LONG	70 LAT	70 LONG	100 LAT	100 LONG	135 LAT	135 LONG	160 LAT	160 LONG	190 LAT	190 LONG	220 LAT	220 LONG
D	1-512	28.9	-22.3	-39	-59.3	14.8	-28.4	114ms 1.0 137ms -1[illegible]7	5.8 -33.7	-26.5	-43.9	176ms 48.8 195ms -21.7	4.3 -20.3	53.0	-20.4
	513-1024	6.2	-36.1	-17.8	-42.2	15.9	-31.4	-23.6	-42.9	13.5	4.3	5.0	-7.8	36.9	-56.1
G	1-512	-53.5	-7.8	-51.2	-33.1	19.7	-10.8	-0.5	-2.2	-16.9	-29.5	57.8	-53.2	34.8	-35.3
	513-1024	9.8	-59.1	-38.4	-69.8	9.4	-15.4	-4.6	-10.5	6.6	-75.6	18.9	9.4	44.6	-30.2
E	1-512	-41.3	13.9	18.9	10.8	19.4	2.4			-33.7	79.9	-35.7	20.0	-51.0	-44.6
	513-1024	-24.4	-31.6	5.4	41.1	5.7	-13.5	61.1	-32.4	-10.9	-37.5			-49.6	-42.2

Table 4 A,B : Intrasubject Comparison of Peak Latencies of a Subject's Right Versus Left Eye for 30 and 60 min of Arc. Subjects activity identified graphically for both the right and left eyes are compared side to side. This is done for both 30 and 60 minutes of arc. I. the nominal 50ms wave, II. the 70ms wave (N70), III. the P100 wave, and IV. the 130ms (N130) wave. The remaining activities are arranged by time (in ms).

Table 4 A : Intrasubject Comparison of Peak Latencies of a Subject's Right Versus Left Eye for 30 min of Arc.

SUBJECTS:

	E		C		A		D		B	
	OS	OD	OS	OD	OS	OD	OS	OD	OS	OD
	.5/4	3		2.5	2.5	1.5			2.5	2
	7.5	(8)	4	5.5	5.5	6	7.5	5	6	6.5
	9.5		9.5	9.5	9			8.5	8	8.5
			13.5	12.5	13	12.5	13.5	13	11	
	15	15	15.5						15	16.5
			18	17.5	17	17	19	17	19.5	19
	20	(20)	23	23	19.5	21.5				20.5
	22.5	24					23	22.5	23	24
	28	(31)		27	26	25.5			26	
				32	30.5	31.5	30.5	28	31.5	29.5
	35.5			36	36		37	39	36	35.5
									39.5	40.5
	42.5		41.5		41.5	40	43		43.5	42.5
	48			47	47.5	48.5	46			
	52		51				52.5		51.5	51.5
									54	54
I.	62	55	59	54.5	56.5	58.5	60	58	69	63.5
II.	76	75	71	72	72.5	71.5	65.5	69	76	78
III.	101	104	100.5	103.5	90	91.5	88	91	98.5	102
IV.	130	127.5	136.5	138	121.5	122.5	119.5	126.5	125.5	132.5
		133.5					135			
	147.5	148				150.5	140	148		
			158.5	168.5			160		168	
	170	165.5			170	182.5		171		
							184			182
	179.5	188.5								
			193.5	200			208.5	207.5	207.5	
	199									
					217.5					
	223	224.5				237.5	230	231	224.5	
			234	238.5						237

Table 4 B : Intrasubject Comparison of Peak Latencies of a Subject's Right Versus Left Eye for 30 and 60 min of Arc. I .

SUBJECT:

	G		B		D		E	
	OS	OD	OS	OD	OS	OD	OS	OD
			.5					
	2.5		2.5	3	1.5	1.5	2.5	2.5
		4.5	5.5	6.5	5.5	5		6
	7.5			9		8.5	8.5	9.5
			11	11.5	10.5			
	13.5	13.0	14	14		14.5	13	
		20.5	16.5		17			16
	24		18	18.5	19.5	21	19	
		29	22.5	22	23		21.5	21.5
			23	26			25.5	
	34.5		31.5	28.5	28	30	33	32.5
			35.5	33.5	32		37	38.5
	42.5	42.5	38	38.5	39.5	36.5	40.5	45
	44.5	46	41.5	46			49/56.5	55.5
I.	55	53.5	58.5	55.5	55.5	54.5	62	58.5
II.	70	72	73	72	67	65.5	72.5	74.5
III.	108.5	104	104	103	86	92.5	104.5	95
IV.	130.5	128	132	136	114		123.5	129.5
					137	130.5		138.5
	147.5		145		151.5		150.5	
			156	156.5	159.5			
	167	163	172		176	172.5	175.5	183
				189				
	201	198		200.5	195.5	194		
			210					
	230	230.5	219	226	230	225	226.5	228.5
				245.5				

Table 4 B : Intrasubject Comparison of Peak Latencies of a Subject's Right Versus Left Eye for 30 and 60 min of Arc. ||,

SUBJECT:

	C		A		F	
	OS	OD	OS	OD	OS	OD
	.5		1.5	.5/3		2.5/3.5
	4		5	6.5	4.5	5.5
			7		8	
	9	9		9	10.5	11
			11.5			
	13.5		14	14		
	15.5		16.5	17	16	15
					20.5	22
	23.5	22.5	21.5	22.5		
			25.5			
	29		28	27.5	27	27
				30.5		
	35	36	35	36		
			40.5	40		
	43.5				43.5	44
	51	47	47	45		
			51.5	53		
I.	59.5	55	54	59	53	56.5
II.	74	72	71.5	69.5	73.5	74.5
III.	100	104	94.5	100	98.5	95
IV.	137	137.5	118		136	129.5
			138	133		138.5
	169	163				
			176	182	182	183
	195	200.5				
			204	213	219	
	227.5	231				228.5
			243.5	252		

Table 5: Graphical Analysis of 2 Selected Closed Door (null) Studies. In these noise records, peaks were identified graphically using the same visual criteria as with actual evoked potentials. (See text for additional details of study). The first 65 ms are included in the table, peaks of activity continue to occur at 2-5ms intervals throughout the 250ms epoch.

Table 5 : Graphical Analysis of 2 Selected Closed Door (null) Studies.

SUBJECT :	H		I	
	LEFT	RIGHT	LEFT	RIGHT
	5.5	5	3	1.5
	8.5	9.5	10.5	4.5
	11.5	13.5	14.5	12
	16.5	17	17	16
	19	19.5	19	19
	25	21	21	23
	27	24.5	29	27
	30	29	31	35
	34	32.5	34	39.5
	36.5	35.5	37	43.5
	41.5	38.5	40	48
	45.5	40.5	45	56
	48.5	46.5	49	60
	54	50.5	52	65
	57	59.5	56	
	59	63	60	
	62.5		65	

Table 6: Table of Subject Test-Retest. Subjects were tested and at a later time retested (subject G - 1 month later, subject H - 5 hrs. later) under the same stimulation parameters (full field, 60' of arc). Visually identified peaks from the vector graphic display show a high degree of similarity throughout the recording epoch . Activities were identified graphically, with no prior knowledge of wave times of the paired study. The paucity of early activity (6-11 events) prior to the 65ms suggest while some of the activity may be noise, it is unlikely it is all noise in as much as closed door studies have an average of 15-20 events in this time range. Brackets ( ) around a number indicates a poorly defined wave. I. the nominal 50ms wave, II. the 70ms wave (N70), III. the P100 wave, and IV. the 130ms (N130) wave. Other identified peaks of activity are paired by similar time.

Table 6 : Table of Subject Test-Retest.

Subject :	G				H			
Test # :	1	2	1	2	1	2	1	2
Eye :	OS	OS	OD	OD	OS	OS	OD	OD
	2.5	2.0				1.0		
		4.0	4.5	5.0	3.0			3.5
	7.5	7.5			8.5	9.0	8.0	
								10
	13.5	10.5	13	11	13.5	14.5	12	15.5
		(18)					15.5	18
		21.5	20.5	21.5		20.5		21
	24	(24)				27	27	23.5
		29.5	29	32	32.5	32		31.5
	34.5	35					39	41.5
	(42.5)	(43)	42/5	(43)	38	59.5	52	48.5
			(46)					57.5
I.	55.5	51.5	53.5	51.5	68.5	73	68.5	78
II.	70	71.5	72	68.5	86.5	82.5	87.5	91
III.	108.5	107.5	104	104.5	110	103	108	108
IV.	130.5	135.5	128	125.5		127		
	147.5				149.5	140		
							154.5	152
	167.5	170	163	164.5		160		
					185		184.5	183.5
	201	196.5	198	194.5				
						218		219.5
	230	229.5	230.5	225.5	232		237	234.5

Table 7 : Graphically Identified Peaks in Subject G's VVEP's Recorded at 60 minutes of arc for, Left and Right eye, Full Field and Hemi-Fields (6 studies). On graphic analysis of these six different studies, the activities post 50 ms are almost identical, showing an extreme degree of reproducibility within a subject. (See text for further discussion).
I. the nominal 50ms wave, II. the 70ms wave (N70), III. the P100 wave, and IV. the 130ms (N130) wave. The other identified peak times are lined up by time, in ms.

Table 7 : Graphically Identified Peaks in Subject G's VVEP's Recorded at 60 minutes of Arc for, Left and Right Eye, Full Field and Hemi-Fields (6 studies).

	OS	OD	OSt	OSn	ODn	ODt
	2.0		2.0	(2.5)	1.5	
	4.0	5.0	5.0		6.5	(5)
	7.5		8.0	8.0		
	10.5	11	10	12.5	11	(11.5)
	(18)	15				
	21.5	21.5	22.5	25	16	25.5
	(24)					
	29.5	32				
	35		(37.5)	(36.5)	(37.5)	
	(43)	(43)		46.5		44.5
I.	51.5	51.5	55	52.5/62.5	51	51
II.	71.5	68.5	72	79.5	69	70
III.	107.5	104.5	107.5	104.5	104	100.5
IV.	135.5	125.5	138	139	136	132.5
	170.5	164.5	168	172	171.5	169
	196.5	194.5	192.5	202	190.5	199.5
	229.5	225.5	218.5	243	221	231

Table 8 A-D : Intersubject Comparisons of Peak Activity Identified from Graphical Observation of Hemi-field Stimulation for OS and OD Nasal and Temporal Retinal Fields. Different subjects were chosen for each hemi-field comparison. As with the previous tables, I. the nominal 50ms wave, II. the 70ms wave (N70), III. the P100 wave, and IV. the 130ms (N130) wave. The other numbers are lined up by time, but as explained in the text may not be the same physiological events. Peak times are given in ms. Of note, subject D and A have very early P100 waves, this shifts both pre and post activity accordingly.

Table 8 A : Intersubject Comparisons of Peak Activity Identified from Graphical Observation of Hemi-field Stimulation for OS Temporal Retinal Fields.

Subject :	G	C	D	F	A
	2.5	1.5		2.5	
	6.0	5.5	7	5	5.5
		10			9.5
	13	14	14	12.5	13
	19.5	18.5		18.5	19.5
	21.5	21.5	21.5	21.5	
	25			25	24
	28.5	28			29
		32.5		32	
	36.5	37		39	37.5
					40.5
	40				
	47			48.5	
	50			51.5	
I.	57.5	51	46.5	56.5	45.5
					(52/63)
II.	72	73.5	62.5	76	68.5
III.	106	101.5	84	98.5	87.5
IV.	135.5	136.5	116	135.5	113.5
			146.5		142
	169.5	169.5		161	
			182.5		182
	202.5	199.5		188/200	
		217.5			
	232		232	230	
		242.5	243.5		241.5

Table 8 B : Intersubject Comparisons of Peak Activity Identified from Graphical Observation of Hemi-field Stimulation for OS Nasal Retinal Fields.

Subject :	G	C	D	E	A
	2.5		2.0	1.5	
	5.0	6.0	6.0	6.5	4.5
	7.0				
	10.5	9.5	9.5		9.0
	14	14	16.5	15	15.5
				18.5	
	19	20	21		22
		24			25
		26.5		28	
	35.5	30			30
		33.5	33	32.5	
		36.5			38.5
		39	48	47	45
					48
I.	42	50.5	51.5	55	54.5
II.	62	67.5	63	66/73	68
III.	105.5	101.5	84	95	88.5
IV.	143	134.5	117.5	125.5	115.5
			145.5	133/140	135.5
		198	176.5	183.5	176.5
	212	207		219.5	
			232.5		
		242	252.5	243	240

Table 8 C : Intersubject Comparisons of Peak Activity Identified from Graphical Observation of Hemi-Field Stimulation for OD Temporal Retinal Fields.

Subject:	C	F	G	K	E	A	D
	2.0	2.5				3.5	3
			4	6	4.5		
	7.5	8	8			8	7
		11		10	9.5		8.5
	13.5	14	14		13	12.5	
							15
	17.5	16.5					
			18	18	20.5	18	18
	22						
	25.5	24.5	23.5	24	23.5	23.5	25.5
		28.5			27.5	27.5	
	30	31.5	30	29			31
	33.5					32	
			35				36.5
	37.5	37.5		37.5	37	37	
		42	41.5	42	42.5		40
	49.5	47.5	44			48	
		53.5		50.5	49		
		59		61			
I.	61.5	61.5	48	68	55.5	52.5	51
II.	72	76	71.5	74.5	73.5	66	70
III.	97	97	97.5	94.5	98	90.5	92.5
IV.	137.5	118.5	131.5		133.5	117	135
		136.5					
		147.5		147			150/170
		158.5				162.5	
	188.5	185	171	186/196			181.5
					190/200	200.5	
	202	206	199.5			212	210
		224	215.5	224	220	226	225.5
	240.5				234	237	

Table 8 D : Intersubject Comparisons of Peak Activity Identified from Graphical Observation of Hemi-Field Stimulation for OD Nasal Retinal Fields.

Subject:	C	F	G	K	A	B	E
	2		1.5			3.5	
		5	5.5	4.5		7	4.5
	9			7.5	9.5	9.5	8
			12	11	13.5		10.5
	15	16.5	14.5	15.5	16	14.5	16
	18				18.5	18	18
	21	20	22	22	21	21.5	20
						25.5	22.5
	26.5	26.5	28	27		27	25.5
					27.5/30		
	30.5	29.5	30	31		30	
		33			34.5	33.5	
	36.5		36.5	36.5		36.5	36.5
					39.5	39.5	40.5
	42					42	
	46.5		45	42/47.5		44.5	44
	49					46/48	50
						52.5	
	57.5					57.5	
						61	
I.	65/69	46.5	58.5	53	45.5	66/67	55.5
II.	73.5	75.5	66.5	73.5	65	73	76.5
III.	98	99	101	96	90.5	96	96.5
IV.	133	120/125	133	132	110		128.5
		146				142.5	
			159	161.5	159.5		162.5
	177/187	172			168.5	169	
		187.5		189.5		191	
	204/233		194.5		214		197.5
		233.5		235		234.5	227
	248				241.5		251

Table 9: Intrasubject Comparison of the Graphically Identified Peak Latencies of the Four Hemi-fields in Three Subjects. Again the activities are grouped for the previous table(s). OSt is left eye, temporal retina stimulation. OSn is left eye, nasal retina stimulation. ODn is right eye nasal retina stimulation, and ODt is right eye temporal retina stimulation.

Table 9 : Intrasubject Comparison of the Graphichally Identified Peak Latencies of the 4 Hemi-field in Three Subjects.

Subject :	C				G				A			
	OSt	OSn	ODn	ODn	OSt	OSn	ODn	ODn	OSt	OSn	ODn	ODn
	1.5		2	2	2.5	2.5	1.5					
	5.5	6		7.5	6	5	5.5	4	5.5	4.5		3.5
	10	9.5	9			7		8	9.5	9	9.5	8
	14	14	15	13.5	13	10.5	12		13.5		13.5	12.5
						14	14.5	14		15.5	16	
	18.5	20	18	17.5	19.5	19		18	19.5		18.5	18
	21.5		21	22	21.5		22	23.5		22	21	
		24		25.5	25				24	25		23.5
	28	26.5	26.5		28.5		28		29	30	27.5/30	27.5
	32.5	30	30.5	30			30	30				32
		33.5		33.5							34.5	
	37	36.5	36.5	37.5	36.5	35.5	36.5		37.5	38.5		37
		39	42		40			41.5	40.5		39.5	
			46.5		47		45	44				
			49	49.5	50				45.5	45		
			57.5							48		48
I.	51	50.5	65/69	61.5	57.5	42	58.5	48	52/63	54.5	45.5	52.5
II.	73.5	67.5	73.5	72	72	62	66.5	71.5	68.5	68	65	66
III.	101.5	101.5	98	97	106	105.5	101	97.5	87.5	88.5	90.5	90.5
IV.	136.5	134.5	133	137.5	135.5	143	133	131.5	113.5	115.5	110	117
									142	135.5		
	169.5				169.5		159	171			159.5	162.5
			177 /									
	199.5	198	187	188.5				199.5	182	176.5	168.5	
	217.5	207	204 / 233	202	202.5	212	194.5	215.5				200.5
					232						214	212
	242.5	242	248	240.5								226
									241.5	240	241.5	237

Table 10: The Pattern ERG Values for Left and Right Eyes of Three Subjects. These data were derived as shown in Figure 17.

Table 10 : The Pattern ERG Values for Left and Right Eyes of Three Subjects.

	OS		OD	
	early peak	late peak	early peak	late peak
SUBJECT:				
H	27.5ms	46.5ms	25ms	45ms
I	31ms	54.5ms	34ms	56.5ms
J	29ms	47ms	32ms	51ms
Mean:	29.2ms	49.3ms	30.3ms	50.8ms
+/- S.D.: (Standard Deviation)	+/- 1.8	+/- 4.5	+/- 4.7	+/- 5.6

Mean of Both eyes, +/- S.D.:

Early peak: 29.8 ms +/- 3.3

Late peak: 50.1 ms +/- 4.7

FIGURES

Figure 1 : Conventional (Queen's Square) VEP Electrode Montage. This schematic diagram represents the conventional electrode placement based on the Queen's Square Method of Queens Hospital, England. Traditional VEP's are recorded and plotted from the Qz (+)(5 cm above inion), Fz(-), recording site, (a one channel recording).

Figure 2 : "Vector" (3-Channel) VEP Electrode Montage. This schematic, with a hypothetical vector plot, demonstrates the electrode placement pairs used to generate a 3 separate channel recording plot with respect to time. The recording pairs are In (-) to Fz(+), Tr2(-) to P3(+), and Tr1(-) to P4(+). See text for a more detailed discussion.

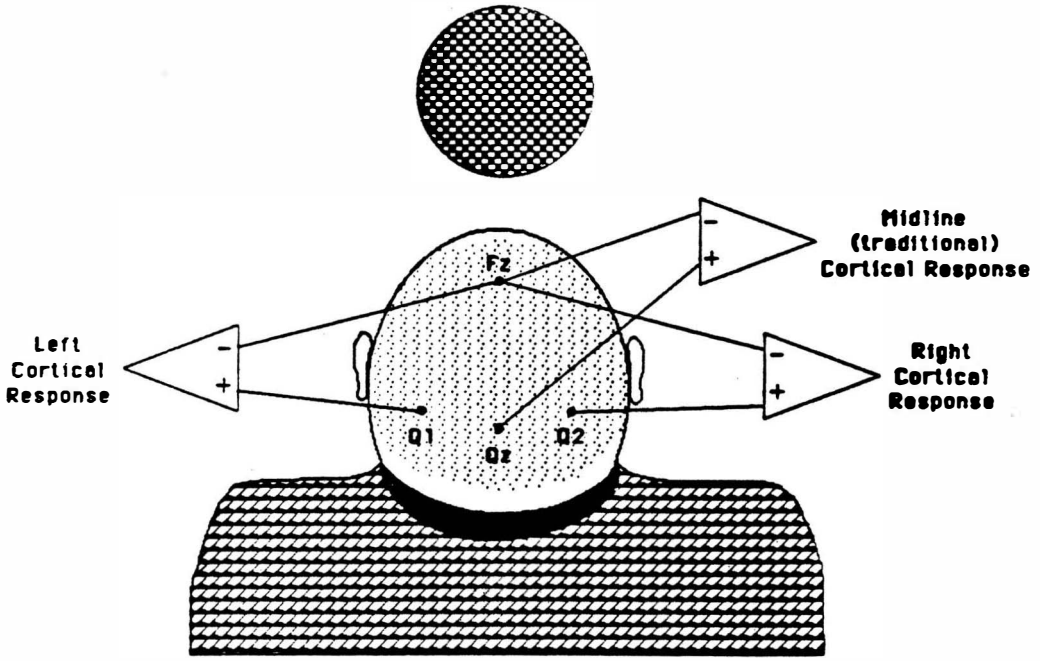

Figure 1 : Conventional (Queen's Square) VEP Electrode Montage.

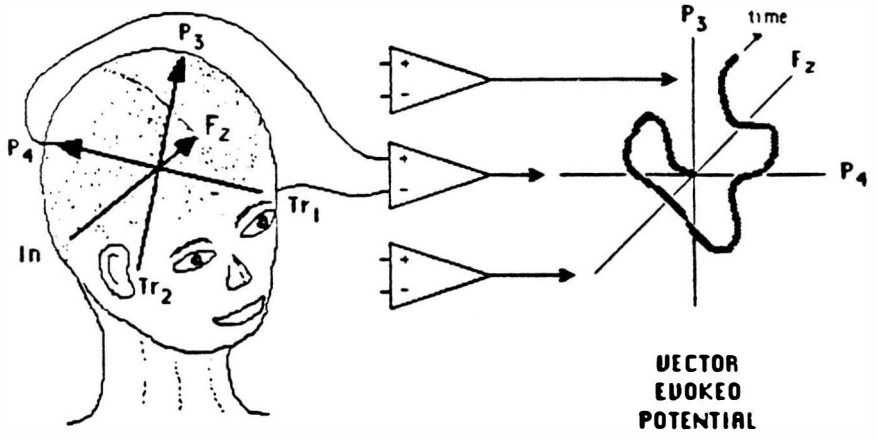

Figure 2 : "Vector" (3-Channel) VEP Electrode Montage.

Figure 3 : 10-20 System of Electrode Placement. This figure shows the designation of the electrode placement sites. (Figure used by permission from Grass Instruments.)

INTERNATIONAL (10-20) ELECTRODE PLACEMENT

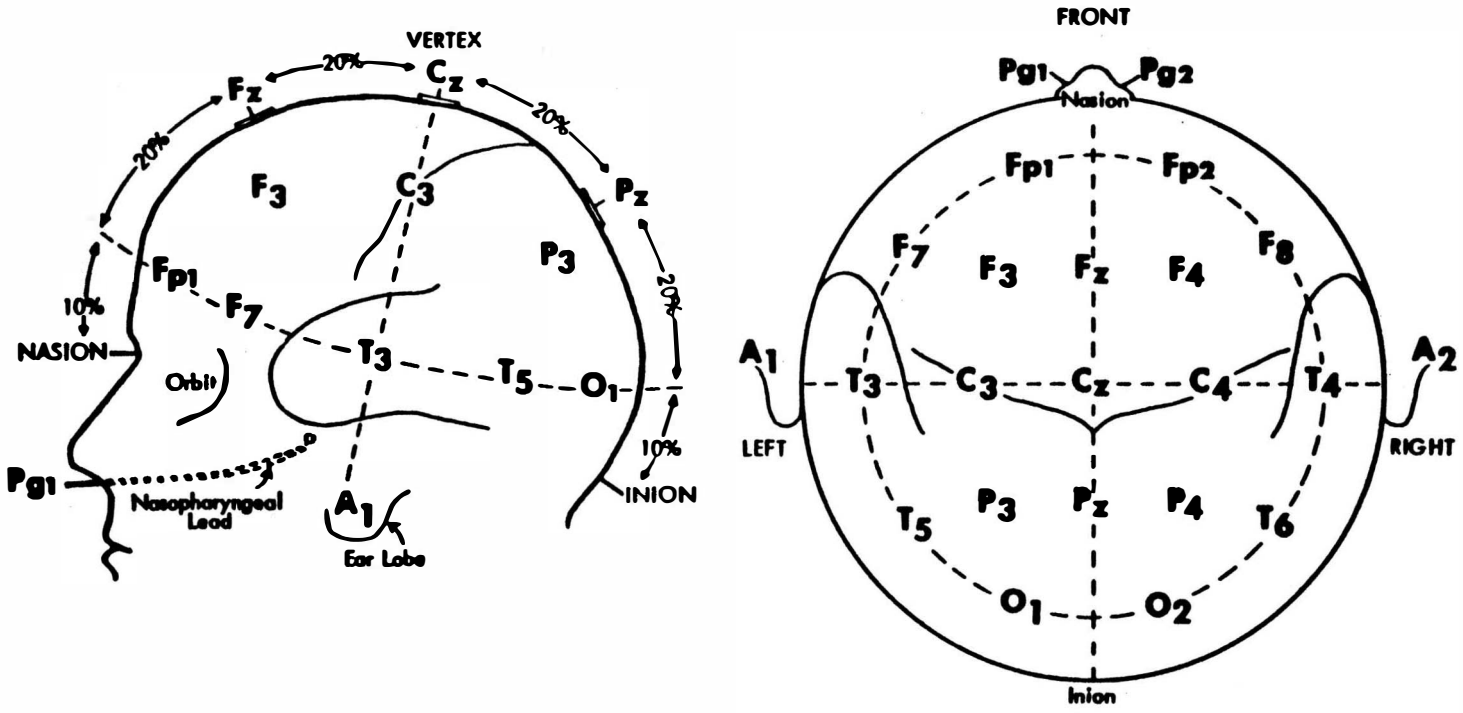

GRASS SINCE 1935 MEDICAL INSTRUMENTS
QUINCY, MASS., U.S.A.

Figure 3 : 10-20 System of Electrode Placement.

Figure 4 : Conventional Plot of Visual Evoked Potential of Left Eye (OS).

Qsz = Midline, 5cm above inion.

A2 = Right ear.

Qsr = 5cm right of Qsz.

Qsl = 5 cm left of Qsz.

Fz= Mid frontal, midline (international 10-20 system), 30% above nasion.

The P100 (100ms) peak is labeled for reference. Note that the P100 occurs at approximately 82 ms in this example.

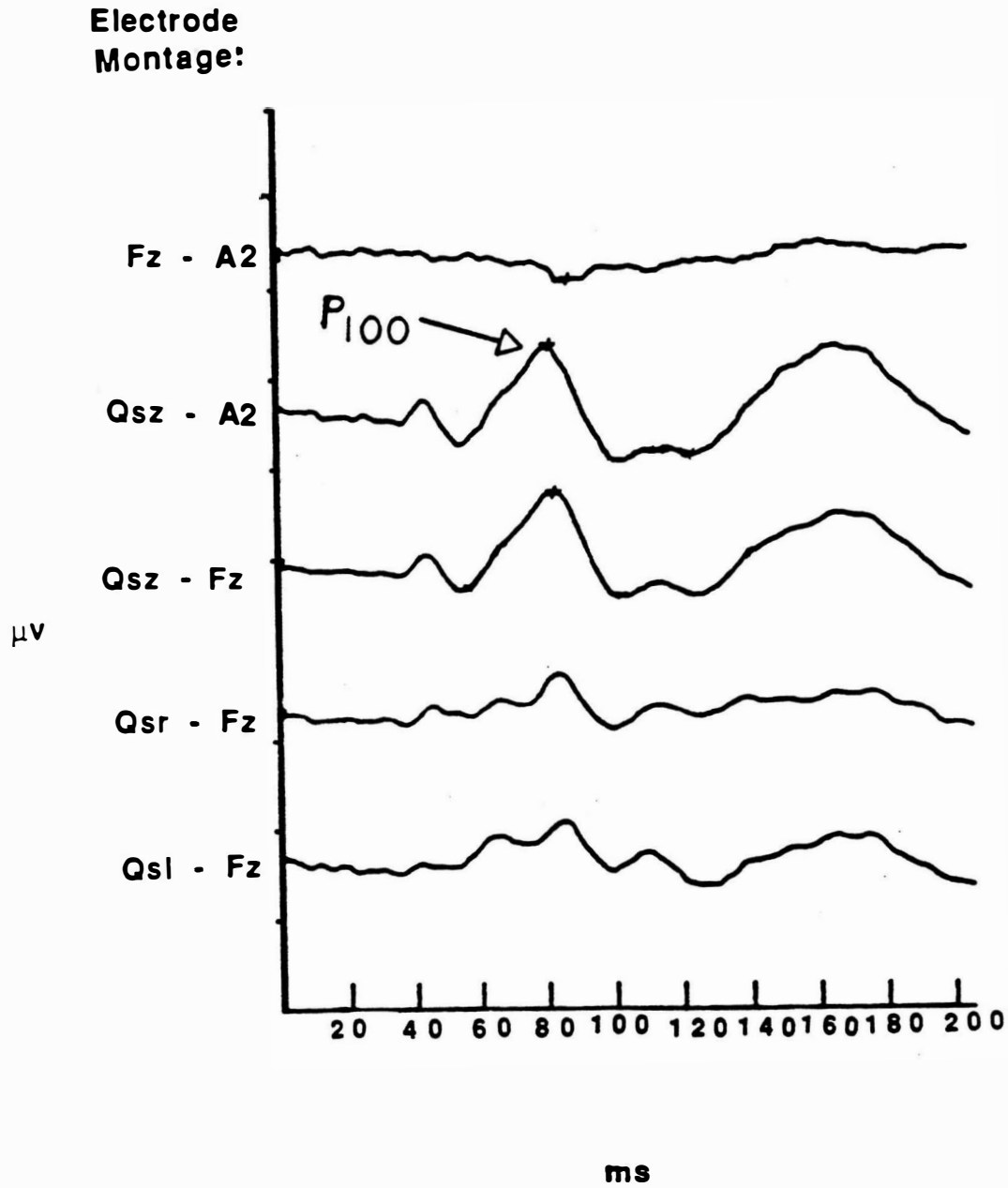

Figure 4 : Conventional Plot of Visual Evoked Potential of Left Eye (OS).

Figure 5 : Plot of visual vector evoked potential. (Vertex View Point). Automatic scaling is used as described in the Methods Section.

A. The entire Vector VEP is shown. The top square is at 75ms, the bottom square is at 100ms. Other markings are used throughout to identify the peaks of activity. Graph is from 0 - 220ms.

B. View of activities prior to the 75ms activity. All times are in ms.

C. Isolated view of activity at 15 and 20ms.

D. Isolated view of activity at 30,40, and 50ms.

E. View of activity at 75 (N70),100 (p100 wave), and 125ms (N125) wave.

F. View of later waves, (activity) at 135, 165, and 210ms.

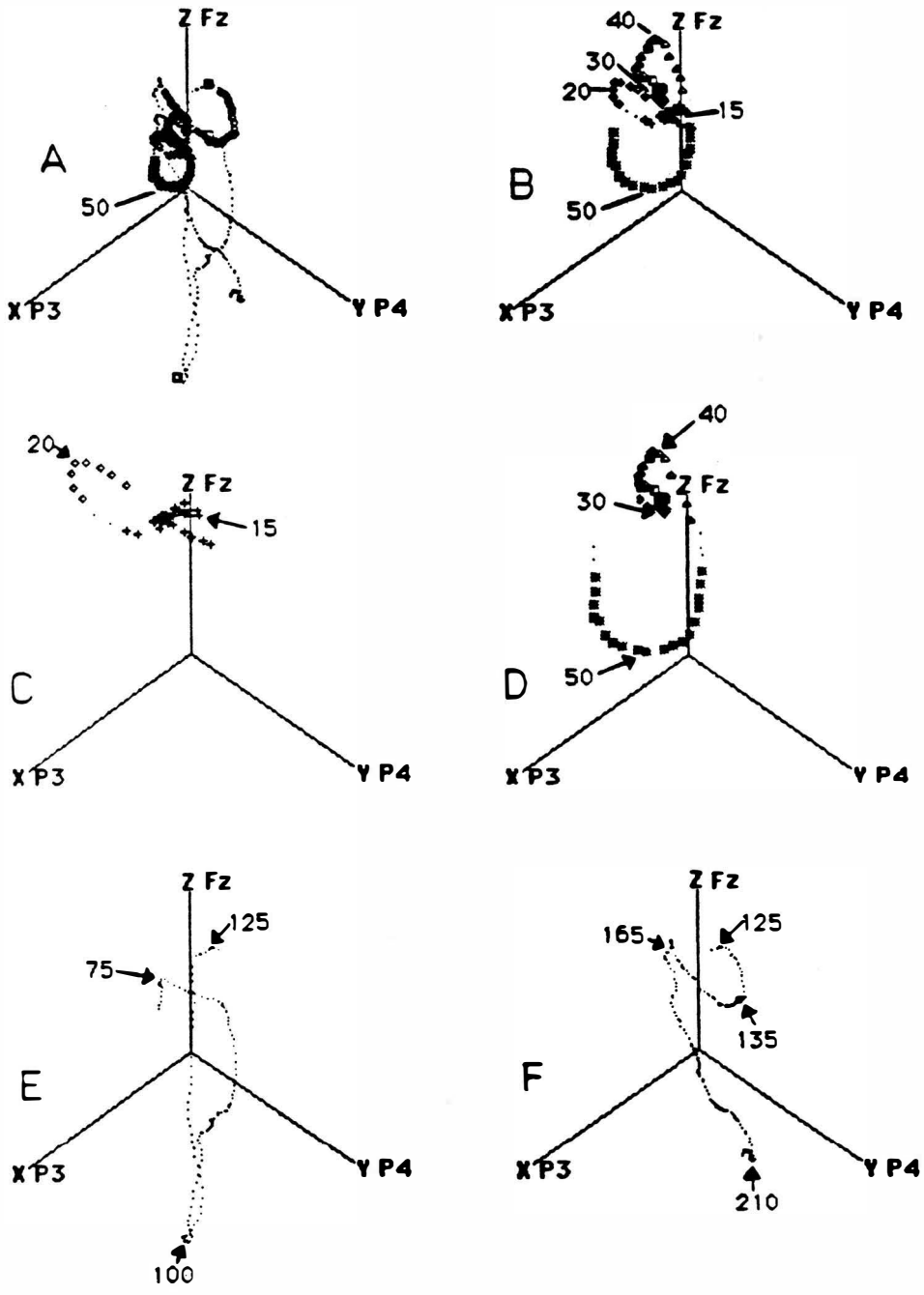

Figure 5 : Plot of Visual Vector Evoked Potential. (Vertex View Point).

Figure 6 : Left and Right Eye Full Field VVEP Progression Plot. A side by side comparison of the left versus right eye full field stimulation evoked potential is shown graphically. (60 min of arc.) The entire progression of activity is shown, broken down into the following segments, with prominent nominal peak latencies labeled.

a. Entire epoch, 0 -250ms, viewed from the side, right eye connected by solid line. View chosen to show superimposable plots.

Figures b-q are vertex views, for a side to side comparison.

b , c.	Left eye,	right eye	respectively : 1-15ms
d , e.	"	"	" : 15-30ms
f , g.	"	"	" : 30-55ms
h , i.	"	"	" : 55-90ms
j , k.	"	"	" : 90-150ms
l , m.	"	"	" : 150-190ms
n , o.	"	"	" : 190-215ms
p , q.	"	"	" : 215-230ms

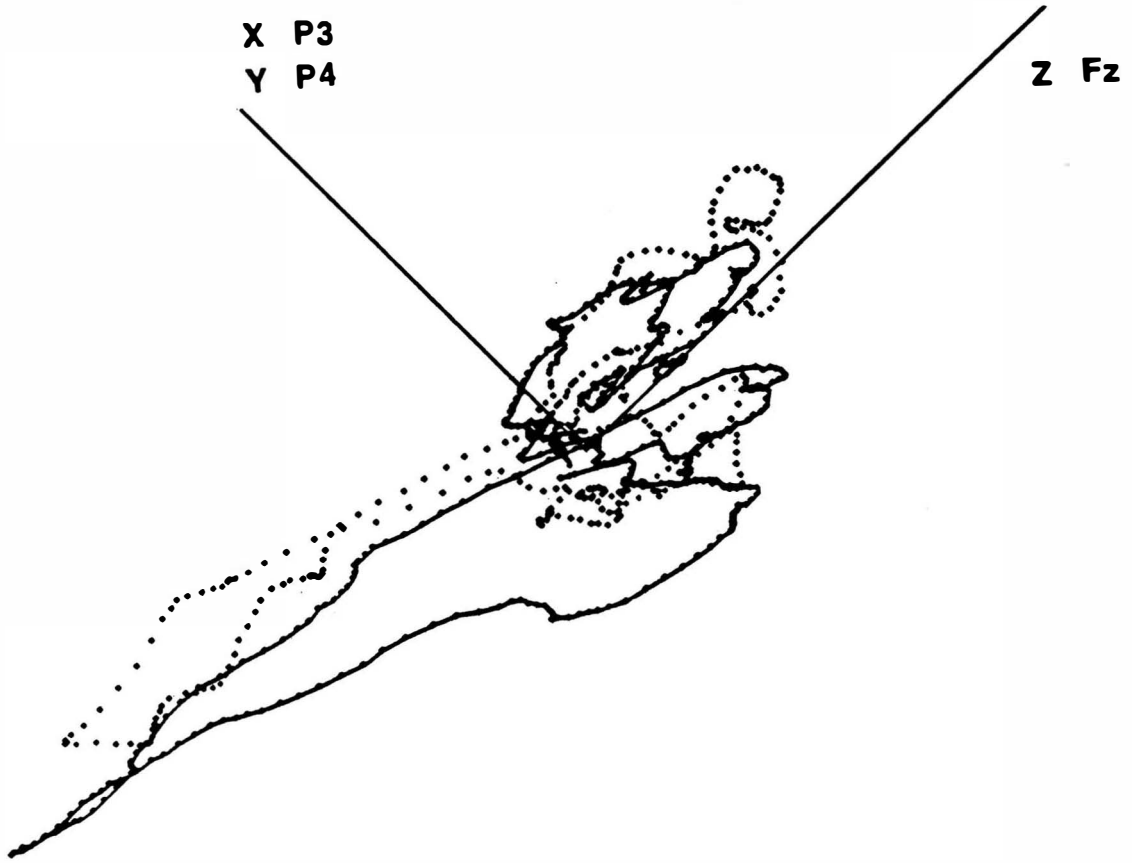

Figure 6 a : Left and Right Eye Full Field VVEP Progression Plot. Right eye connected by solid line.

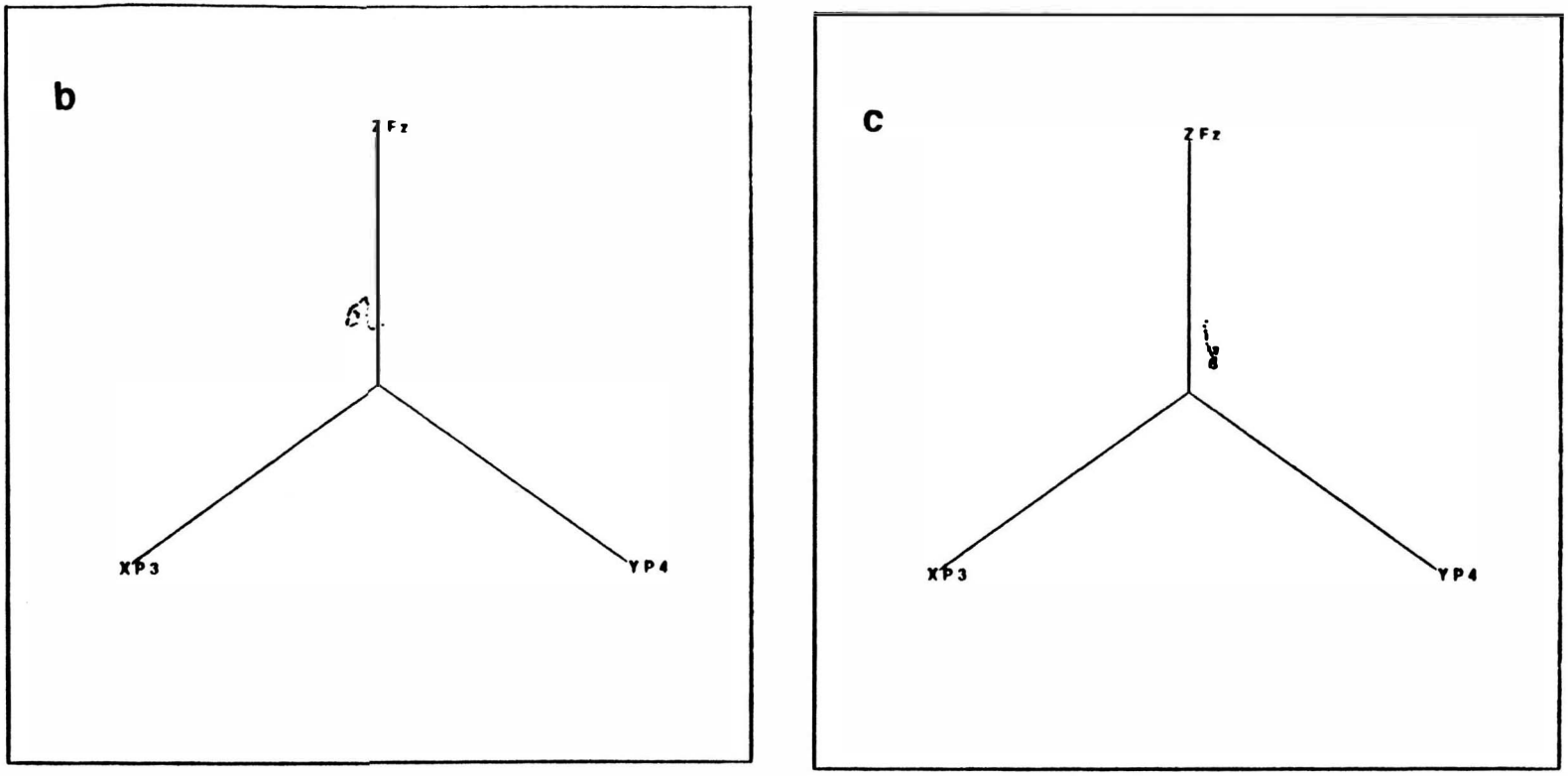

OS OD

1 - 15 ms

Figure 6

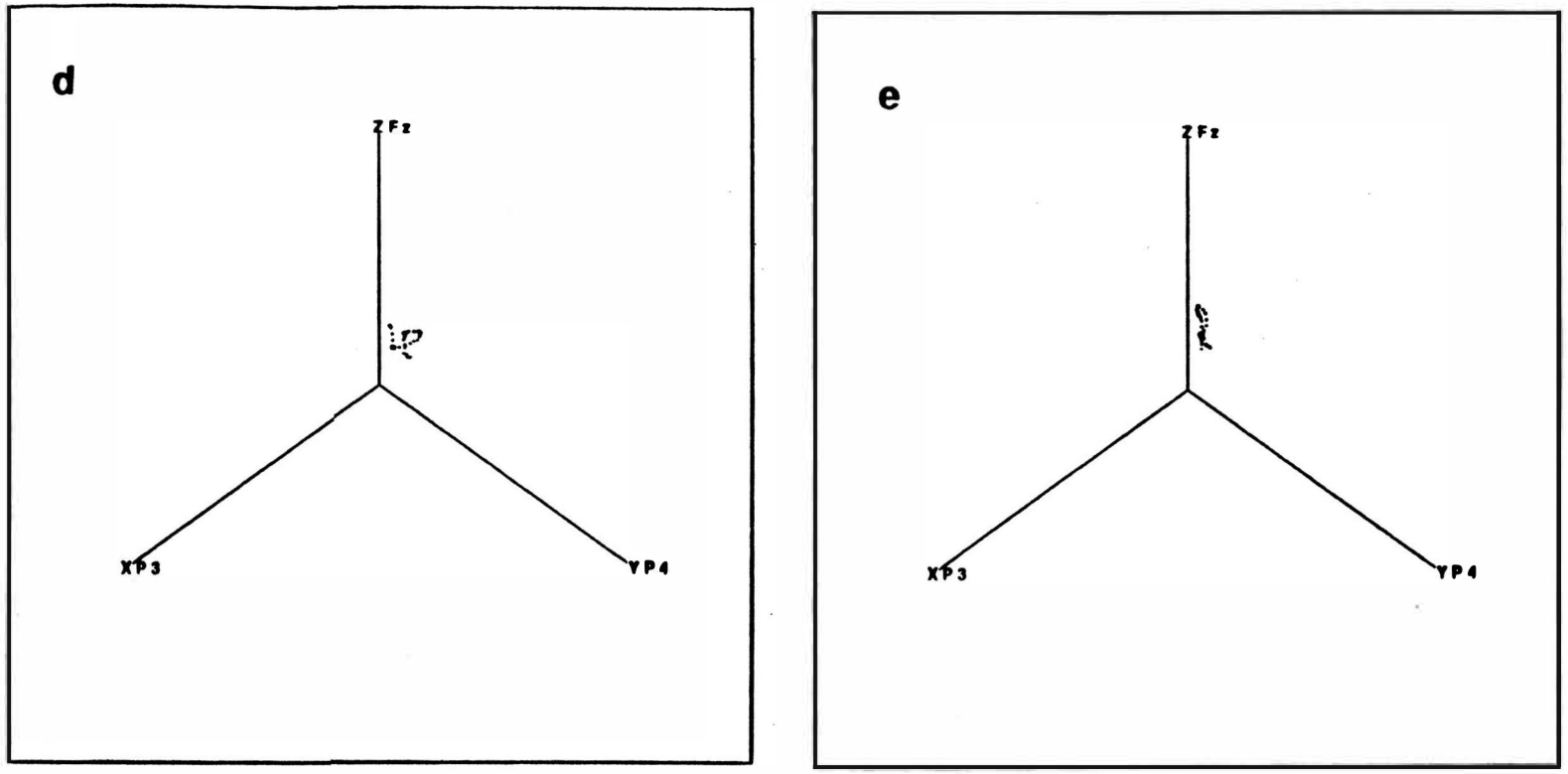

Figure 6

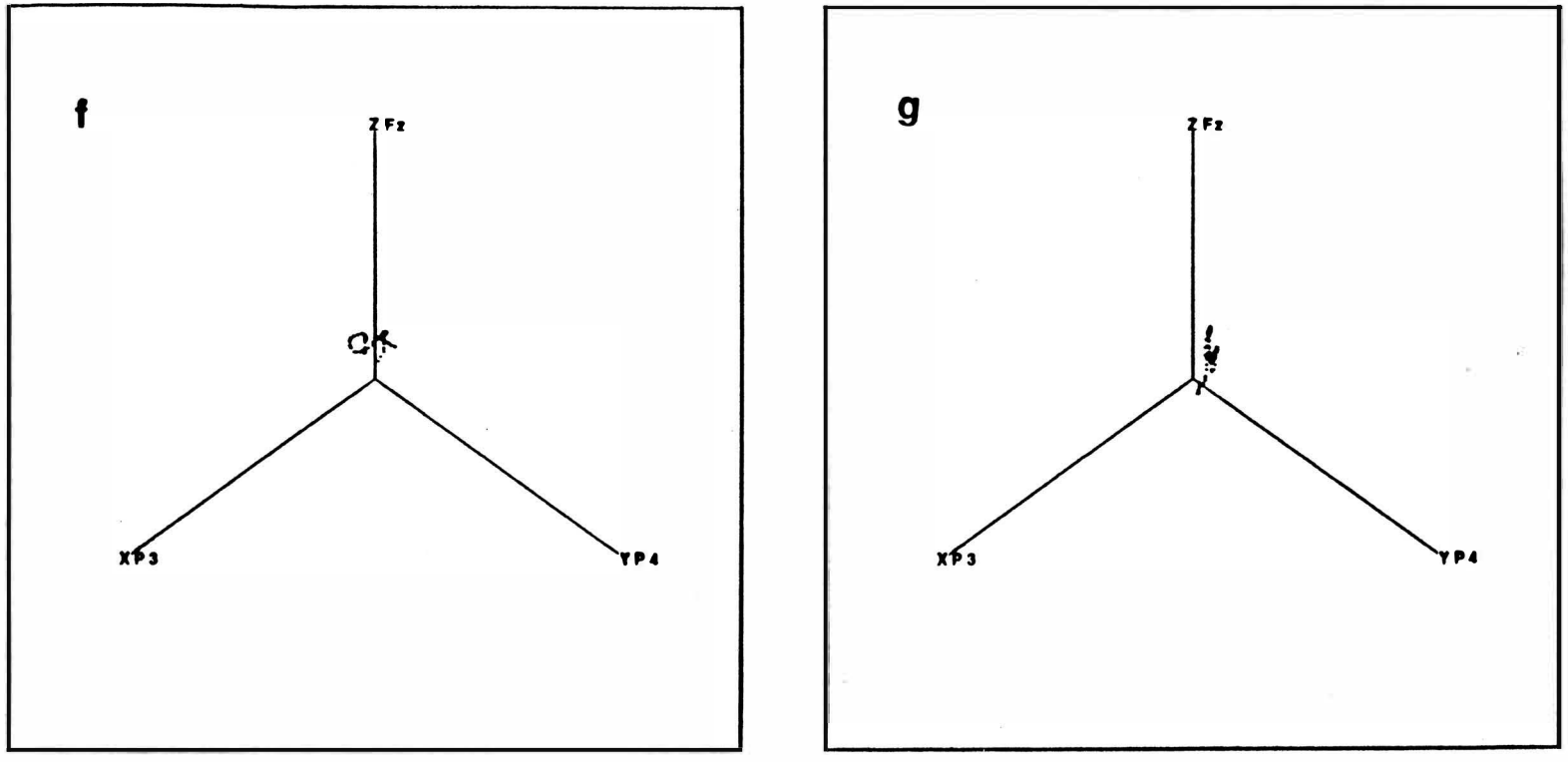

OS

OD

30 - 55 ms

Figure 6

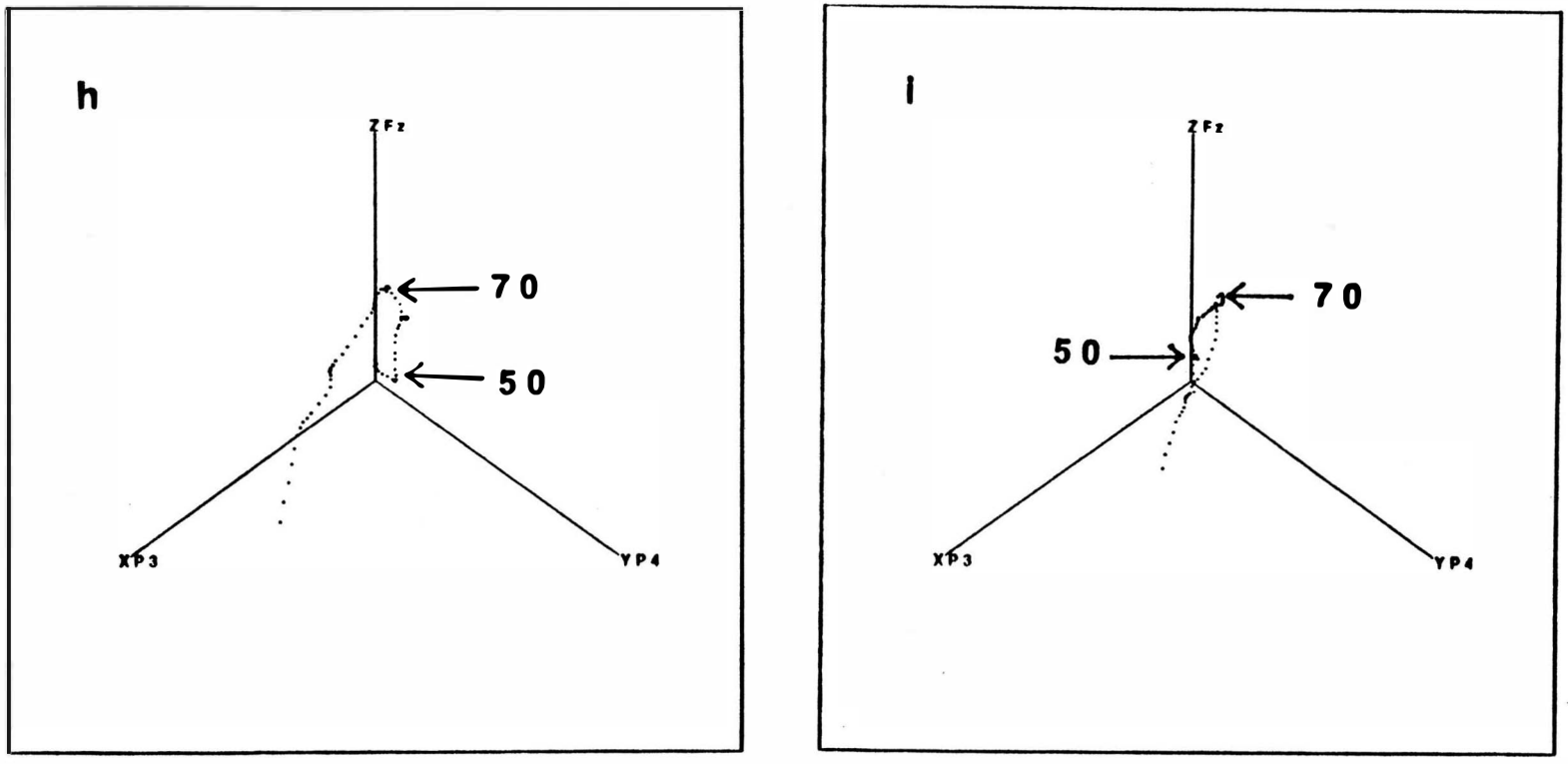

Figure 6

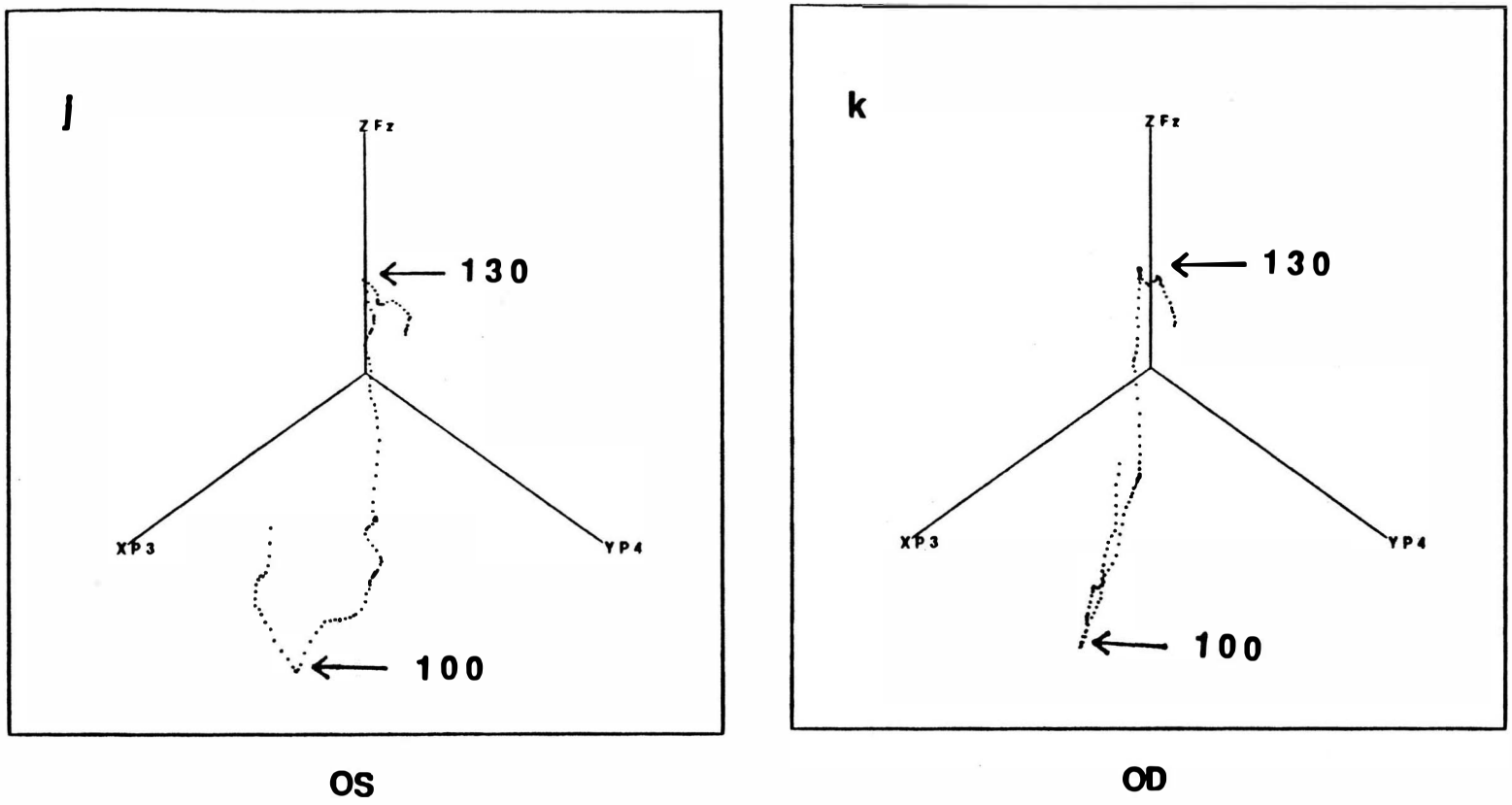

Figure 6

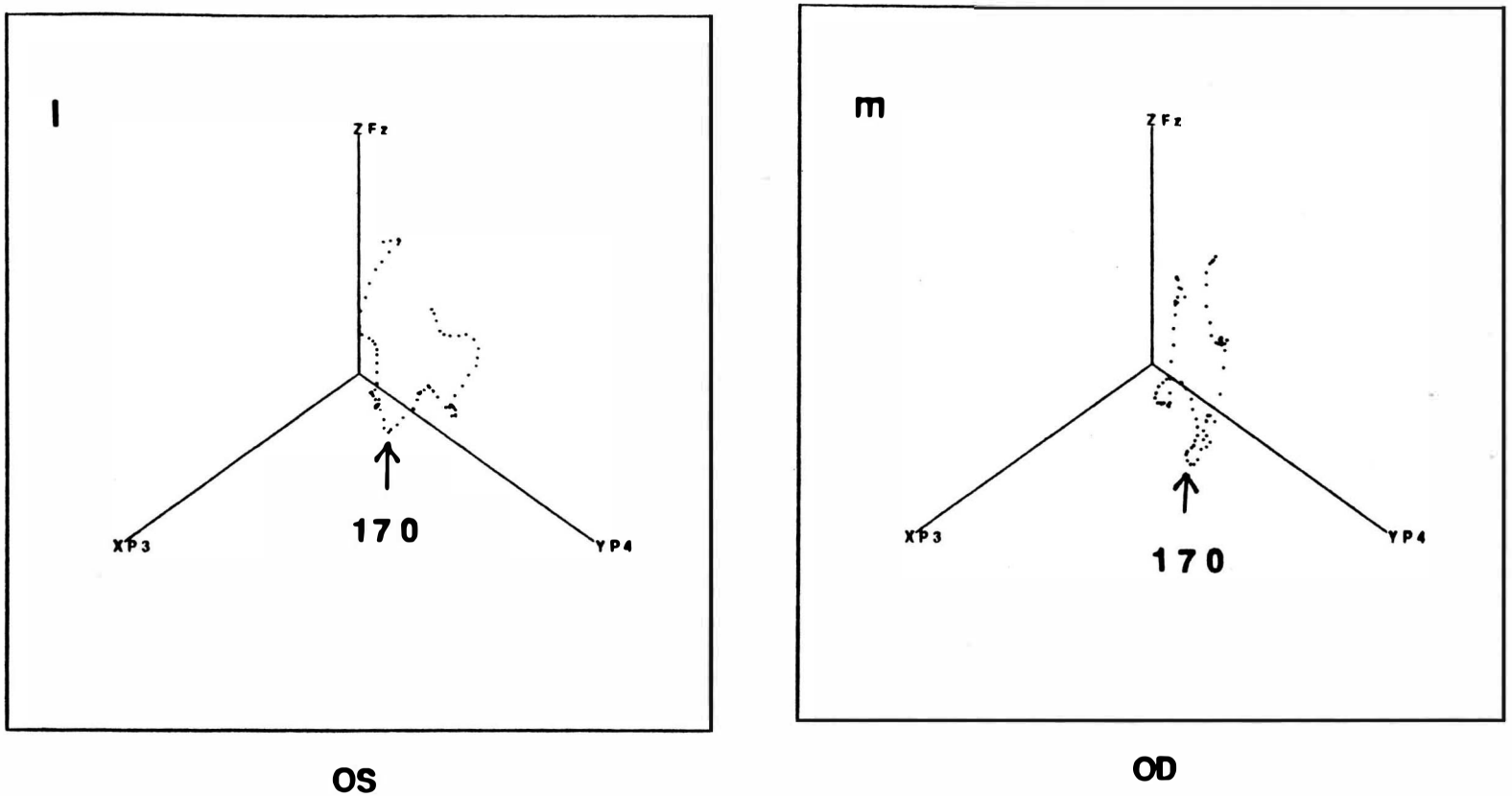

Figure 6

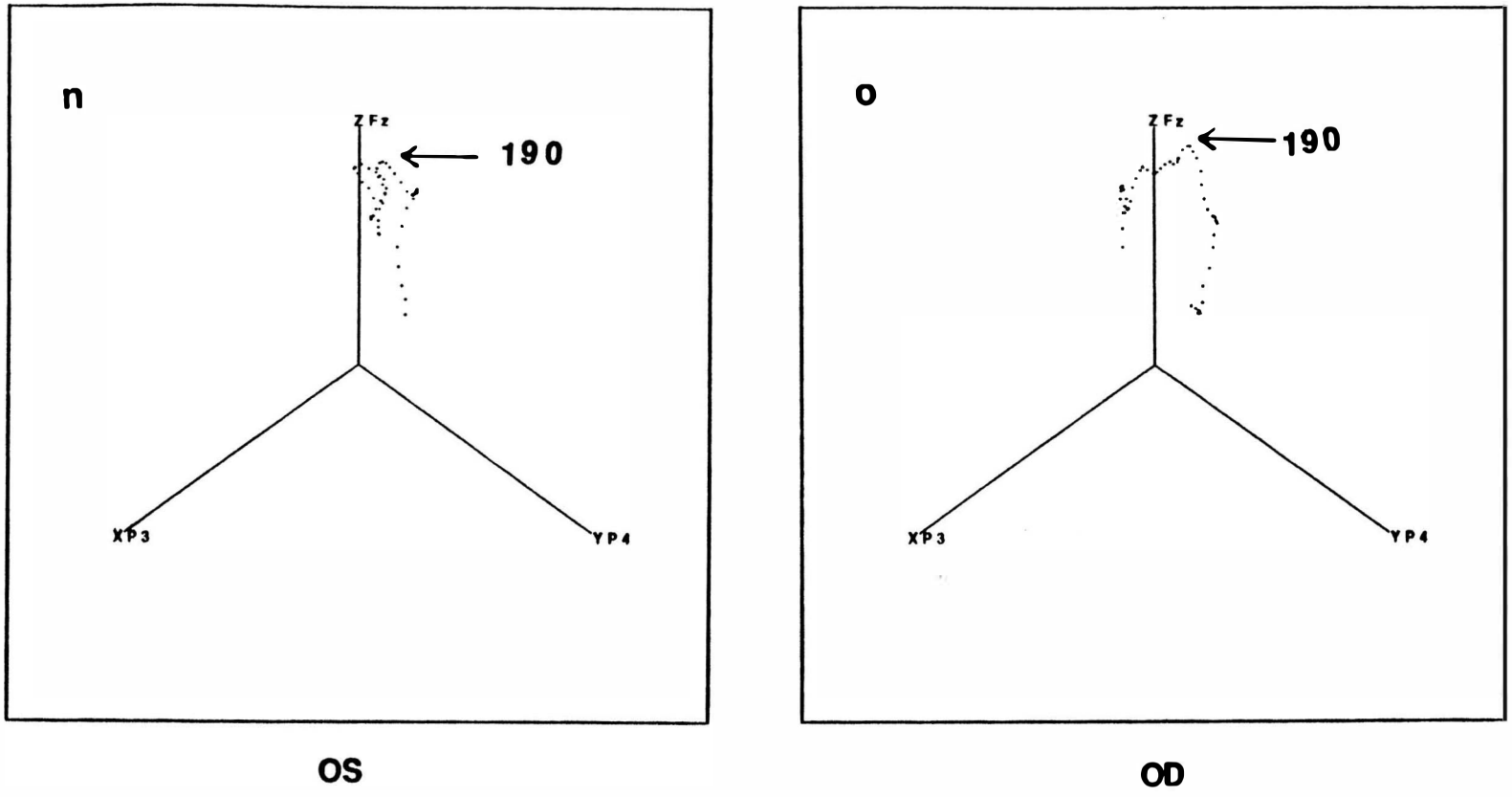

Figure 6

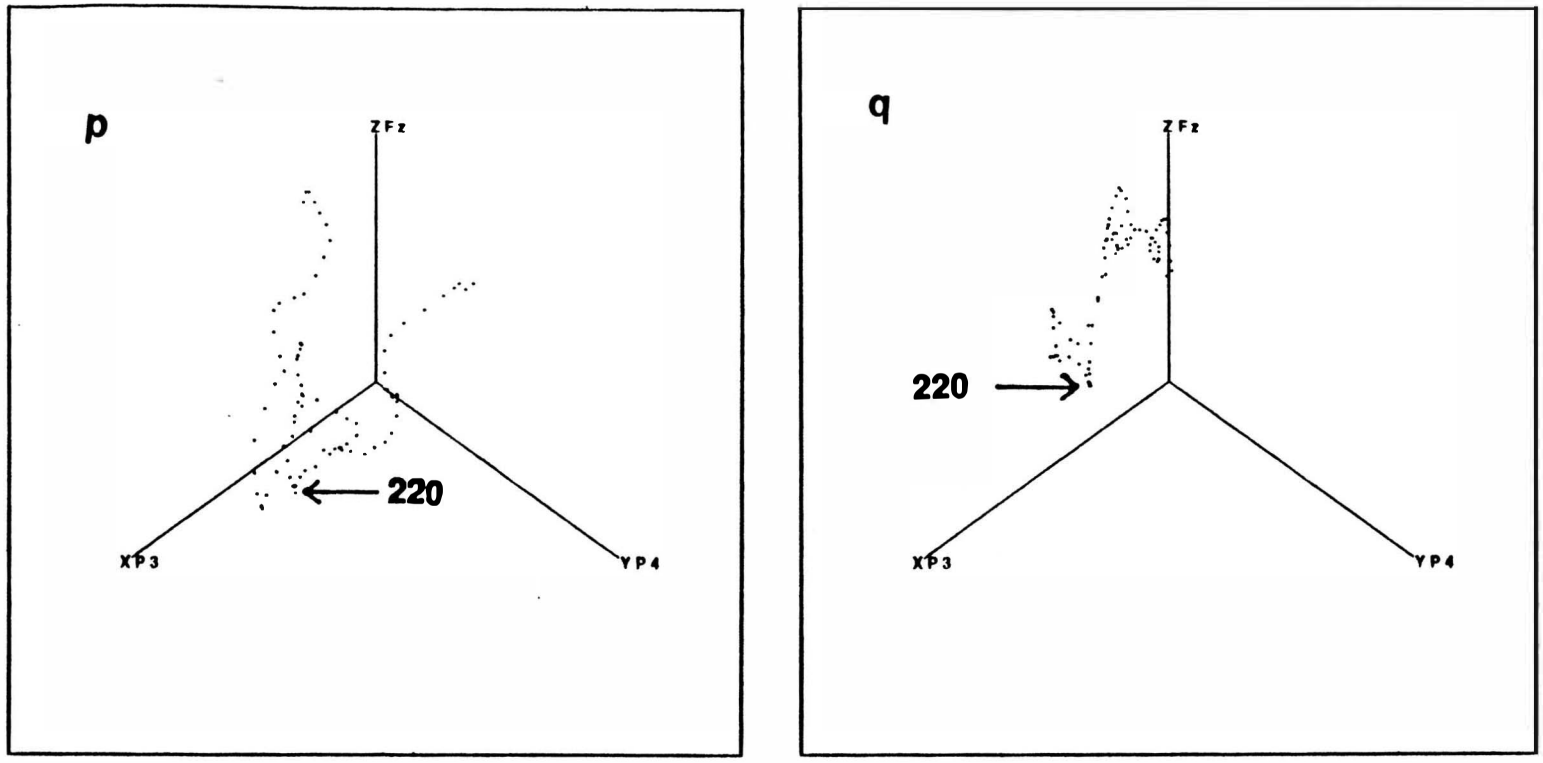

OS OD

210 - 240 ms

Figure 6

Figure 7: Full Field Stimulation Comparison of OS and OD VVEP's. Subject A is vertex view at 30' of arc.

a. Full field 50ms - 250ms, OD connected by solid line.

b , c. 0ms - 40ms, OS, OD, respectively.

d , e. 40ms - 140ms, OS, OD, respectively.

f , g. 140ms - 250ms, OS, OD, respectively.

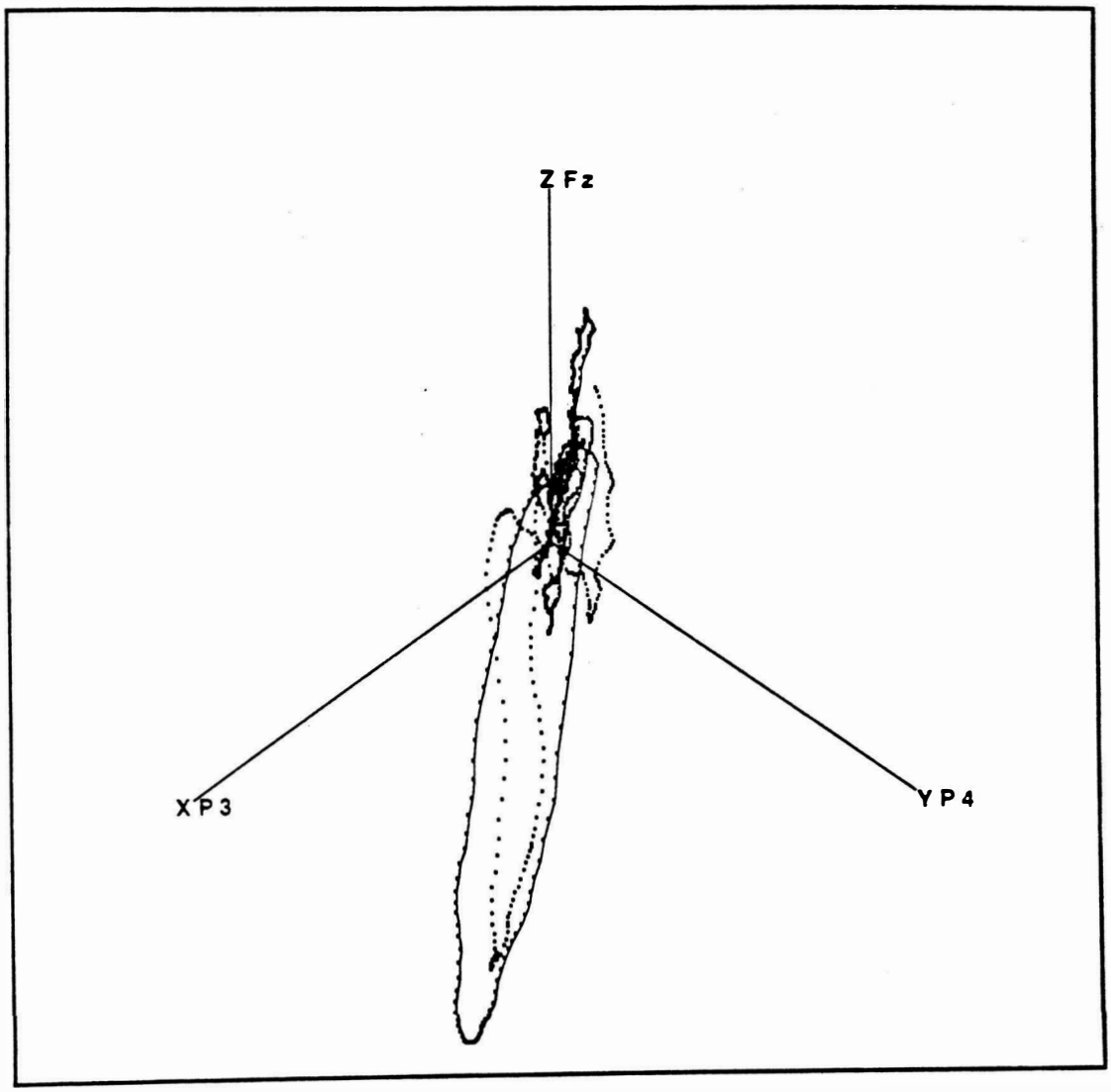

Figure 7a: Full Field Stimulation Comparison of OS and OD VVEP's. (right eye connected by solid line)

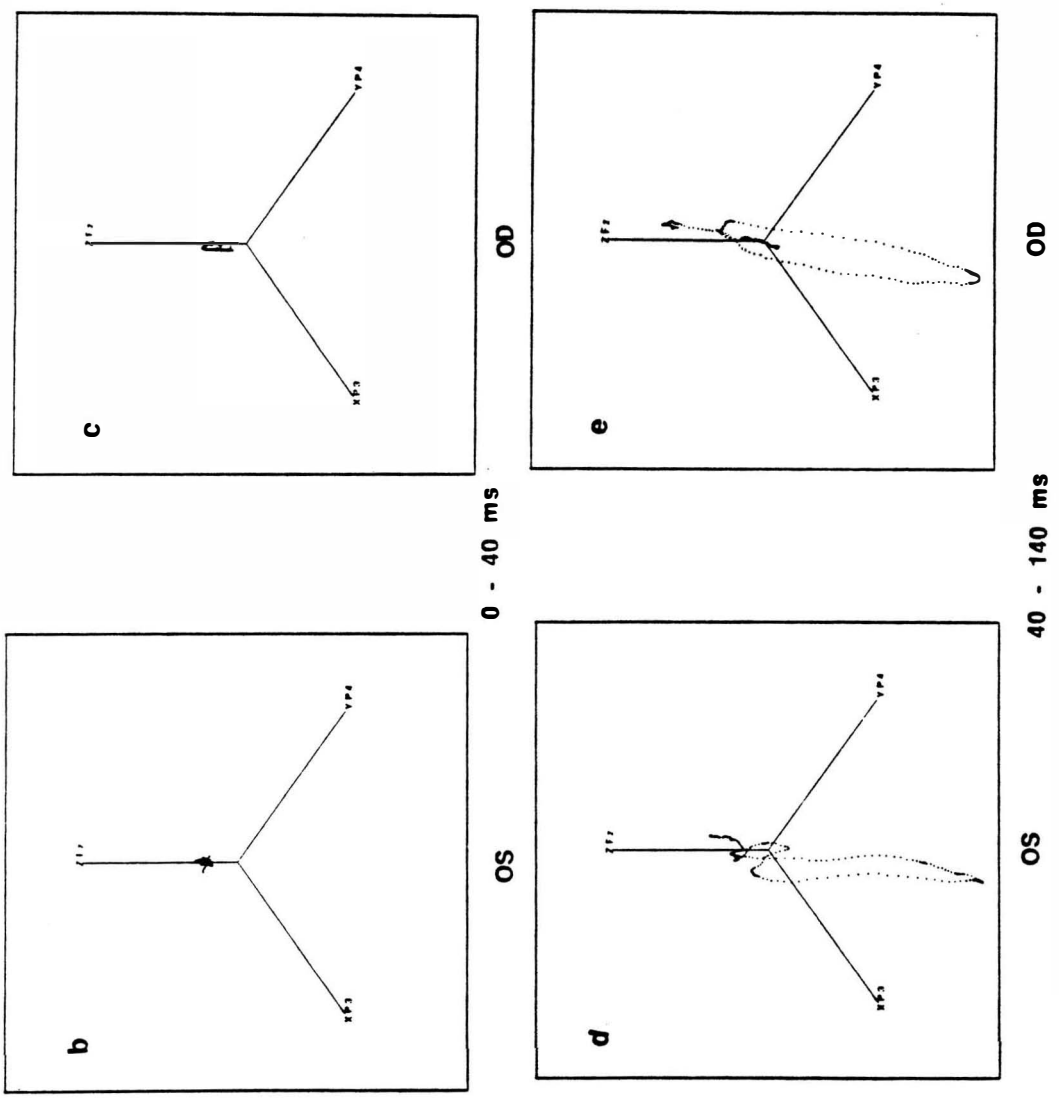

Figure 7

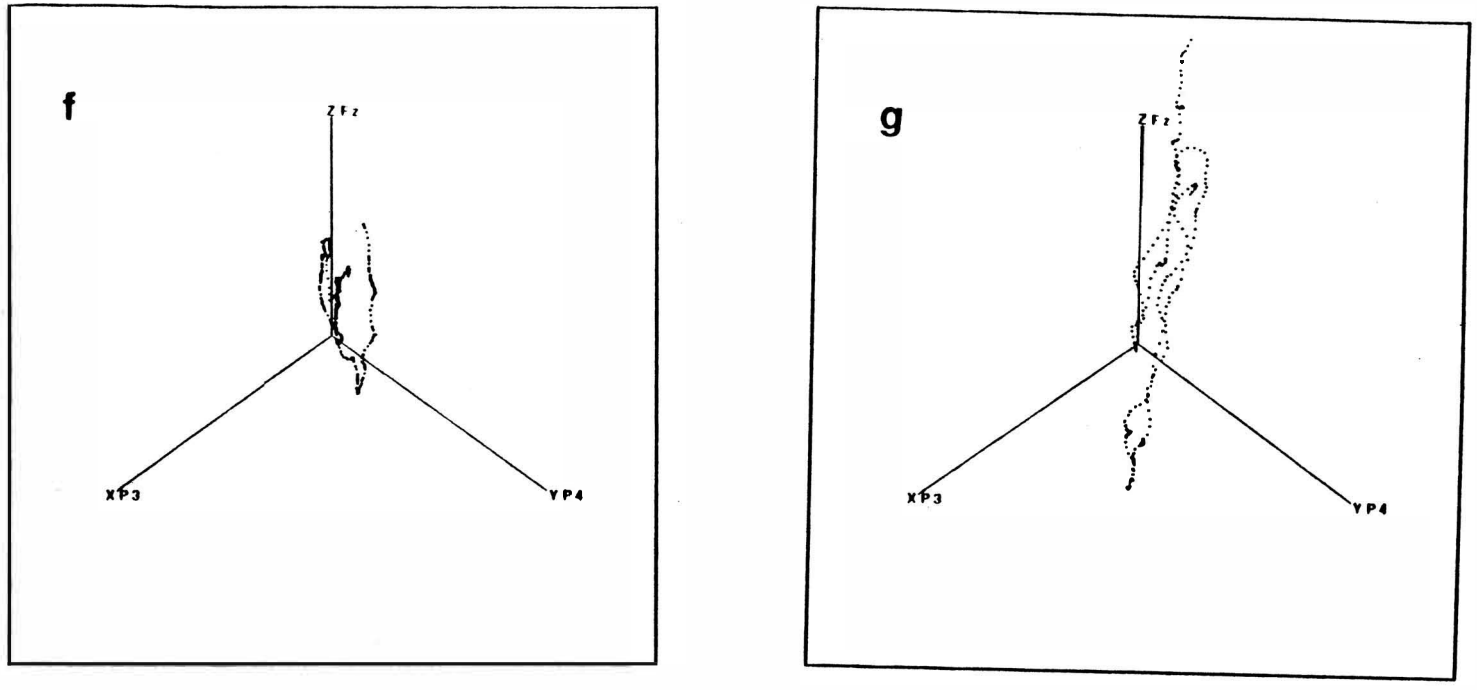

OS

140 - 220 ms

OD

Figure 7

Figure 8: Full Field Stimulation Comparison of OS and OD VVEP's. Subject D is side view at 60' of arc. Lateral views chosen to show similarity (superimposable imagery).

a. Full field 40ms - 250ms, OD connected by solid line. (right lateral view).

b , c. 0ms - 40ms, OS, OD, respectively.

d , e. 40ms - 140ms, OS, OD, respectively.

f , g. 140ms - 250ms, OS, OD, respectively.

(b - g are left lateral views).

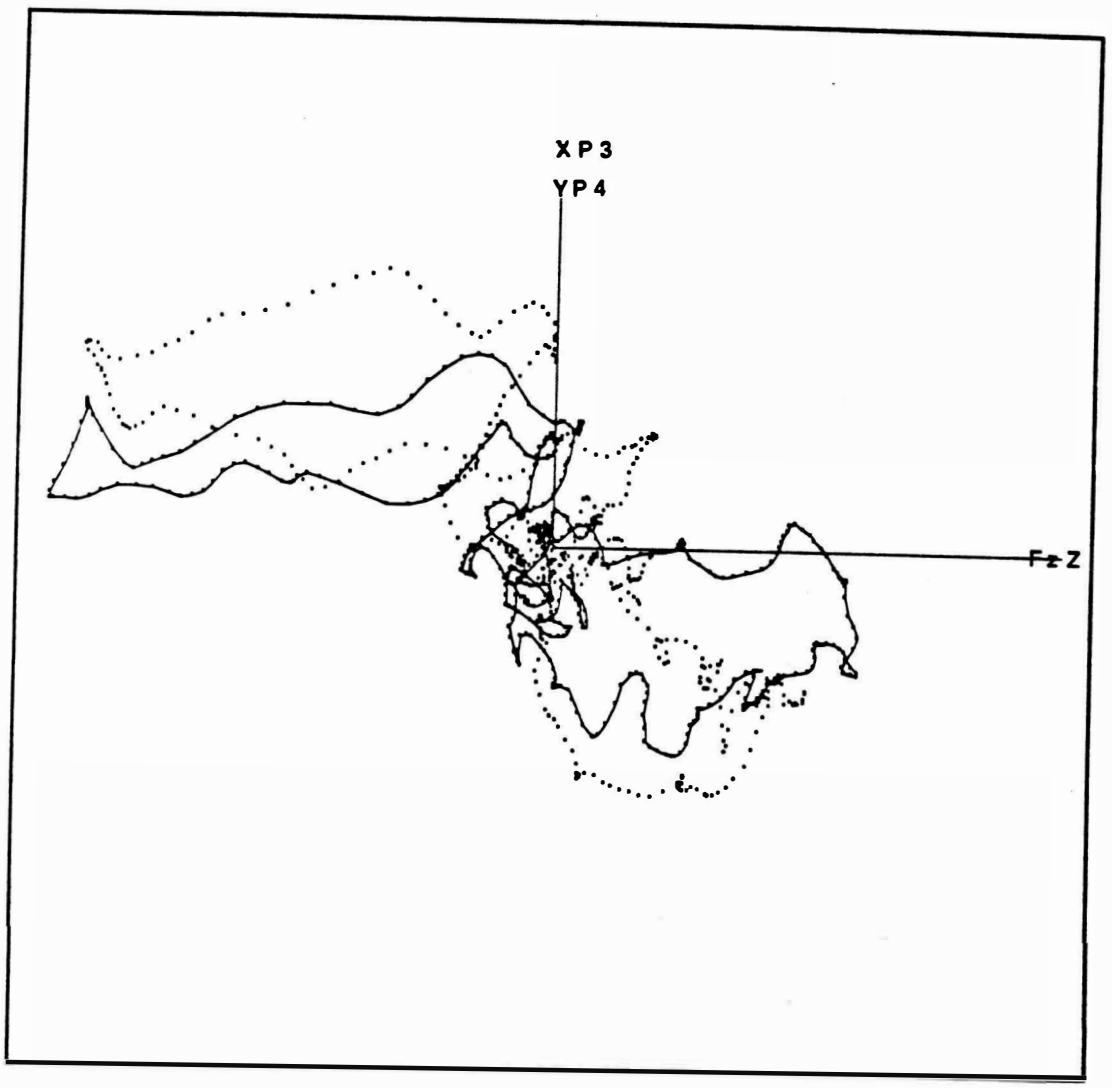

Figure 8a: Full Field Stimulation Comparison of OS and OD VVEP's. (right eye connected by solid line.)

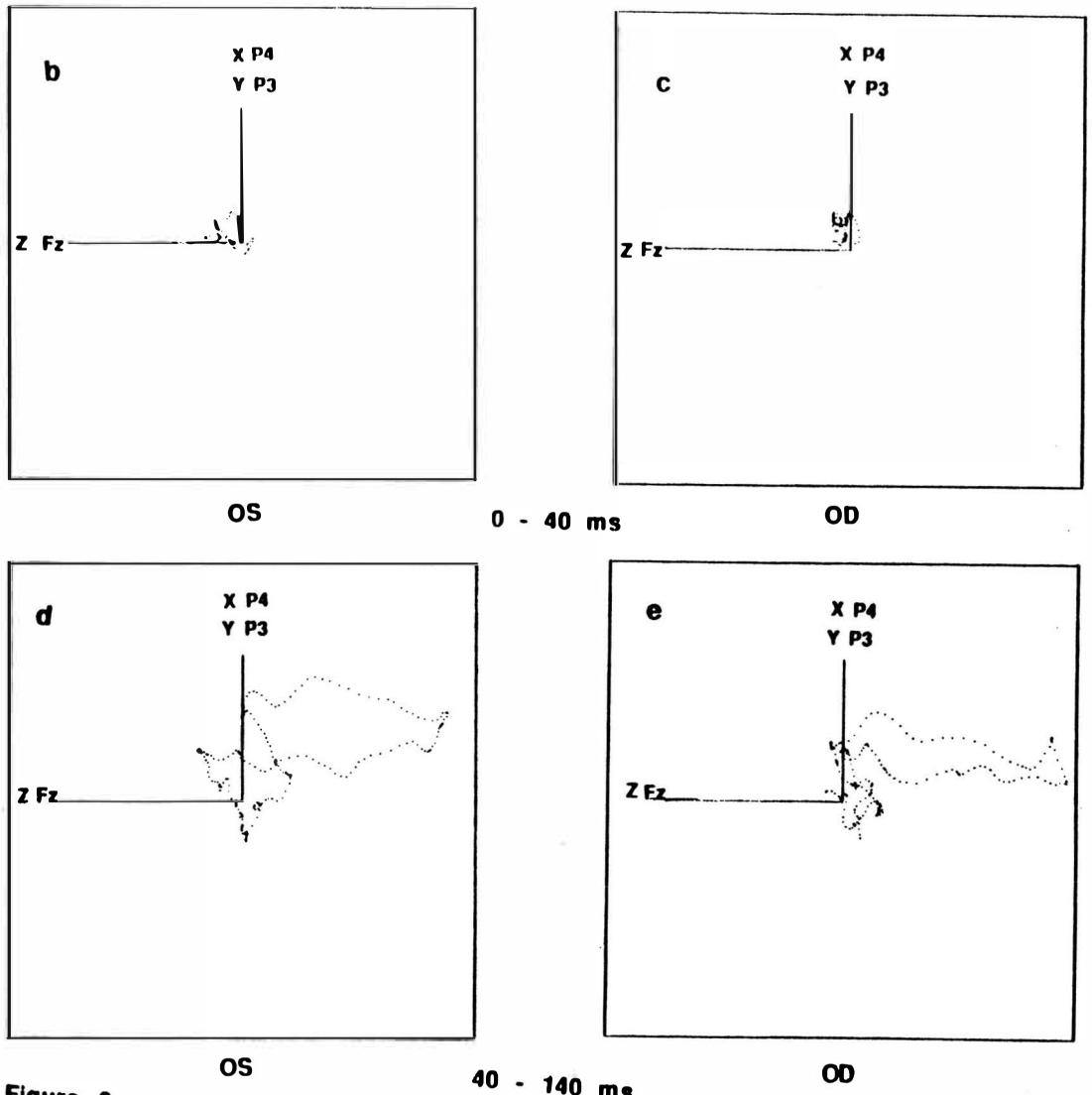
b
X P4
Y P3
Z Fz
OS
c
X P4
Y P3
Z Fz
OD
0 - 40 ms
d
X P4
Y P3
Z Fz
OS
e
X P4
Y P3
Z Fz
OD
40 - 140 ms

Figure 8

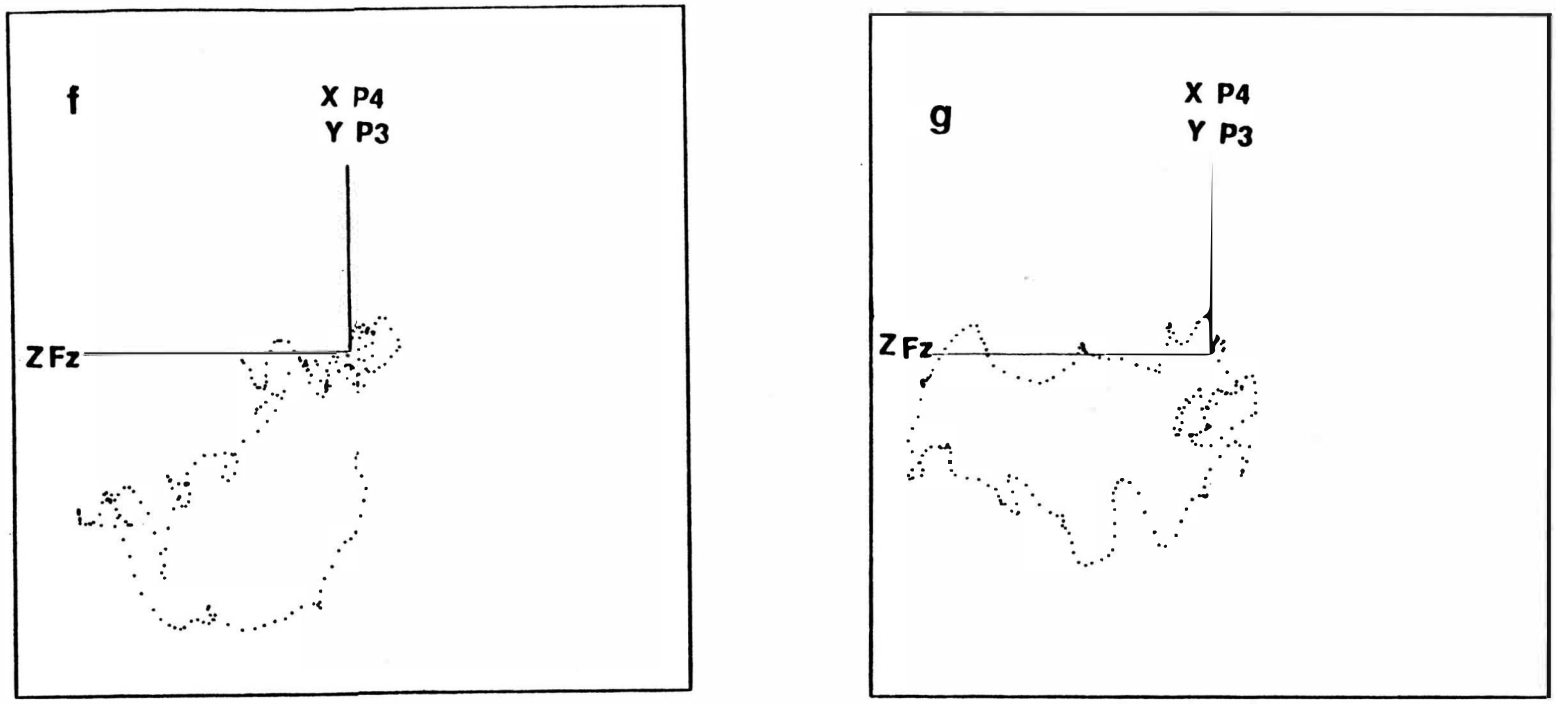

Figure 8

Figure 9: VVEP Hemifield Graph of OD Temporal and OS Nasal Retina Stimulation in Subject C. These graphs show the time sequence from approximately 45ms to 175ms. The reproducibility of similar figures from anatomically overlapping hemi-fields from each eye emphasizes the power of the vector method. The nominal peak times are labeled. An in-depth view and discussion of hemi-fields is found later in the text.

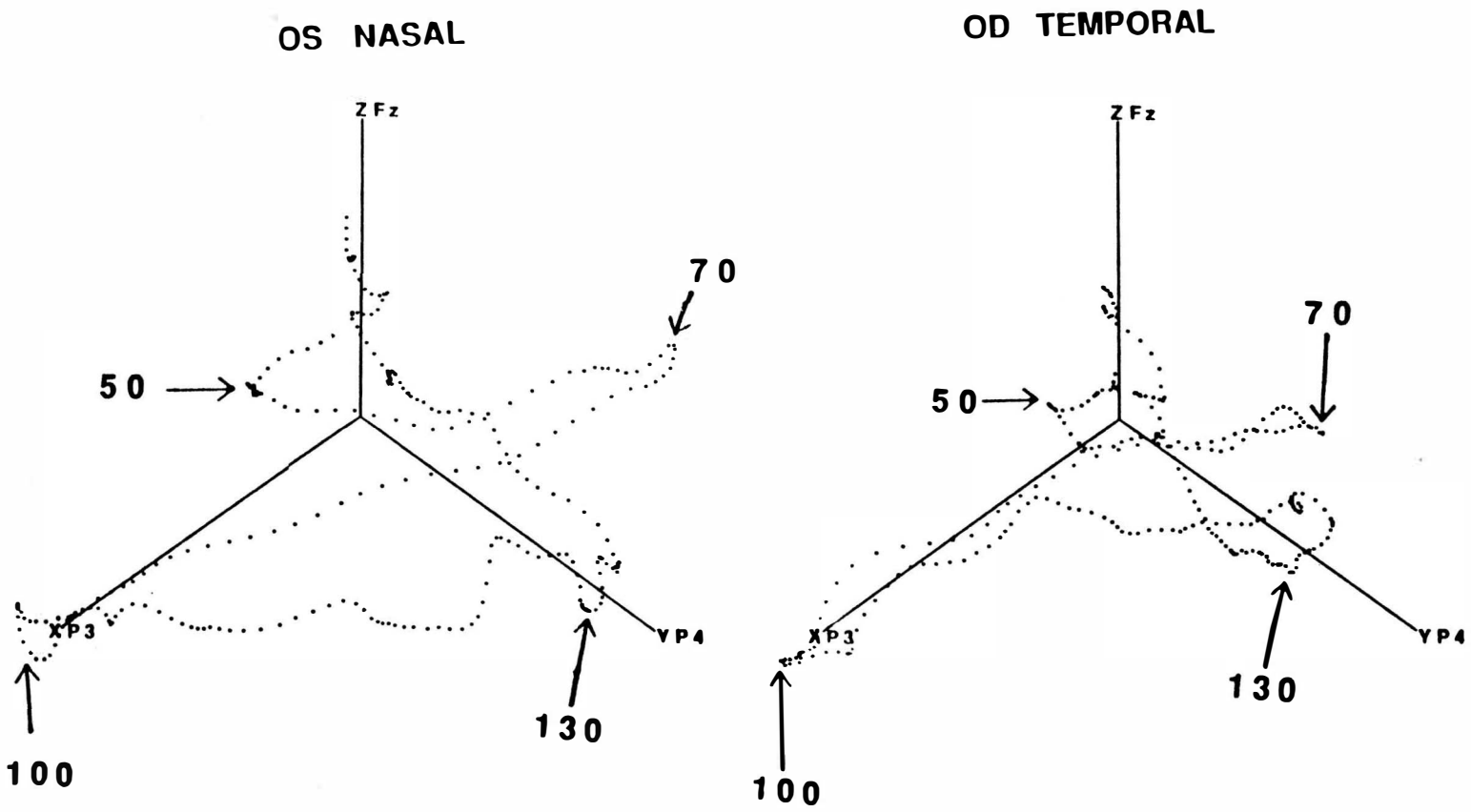

Figure 9 : VVEP Hemifield Graph of OD Temporal and OS Nasal Retina Stimulaltion in Subject C.

Figure 10 : A 0ms - 58ms Epoch of a Left and Right Full Field VVEP at 60 min of Arc, in Subject G, Compared to the VVEP Generated by a "Closed Door" (null) Study in Subject H. The time prior to 50ms, although suggested to be pre-retinal, in this thesis can still show symmetry. **a.** Normal full field study shows far less noise than a "closed door" study. Arrows mark a presumed PERG wave occurring at 51ms at this view point. **b.** "Closed door" noise at the same magnification as a., in which b. has a point included equivalent to the magnitude of a "P100" point to adjust for the automatic scaling, as previously described, as is in a. **c.** is a full scale (enlarged) view of b. The randomness of figure b. and c. become apparent, while a. appears too ordered and too similar in the left and right eyes to be considered random noise.

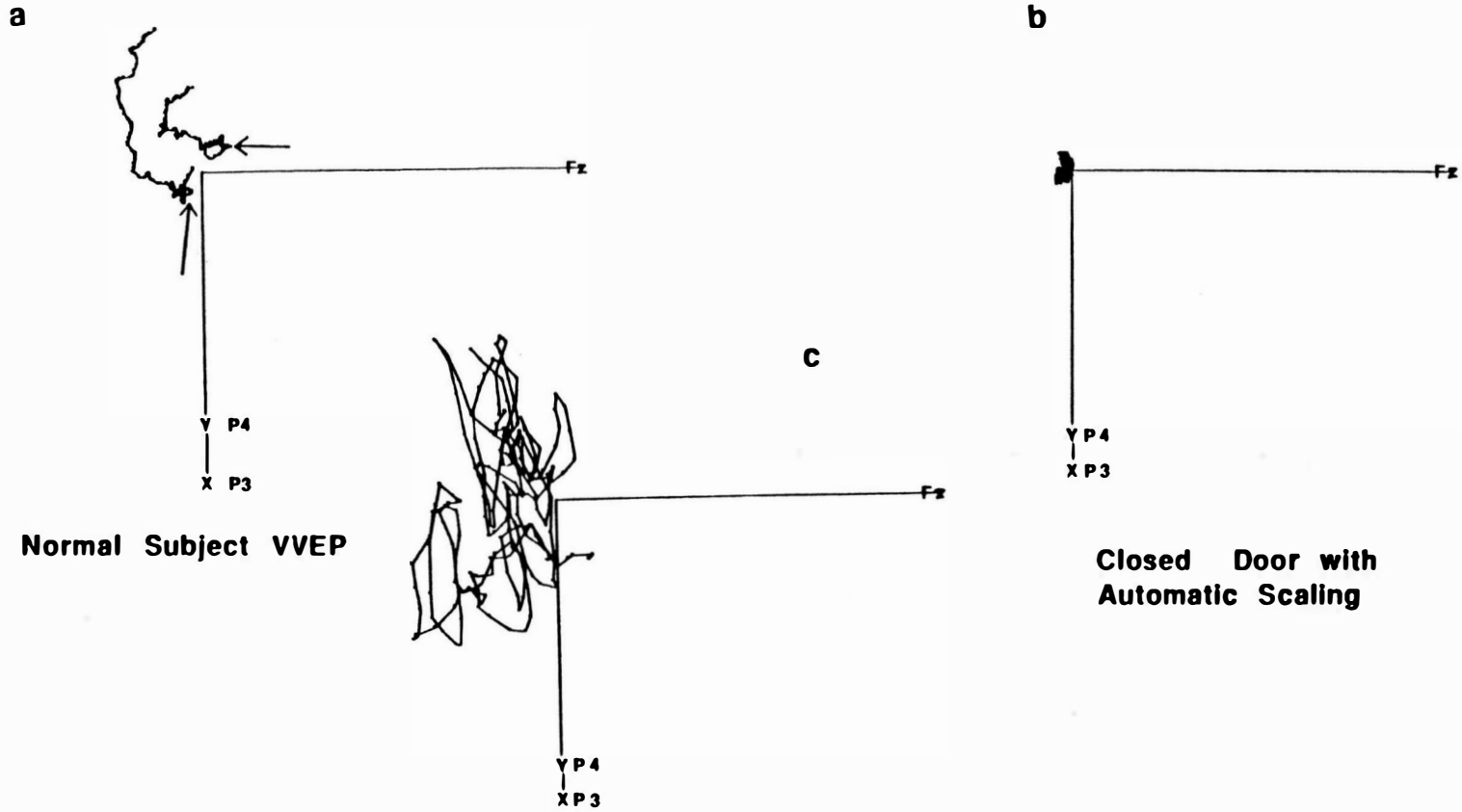

Figure 10 : A 0ms - 58ms Epoch of a Left and Right Full Field VVEP at 60 min of Arc, in Subject G, Compared to the VVEP Generated by a "Closed Door" (null) Study in Subject H.

Figure 11 : Graphic Comparisons of the Same Visual Field (ODn) at Separate Test Times. Subject H was tested five hours apart, time epoch is 51ms-178ms. The nominal P50, N70, and P100 peaks are labeled.

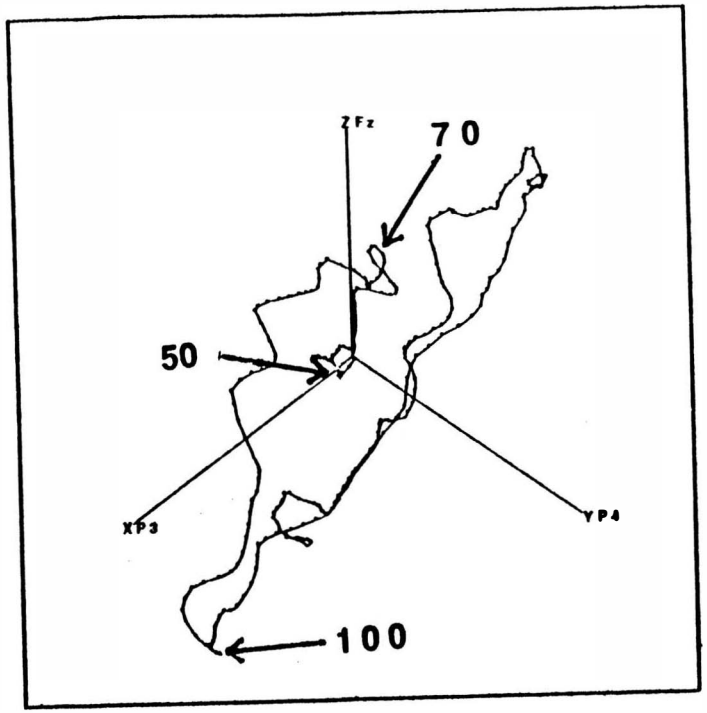

ODn

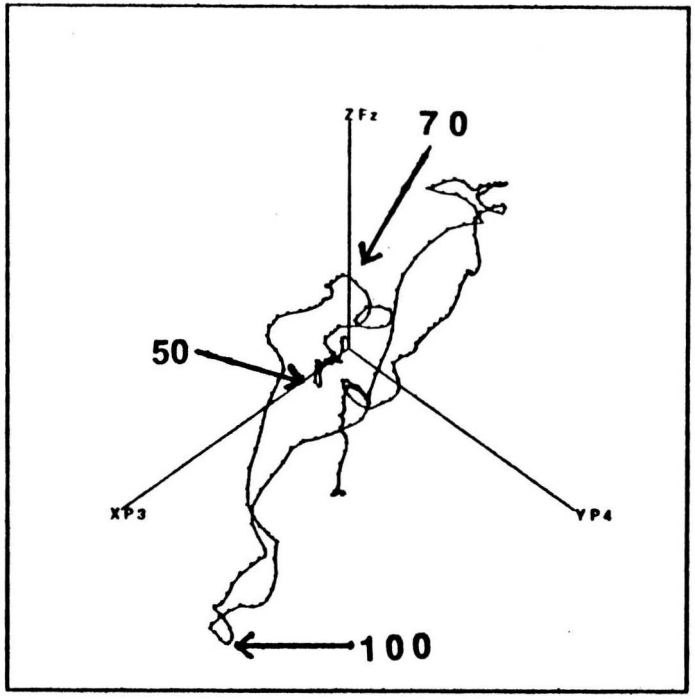

ODn

Figure 11 : Graphic Comparisons of the Same Visual Field (ODn) at Separate Test Times.

Figure 12 A-L : Graphic Comparison of Given Time Segments of the VVEP's of the Four Hemi-fields in Subject E. The top figures are OSn and OSt (left to right), while the bottom figures are ODt and ODn (left to right). Figures are shown in vertex view, with corresponding times given and nominal peak latencies identified.

A : The full epoch for each of the hemi-fields.

B, C, D, E, F: Early Waves. There is little exact symmetry, however equal number of changes often occur, with the activity too ordered to be explained by noise.

G: Formation of peak at 50ms and peak at 70ms

H, I: Peaks are seen at 90ms and 130ms.

J, K, L: Reduced symmetry of later activity is seen.

Note that from G on, there is striking symmetry with the left nasal and right temporal VVEP being very similar while they are almost mirror images to the left temporal and right nasal VVEP which in themselves are very similar.

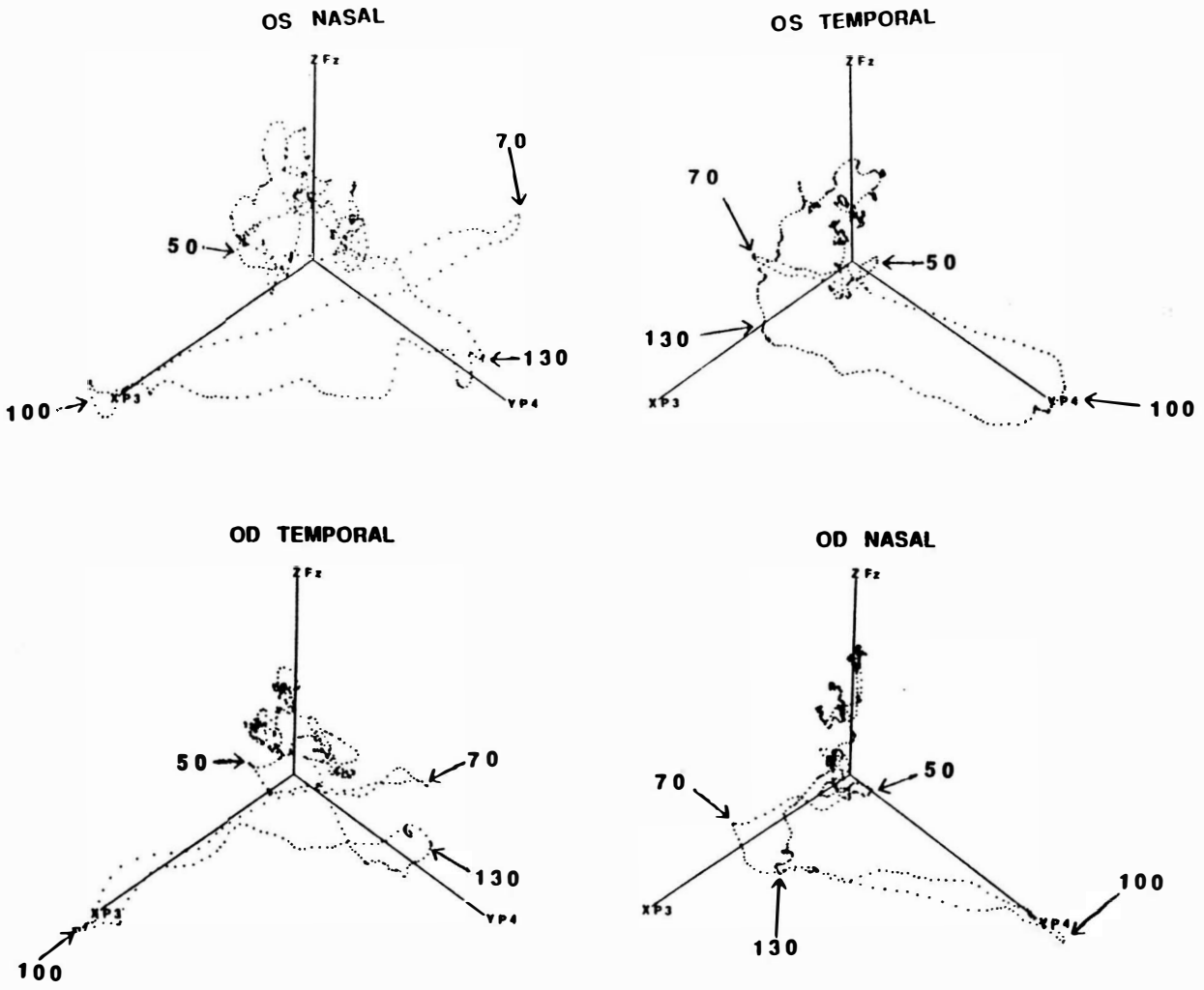

Figure 12 A : Graphic Comparison of Given Time Segments of the VVEP's of the Four Hemi-fields in Subject E.

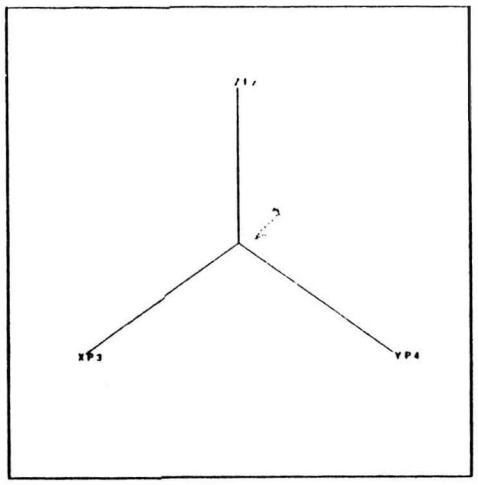

OSn

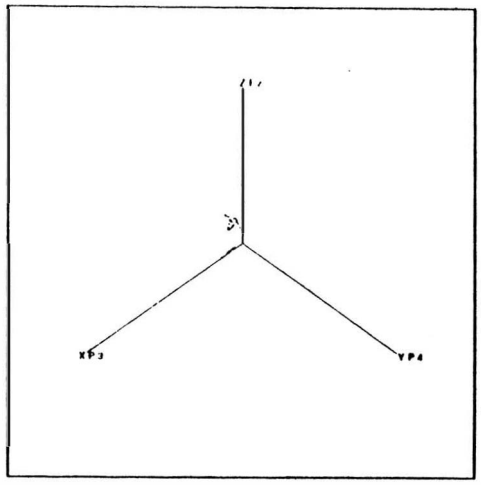

OSt

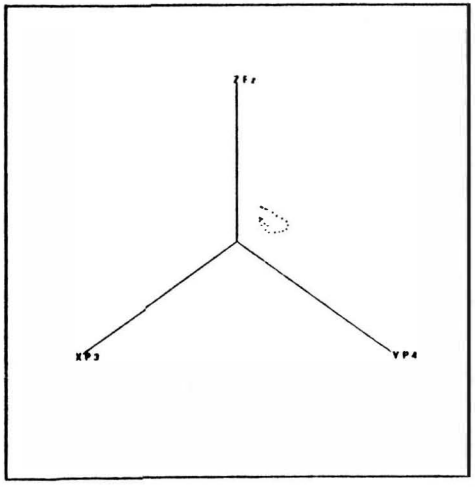

ODt

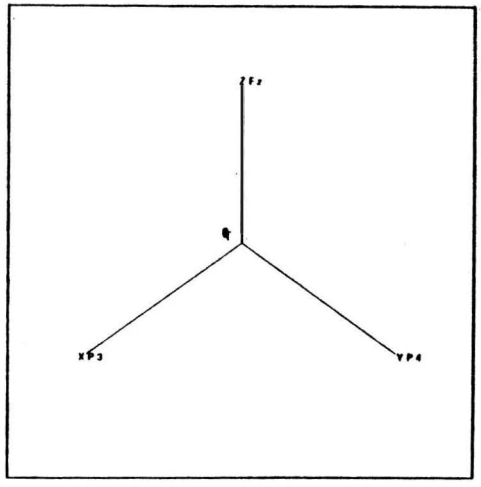

ODn

Figure 12 B 0 - 10 ms

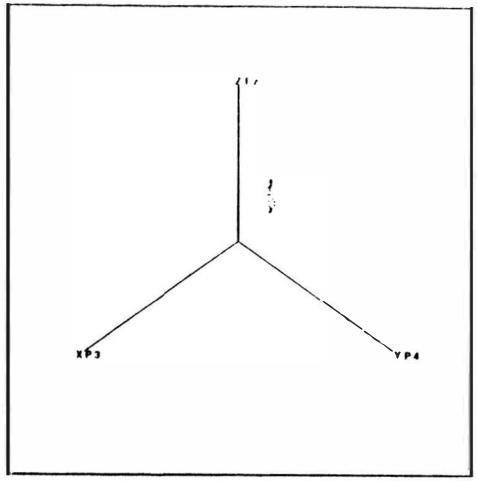

OSn

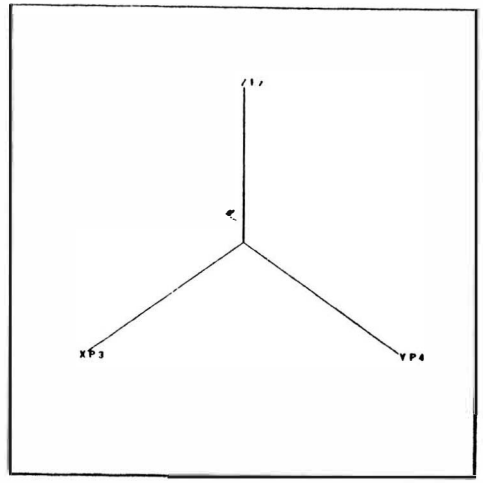

OSt

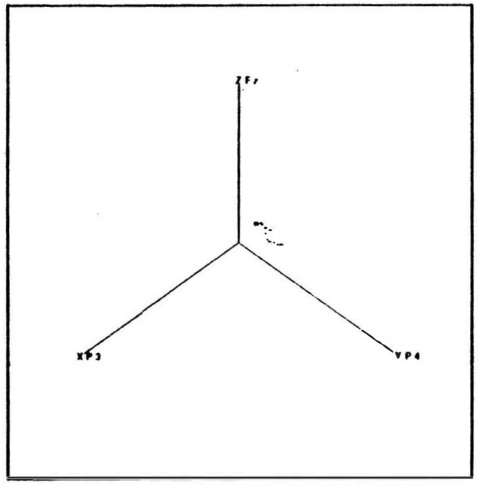

ODt

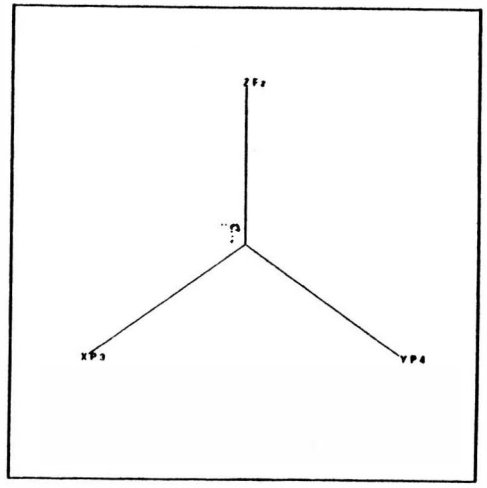

ODn

Figure 12 C 10 - 20ms

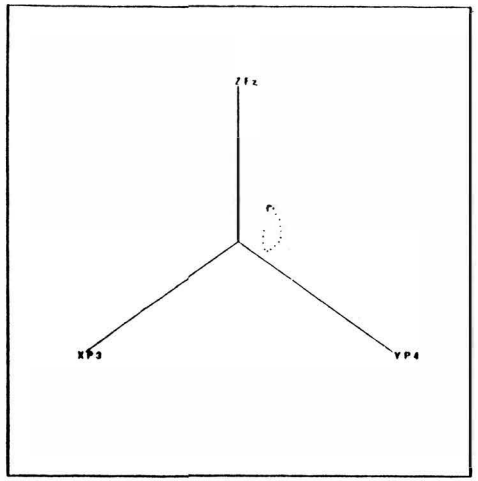

OSn

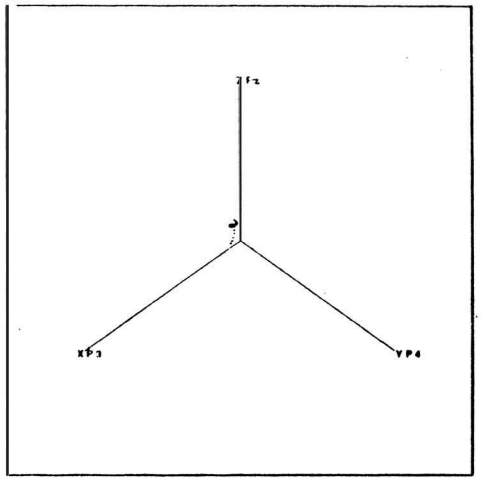

OSt

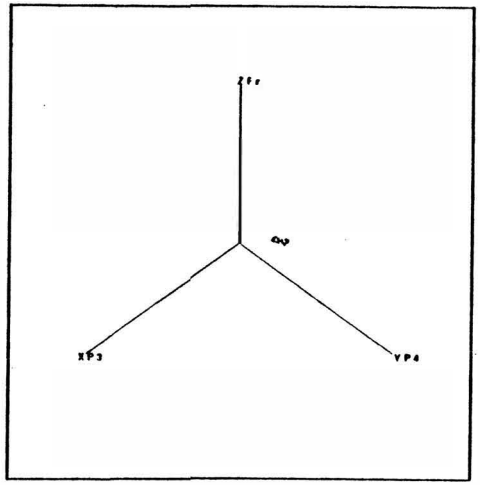

ODt

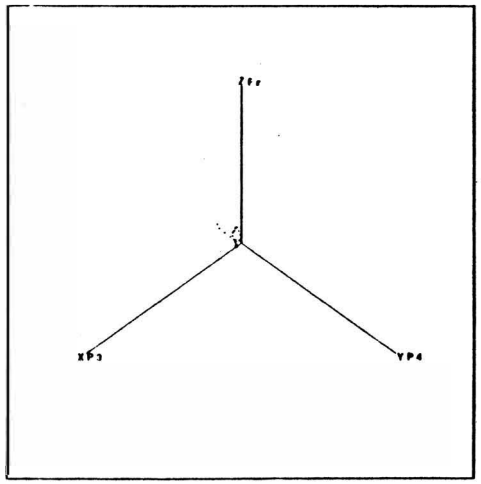

ODn

Figure 12 D 20 - 30ms

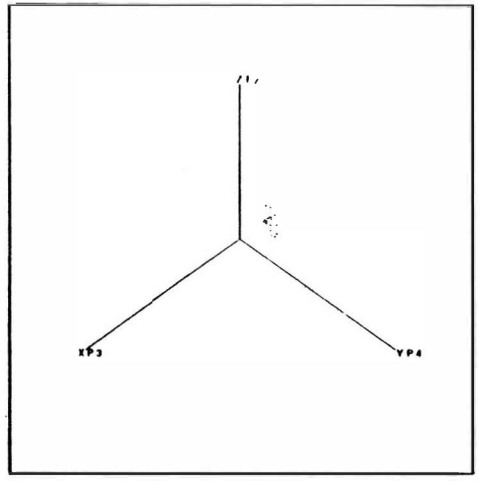

OSn

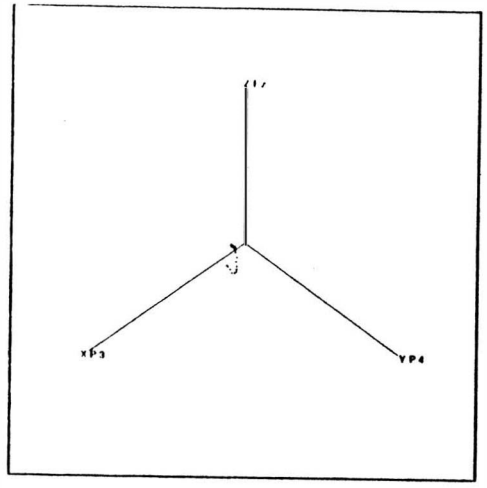

OSt

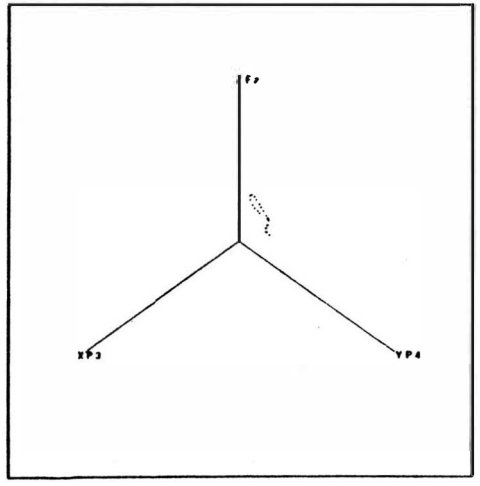

ODt

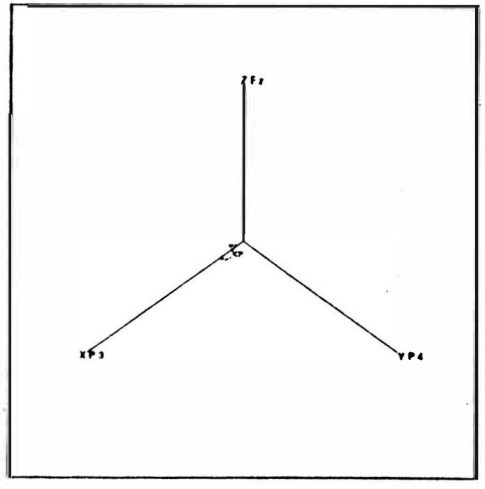

ODn

Figure 12 E 30 - 40ms

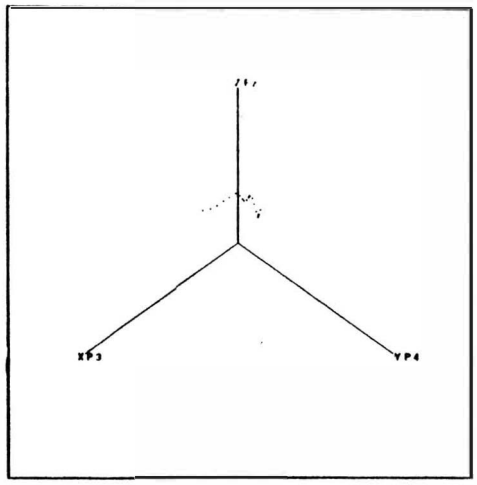

OSn

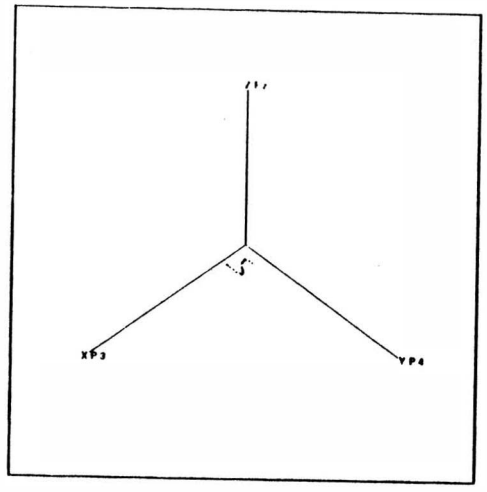

OSt

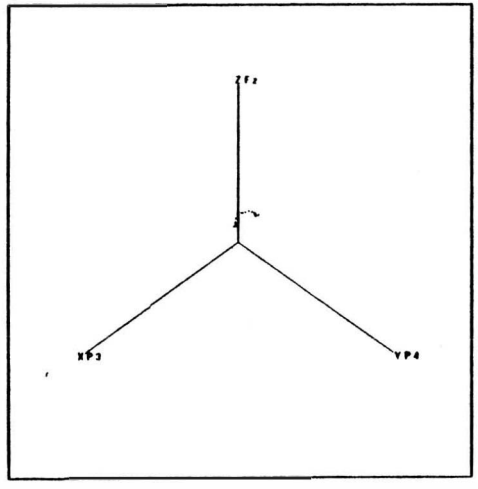

ODt

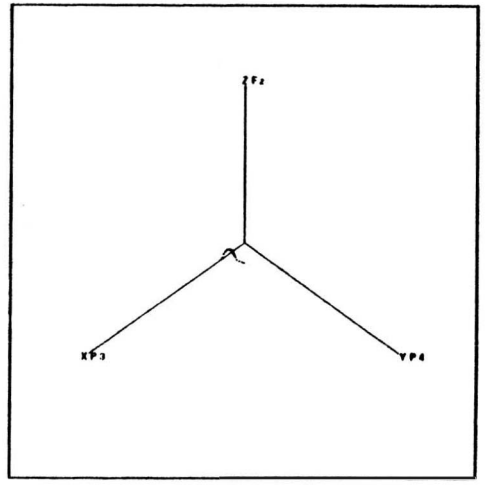

ODn

Figure 12 F 40 - 50ms

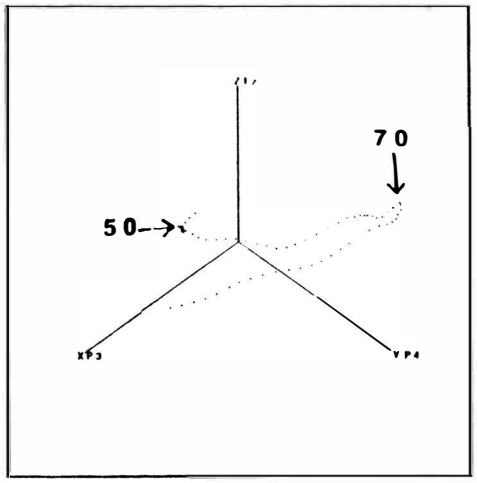

OSn

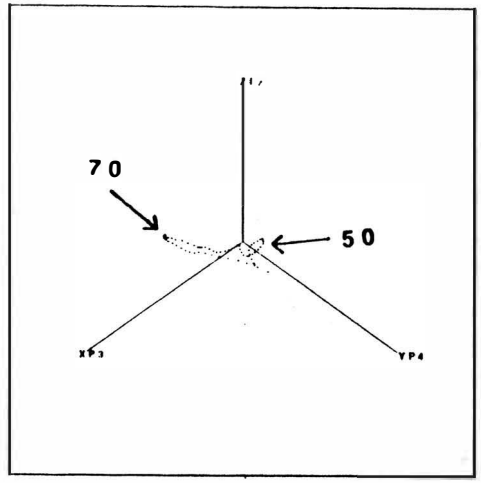

OSt

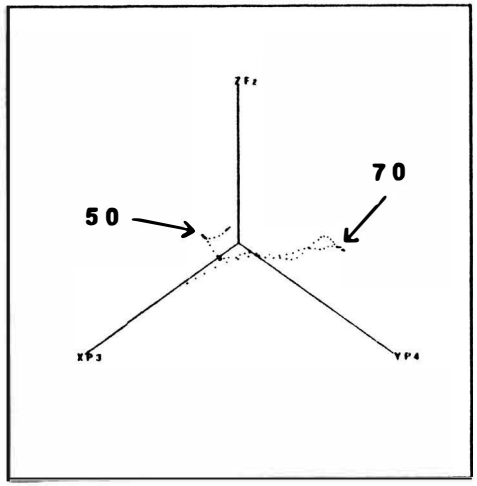

ODt

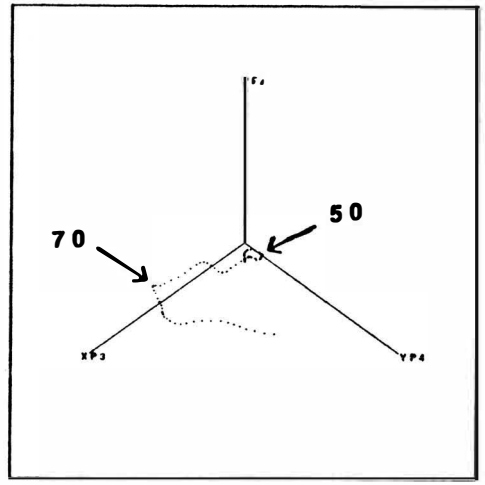

ODn

Figure 12 G 50-85ms

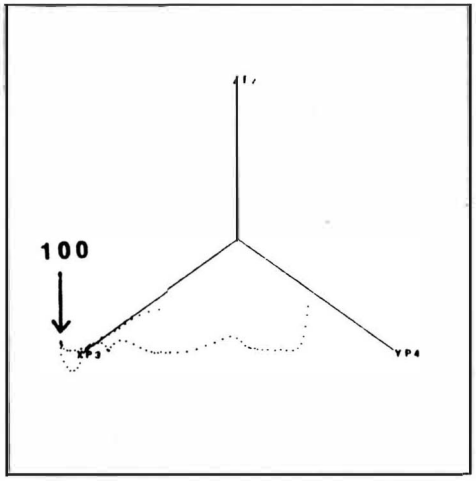

OSn

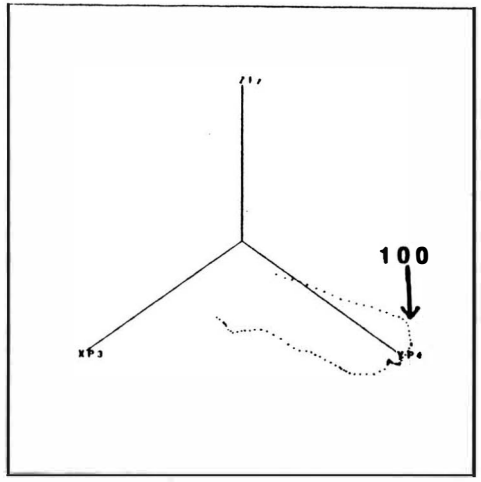

OSt

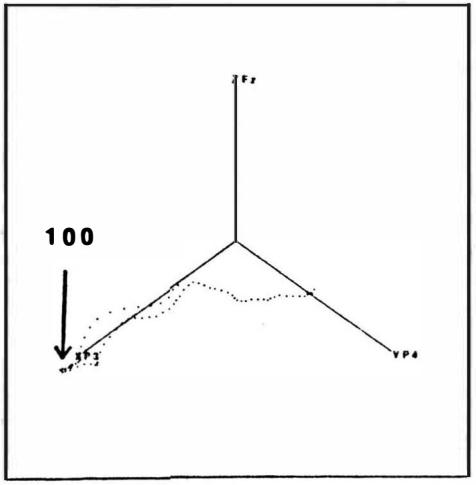

ODt

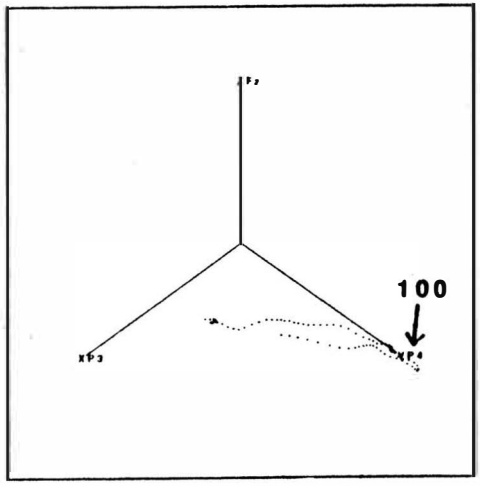

ODn

Figure 12 H 85 -125ms

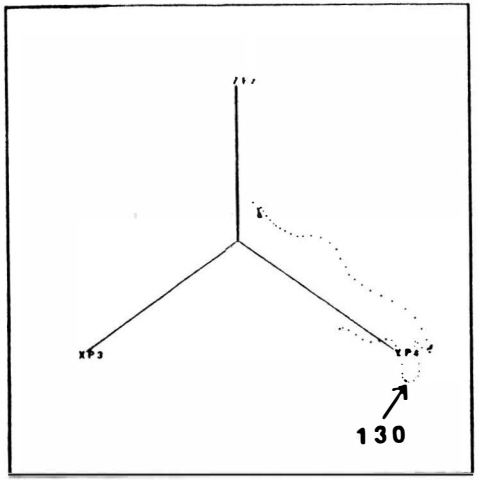

OSn

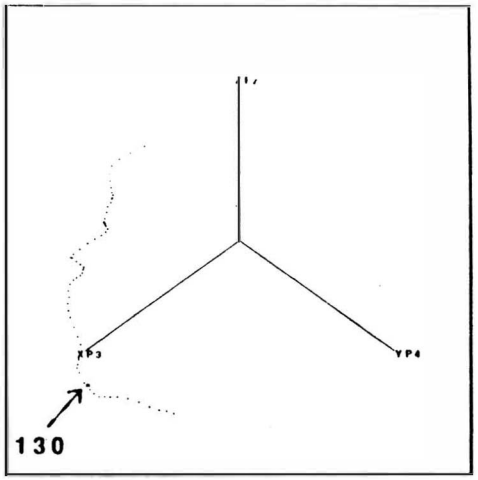

OSt

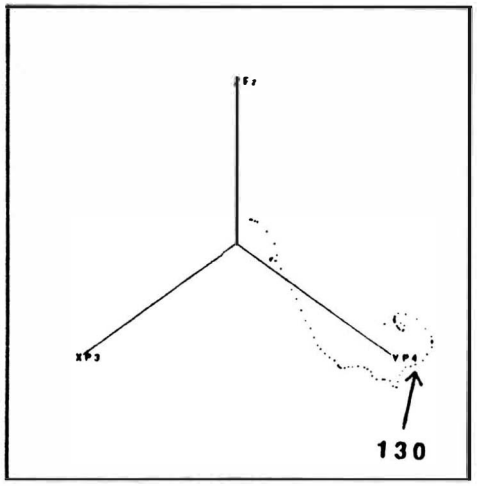

ODt

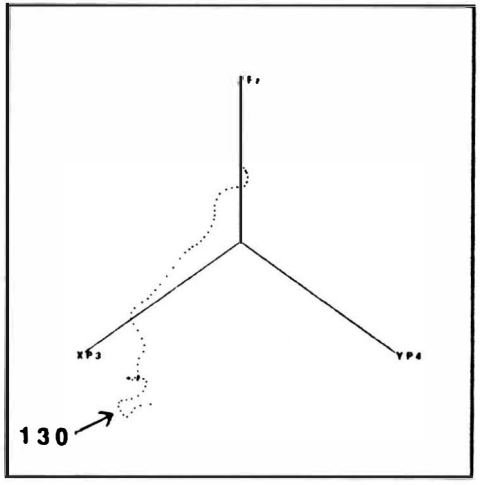

ODn

Figure 12 I

125 -160ms

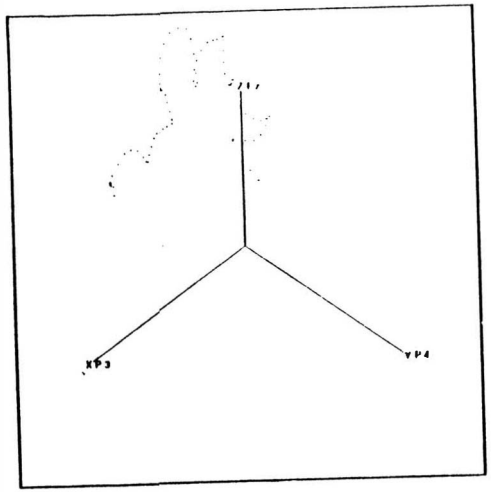

OSn

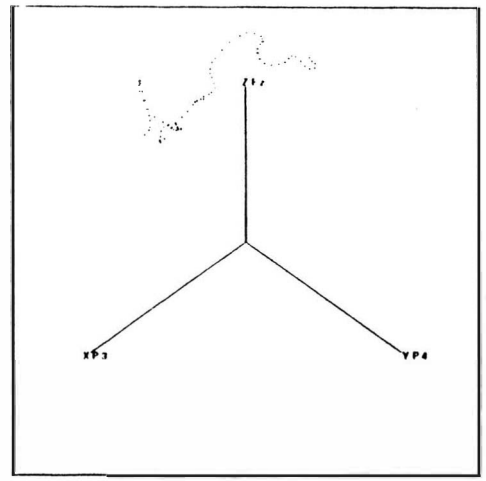

OSt

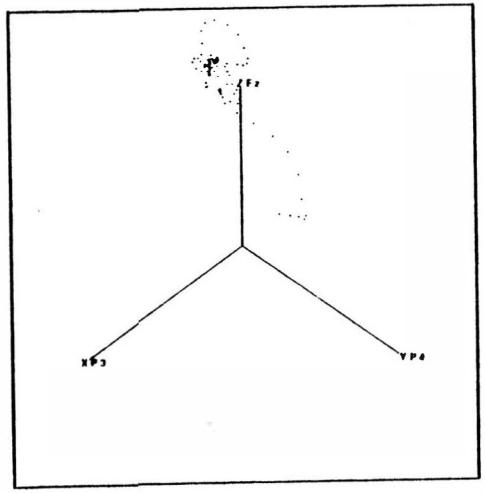

ODt

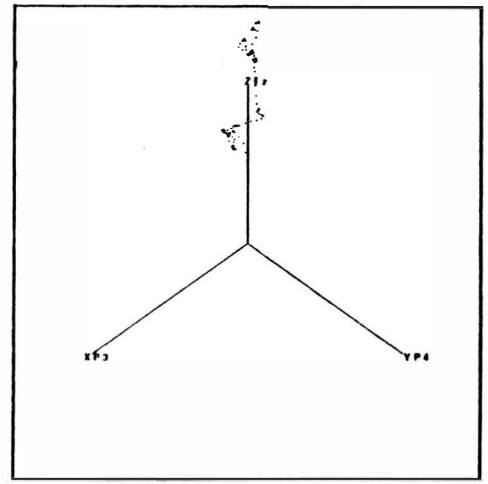

ODn

Figure 12 J 160 - 200ms

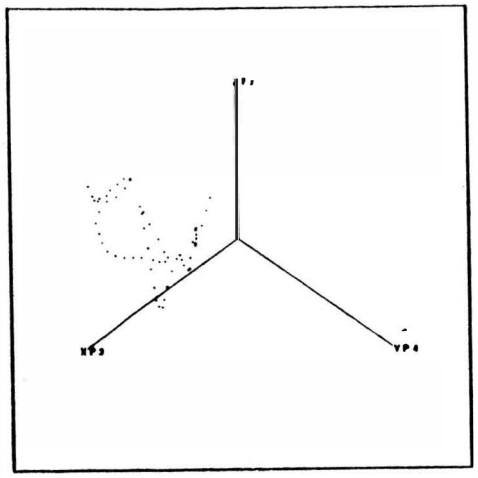

OSn

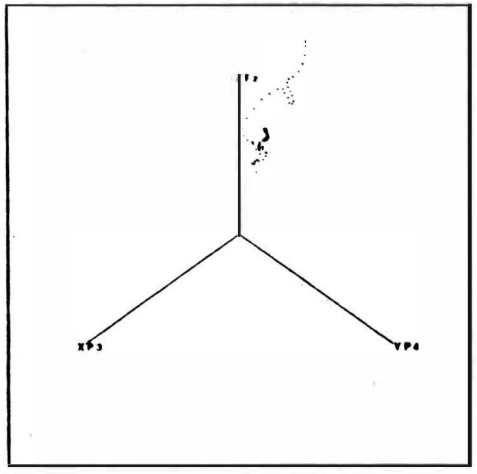

OSt

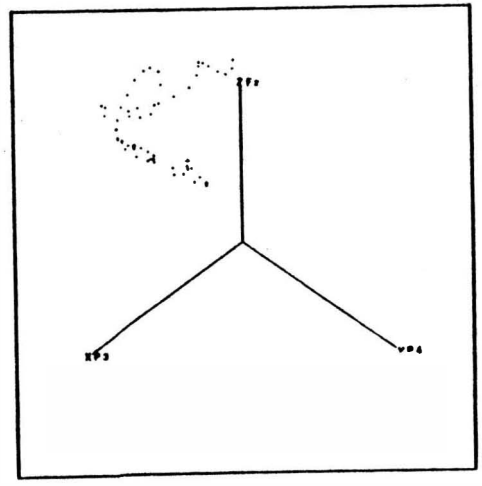

ODt

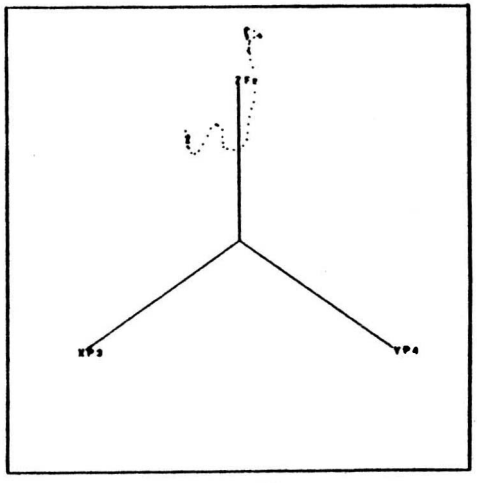

ODn

Figure 12 K 200 - 230ms

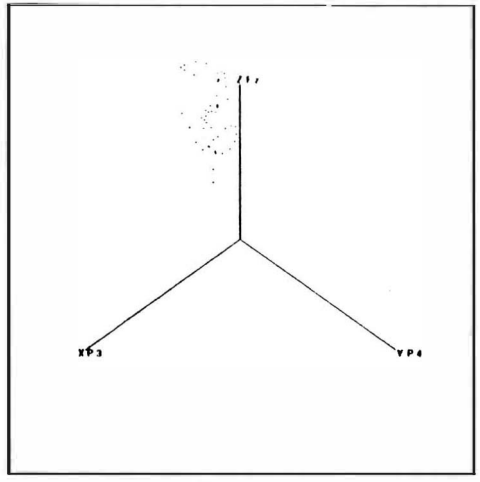

OSn

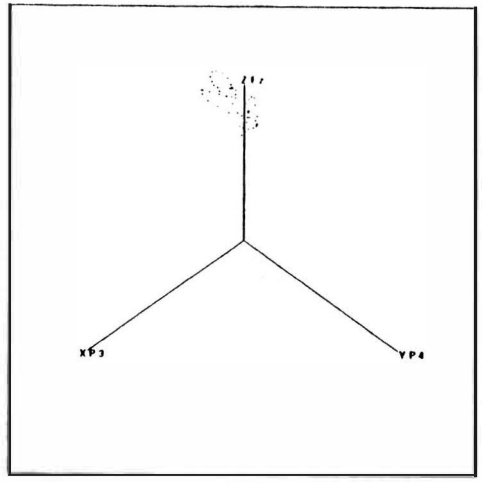

OSt

ODt

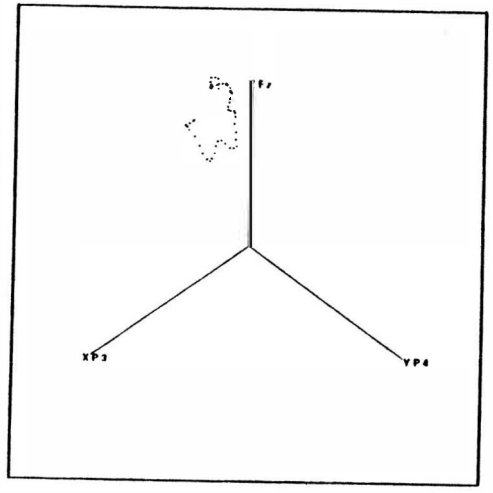

ODn

Figure 12 L 230 - 250ms

Figure 13 : Comparison of Nasal Versus Temporal Hemi-field VVEP of the Left Eye of Subject C. In a-l., the progressive time segments are assigned to show symmetry. The nasal (retinal) evoked potential (OSn) (solid line) is graphed with the temporal (retinal) evoked potential (OSt), for comparison. a-d. show little symmetry (approximately 0 -41.5ms). In e. at approximately 41.5ms mirror symmetry leading into a well defined 50 ms wave occurs (marked by large arrows, small arrows show progression on to the 70ms wave). The remaining figures show a great deal of mirror symmetry. Because the retinal potentials tend to occur at approximately 40ms, the crossing of activity at 45ms, in this subject, may represent the optic chiasmal cross, with the peak at 50ms representing the geniculate potential. Further discussion of this possibility is described in the text.

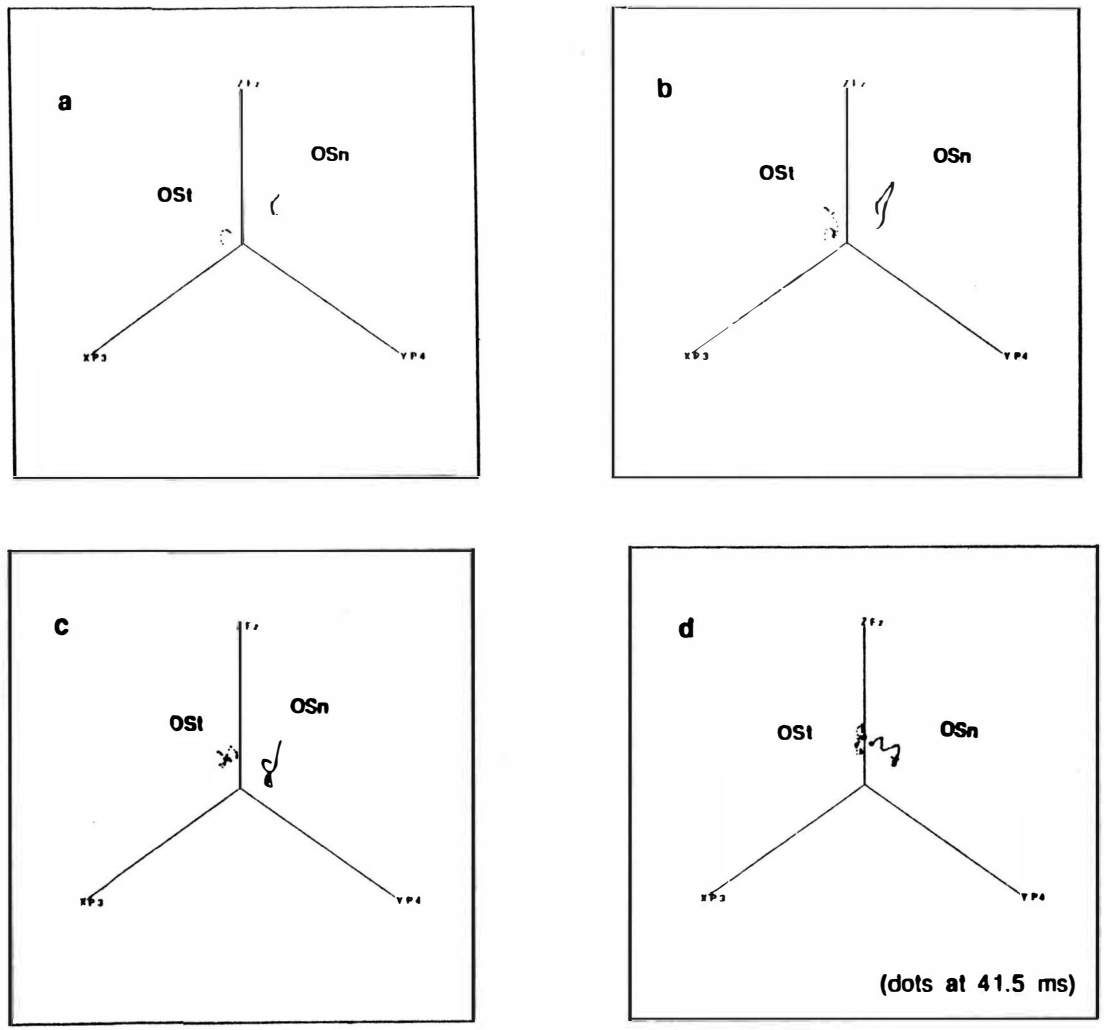

Figure 13 : Comparison of Nasal Versus Temporal Hemi-field VVEP of the Left Eye of Subject C.

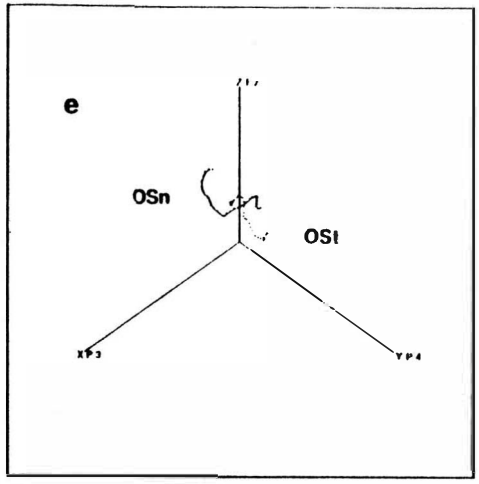

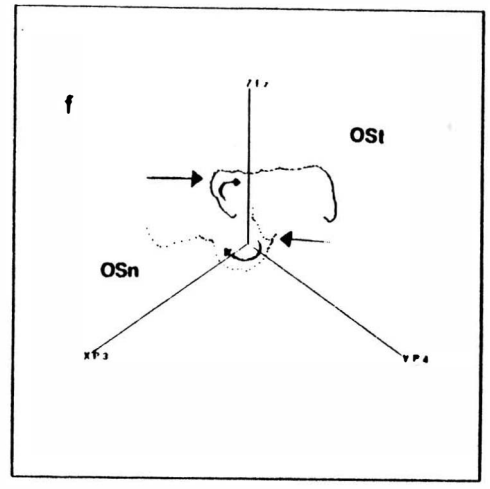

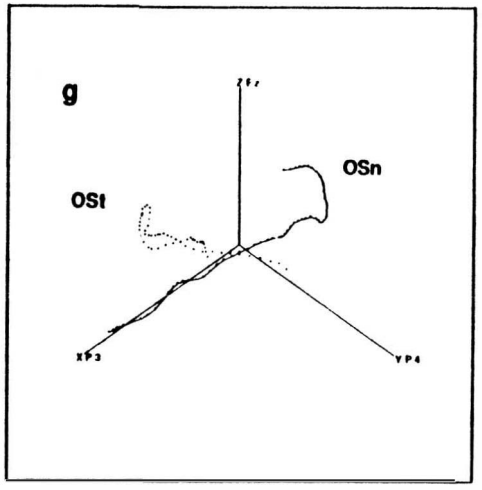

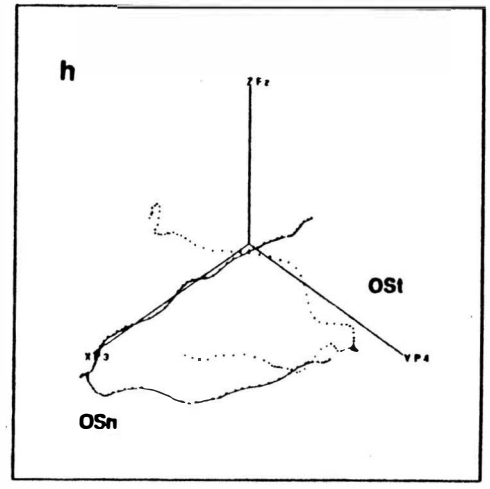

Figure 13

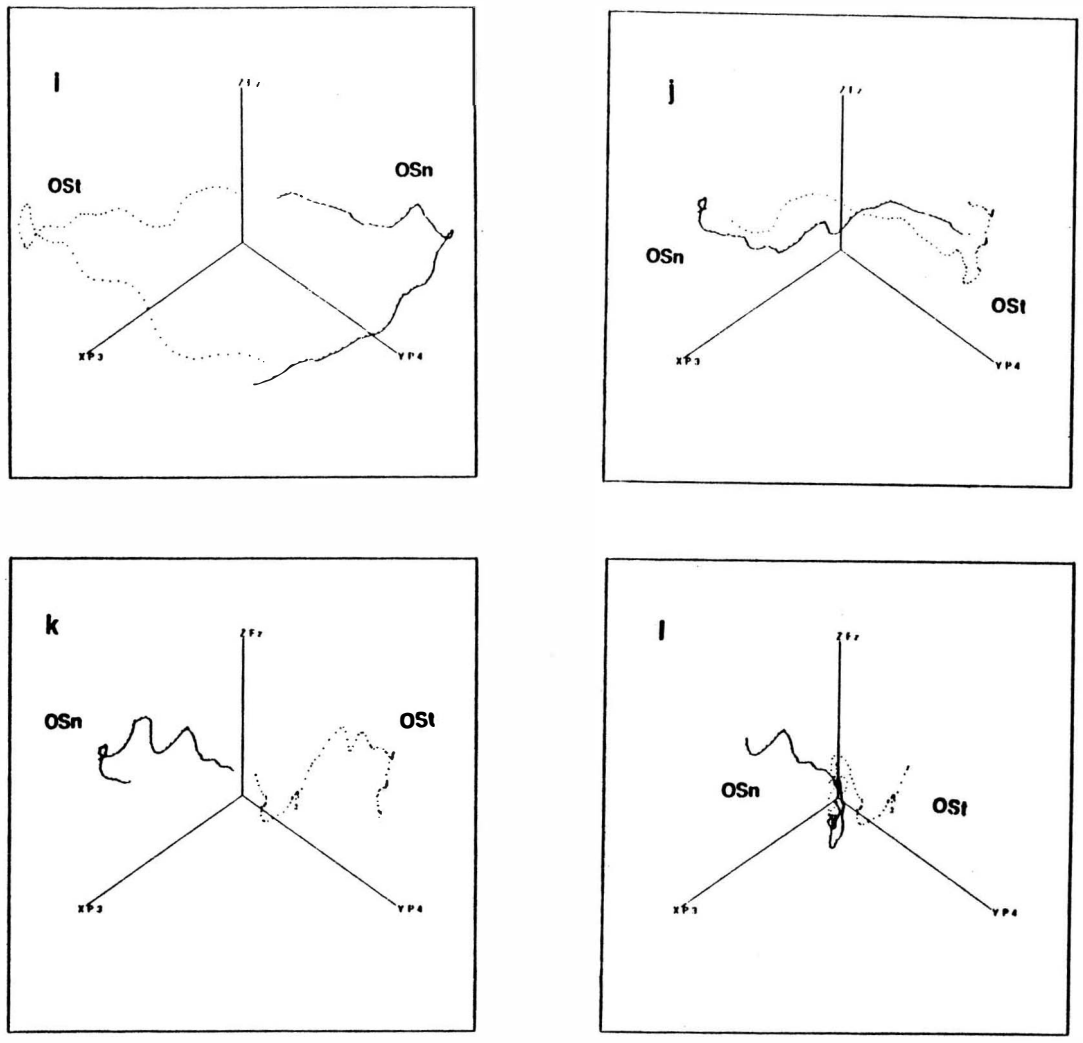

Figure 13

Figure 14 A, B, C : Hemi-field Symmetries in 3 Subjects. Each of the four retinal hemifield stimulation VVEP's are shown for each subject. The upper left plot is ODt, The upper right is the OSn, the lower left is the ODn and the lower right is the OSt. The epoch ranges from 40 or 50ms (as designated) to 225ms. A and B have solid lines to show the 50ms wave giving rise to the N70. The nominal 50ms wave is labeled, while an arrow shows the progression of the plot to the N70 (70ms) wave. The symmetrical similarity nasal-temporal pairs can be seen as well as the mirror symmetry of the nasal-nasal, and temporal-temporal pairs.

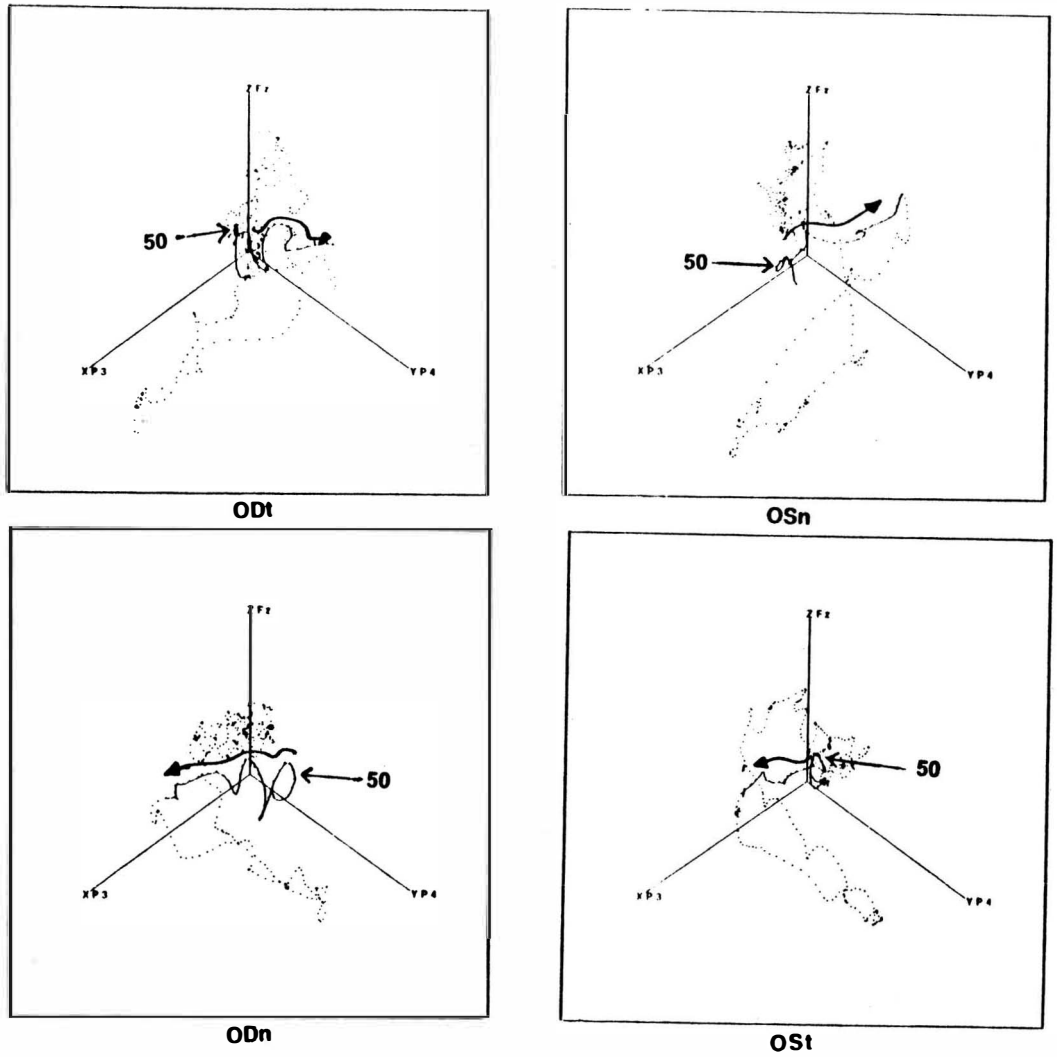

Figure 14 A Hemi-field Symmetries 50 - 225 ms

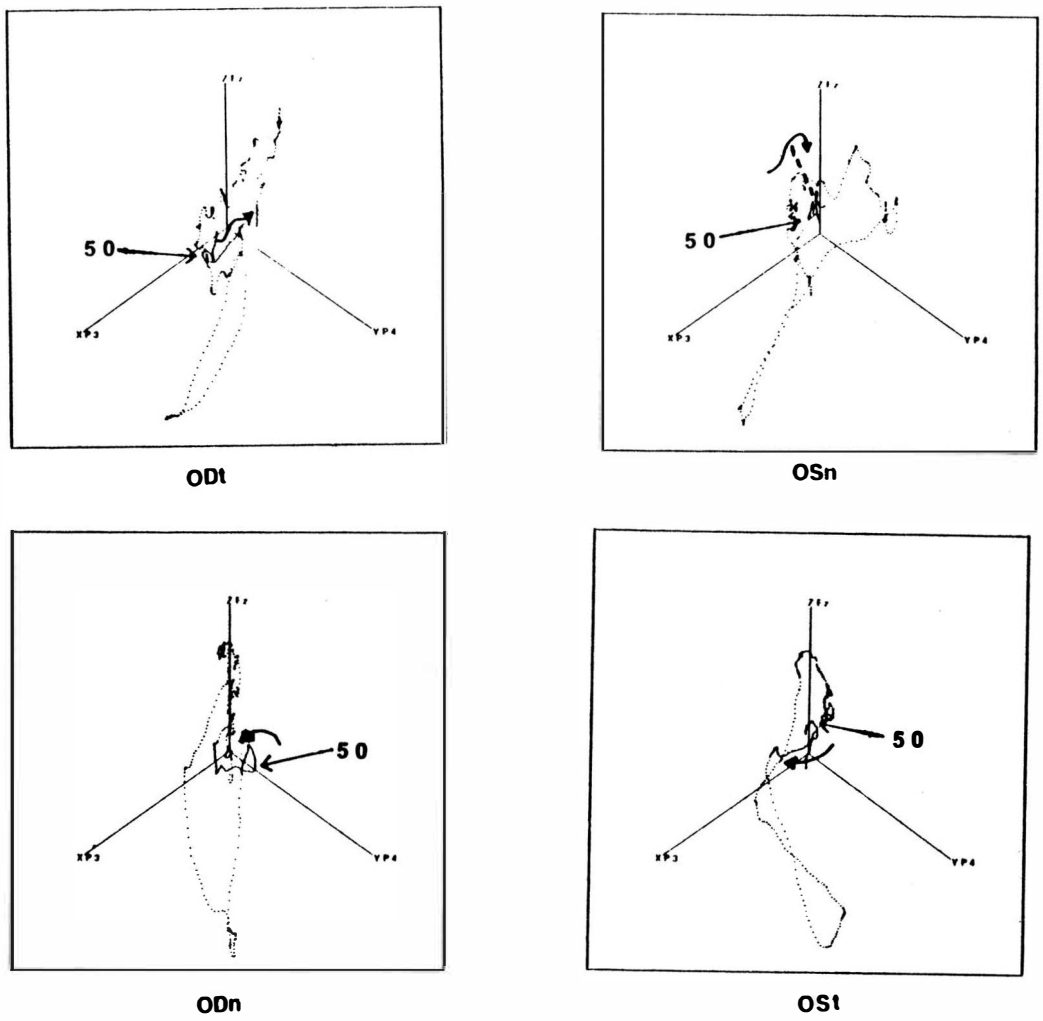

Figure 14 B Hemi-field Symmetries 40 - 225 ms

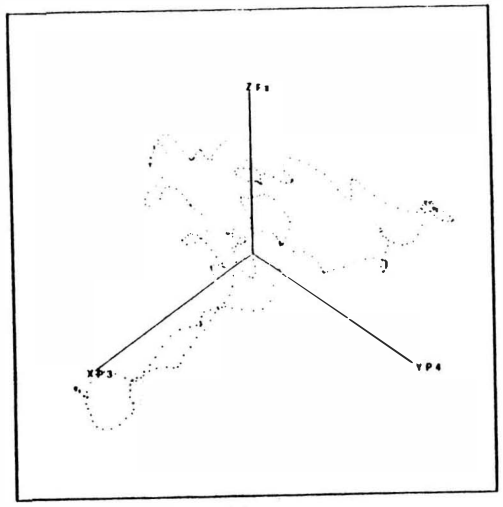

ODt

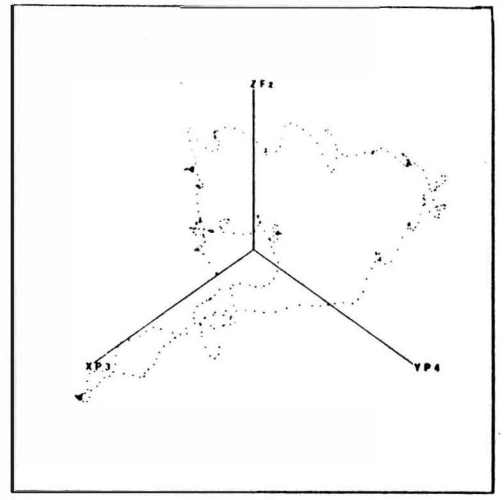

OSn

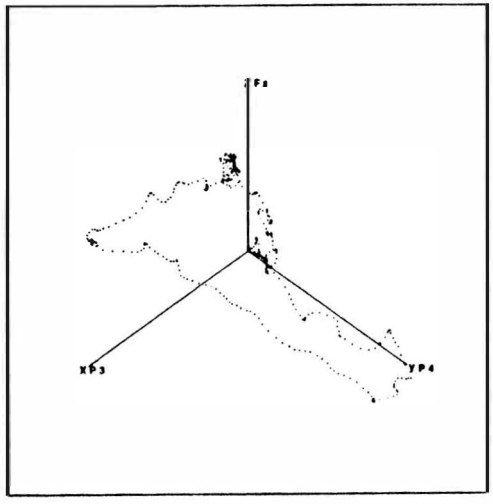

ODn

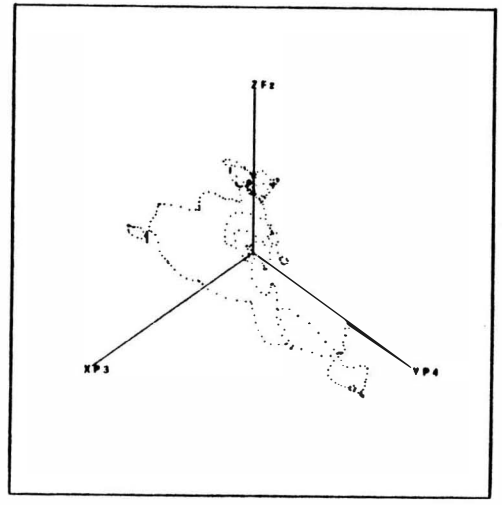

OSt

Figure 14 C Hemi-field Symmetries 50 - 225 ms

Figure 15 : VVEP Hemi-Field Responses of Five Subjects Are Hand Drawn as Smooth Curves of the Approximately 40-135ms Range. These approximations demonstrate the intrasubject similarity among OSn and ODt, and among OSt and ODn as well as the mirror images among ODn and OSt with both OSn and ODt. The 50ms peaks are labeled in each by an arrow. The similarity of the graphs among a given field in the intersubject studies is also apparent.

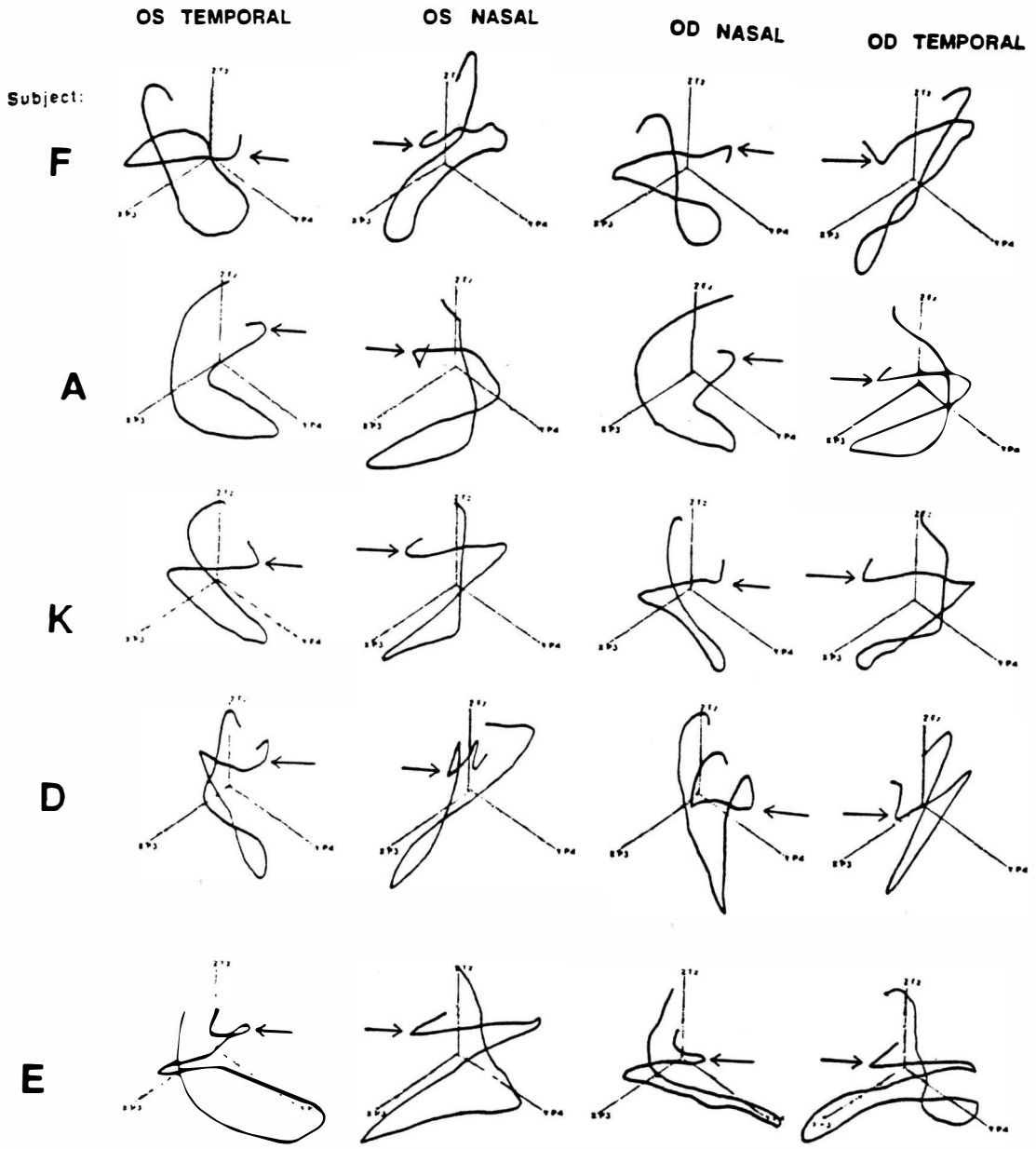

Figure 15 : VVEP Hemi-Field Responses of Five Subjects Are Hand Drawn as Smooth Curves of the Approximately 40-135ms Range.

Figure 16 : Vector Addition of the P100 Wave of Two VVEP Hemi-field Generated Waves. In both these two examples, subjects C and K, a. represents the left eye, nasal and temporal P100 wave. The nasal wave is designated by a solid line, while the temporal activity is designated by continuous points. b. is the vector addition of the temporal and nasal retinal stimulated activities. c. is the vector peak generated by the full field, 60' of arc left eye stimulation. The P100 generated by vector addition is very similar to the full field p100 wave.

SUBJECT:

C

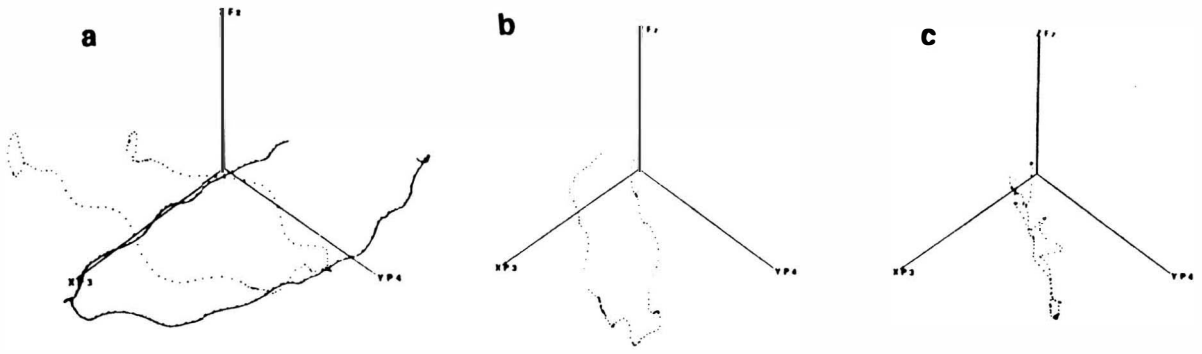

K

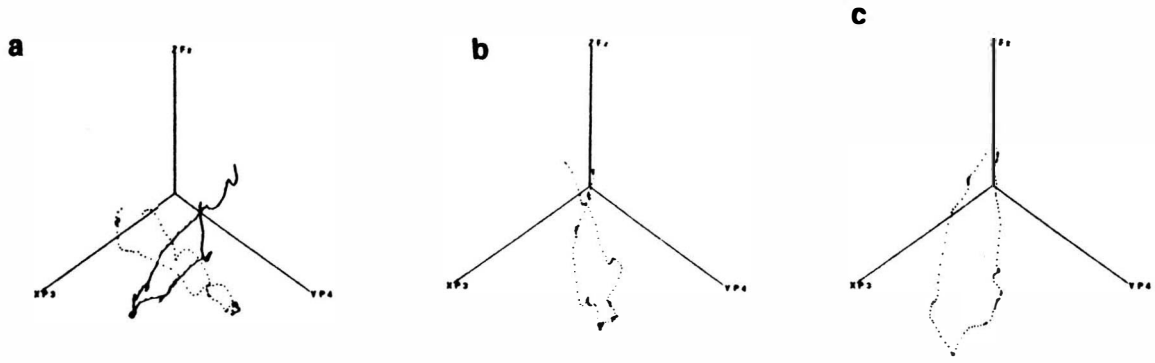

Figure 16 : Vector Addition of the P100 Wave of Two VVEP Hemifield Generated Waves. (Nasal Wave, Solid Line)

Figure 17 : Sample of a Pattern ERG Plot. These data were recorded form an infra-orbital skin electrode referred to the ipsilateral tragus. Pattern ERG of subject H, demonstrates a peak at 46.5 ms in the left eye and 45ms in the right eye. A preceding negative minimal activity (trough) is found at 27.5 and 25ms for the left and right eye, respectively. (60 min of arc).

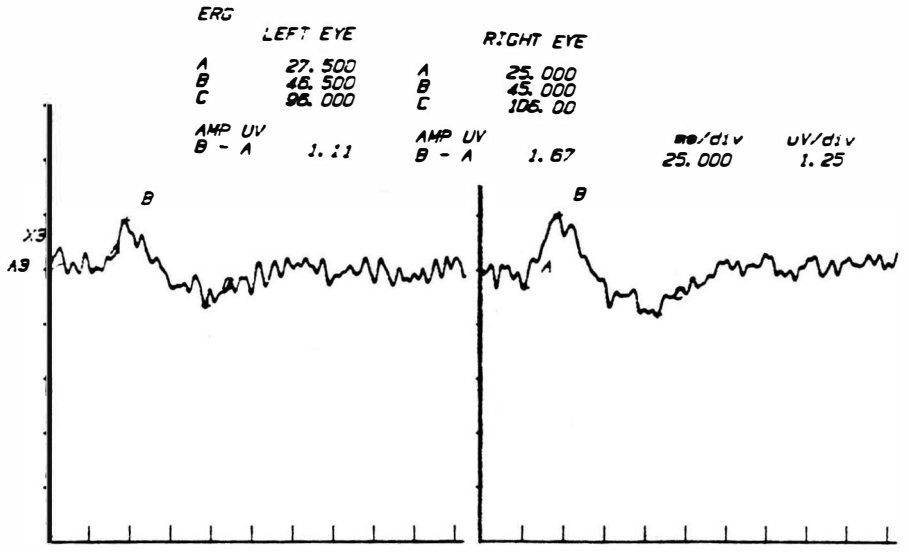

Figure 17 : Sample of a Pattern ERG Plot.

Figure 18 : Comparison of Peak Latency of 50ms Pattern ERG and the 55ms Peak. The ERG time is represented by an asterisk while the 55ms peak (wave) is represented by a square. Trends show the 50ms Pattern ERG occurring at either a cluster of activity (a.) or at a peak just prior to the 55ms peak (b.), with a relatively straight progression to the 55ms wave. (Pattern stimulation at 60 min of Arc). a. and b. are from subject H. c.,d.,e., and f. are from subject I. The view points are selected for best representation of the 55ms wave.

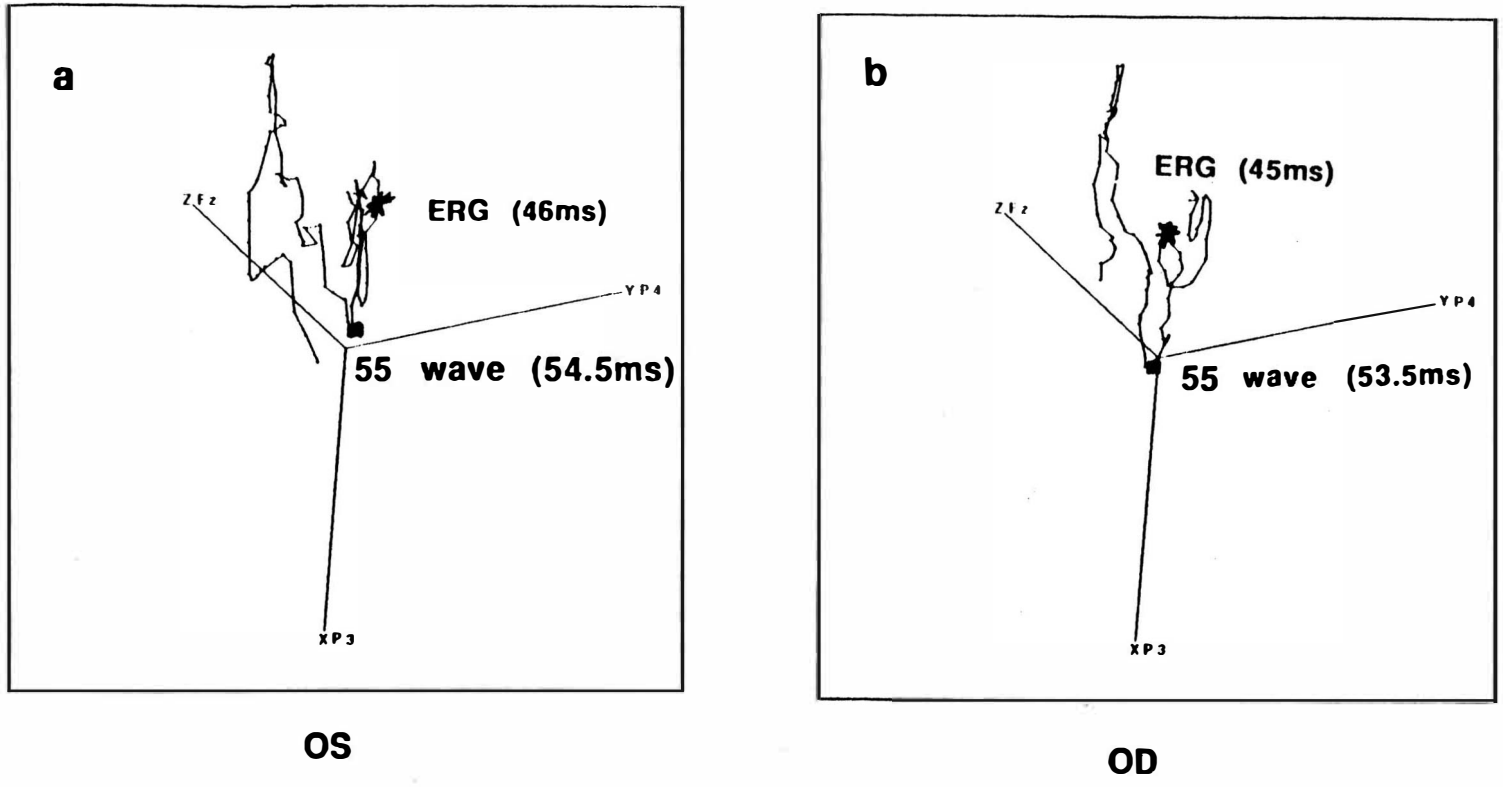

Figure 18 : Comparison of Peak Latency of 50ms Pattern ERG and the 55ms Peak.

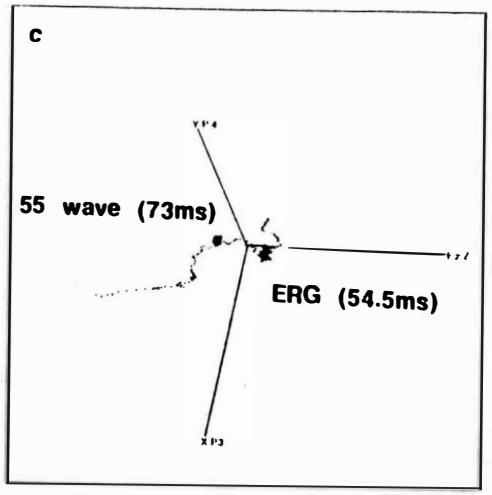

OS

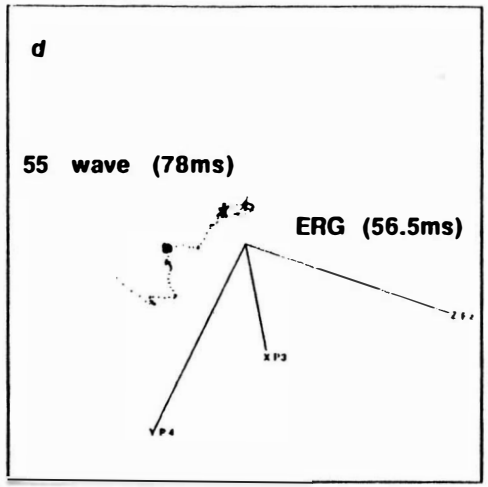

OS

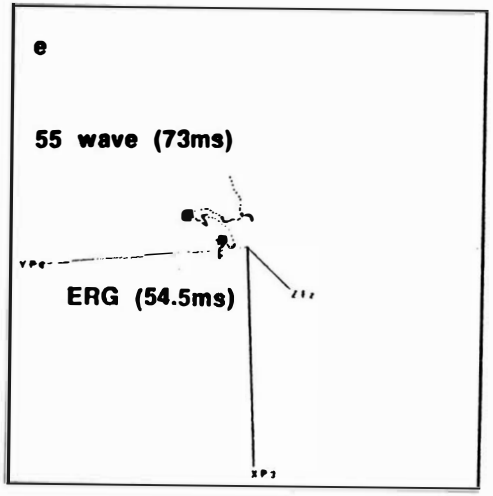

OD

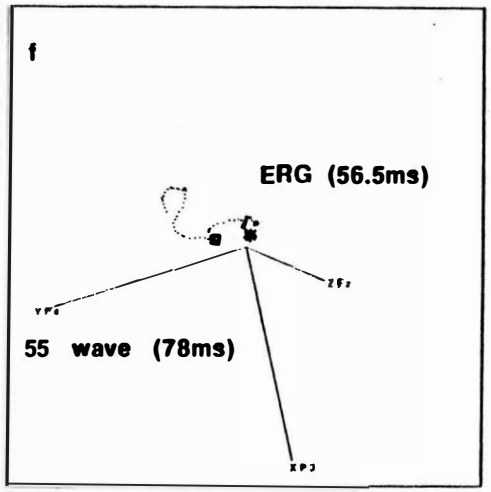

OD

Figure 18 c-f

Figure 19 : Comparison of the 55ms Wave of the Right Eye, Nasal and Temporal Field with a Full Field 55ms Wave of the Same Eye, at Identical Scaling. (60 min of Arc.) **a.** A selected view point to emphasize the 55ms peaks which are not always as apparent in more traditional views (vertex or lateral). Note the lateral orientation by this display of the hemi-field generated 55ms waves. These waves occur at 52ms, with the right peak being the nasal retinal field and the left peak being the temporal field of the right eye. **b.** Note the full field 55ms potential of the right eye is midline, with a peak time of 52ms. The peak occurs near the origin with a reduced magnitude. **c.** The 55ms peak in b. is shown at a different orientation. Note how its potential is perpendicular to the Fz recording axis, i.e. conventional recording axis.

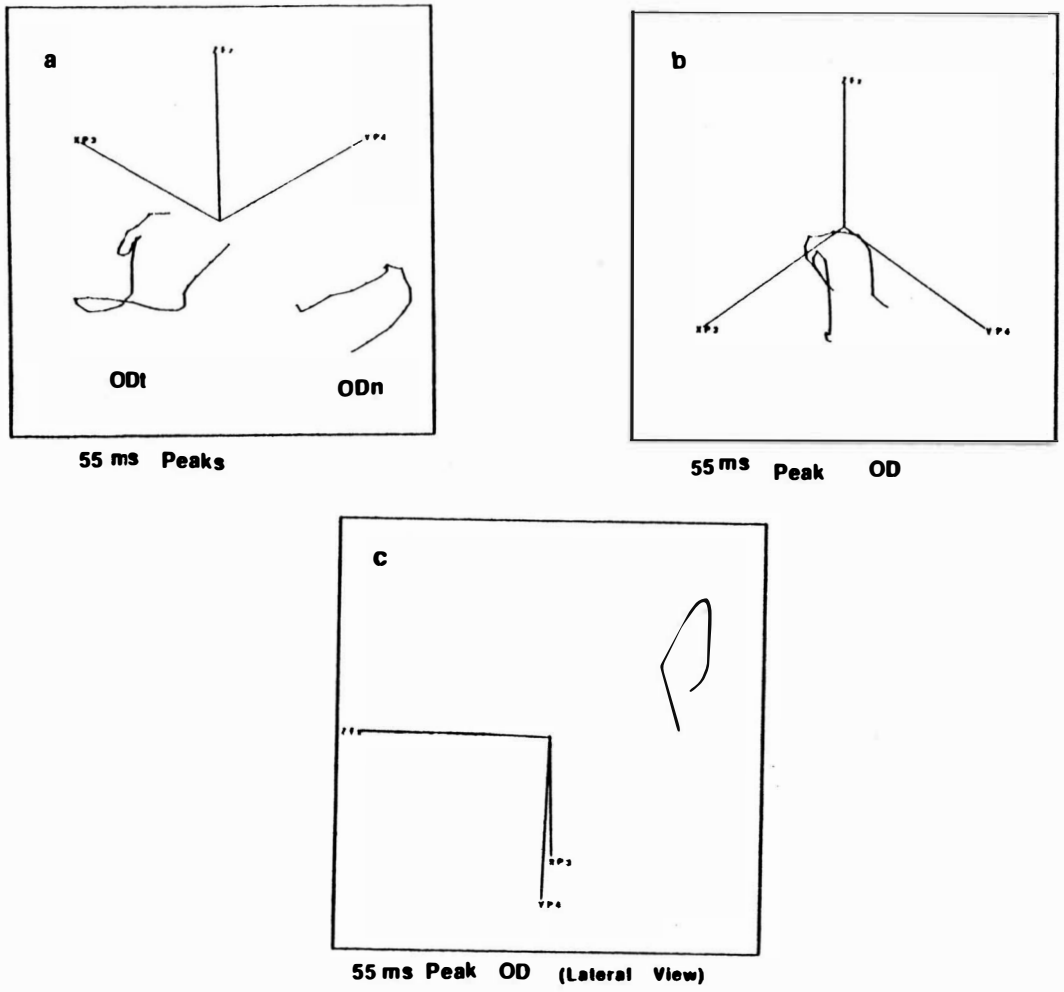

Figure 19 : Comparison of the 55ms Wave of the Right Eye, Nasal and Temporal Field with a Full Field 55ms Wave of the Same Eye, at Identical Scaling. (60 min of Arc.)

Figure 20 : Identification of Occult Peaks Through Rotation of a Group of Data Points of a VVEP. A. A segment of a hemi-field in subject A. The "X" is at the undisputed P100 point, while the square is at an area of change consistent with a probable peak. The diamond is midway between the two for reference. The open circle is at the end of the data set. **B.** The data set viewed at a different angle confirms the identification of a peak at the area of the square. The designation of the apex would probably be at the arrow. Note on these two views no peaks/changes of activity are identified between the open circle and the square. **C.** On this final view point the identification of an occult peak can be made which is marked by the arrow. This peak was not noticeable in the other two view points, also note at this view point the square which lies next to an apiece no longer seems to at this view point. Thus the viewing a VVEP at different rotations (angles) is important to identify all peaks of activity.

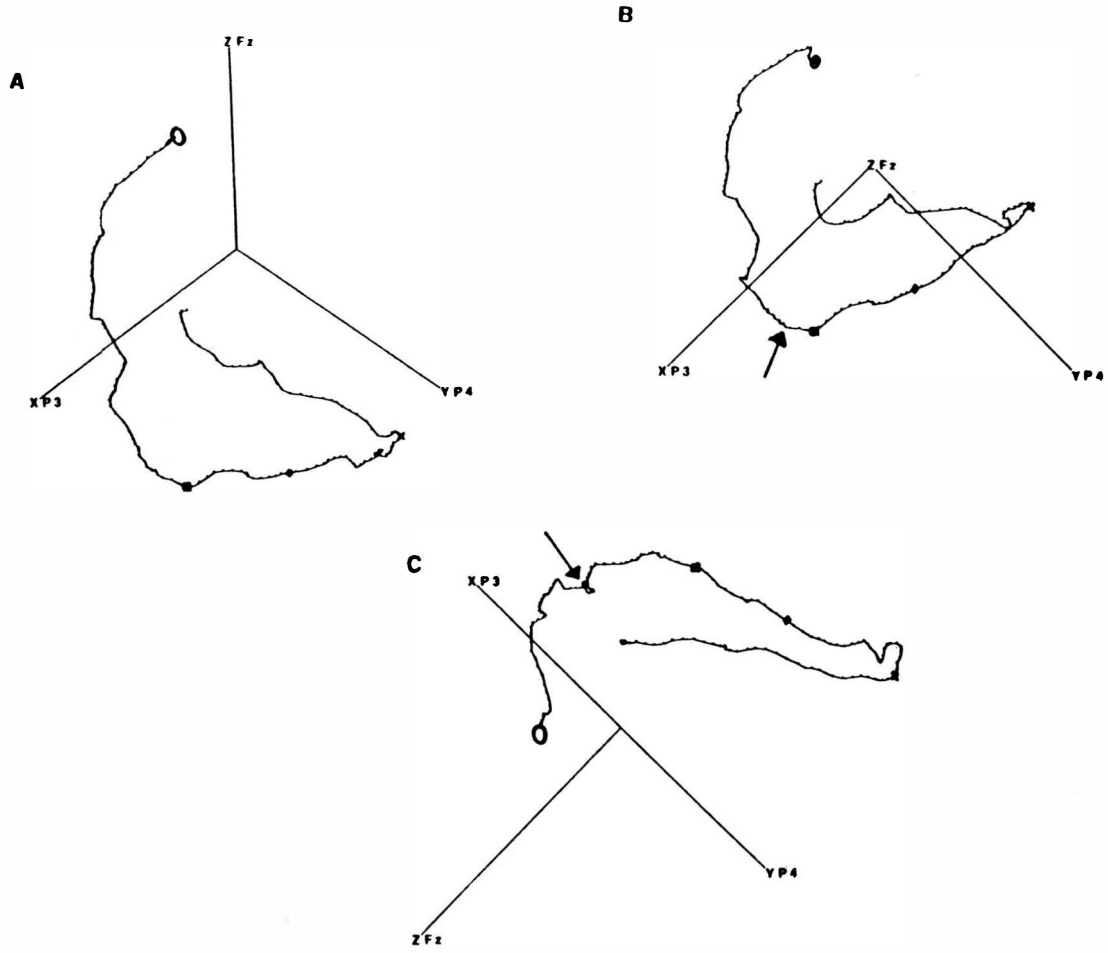

Figure 20 : Identification of Occult Peaks Through Rotation of a Group of Data Points of a VVEP.

Figure 21 : Assigning Peaks to Variations in Displayed (graphic) Data.

A. Cluster of points: The time of the peak in this case is chosen by one of the midpoints of the cluster, assigning an exact direction to this event is not possible, although an approximation can be made.

B. P100 with wave forms pre and post event of no significance: The P100 verging off to the left has an intrinsic wave activity. The most apical point is assigned as representing the peak latency (designated by an arrow).

C. and **D.** General flow is important when noise present: Both show a large amount of noise and small peaks, however the general trend of the flow of progression is what's important, with the peak being assigned to the midpoint of apiece activity.

E. Bimodal peaks: Bimodal peaks were considered one peak (event) if they were co-planar, in which case the midpoint was used for time of occurrence. If each peak had its own direction in space, each peak was classified as its own event using the maximal prominent point as the time of occurrence.

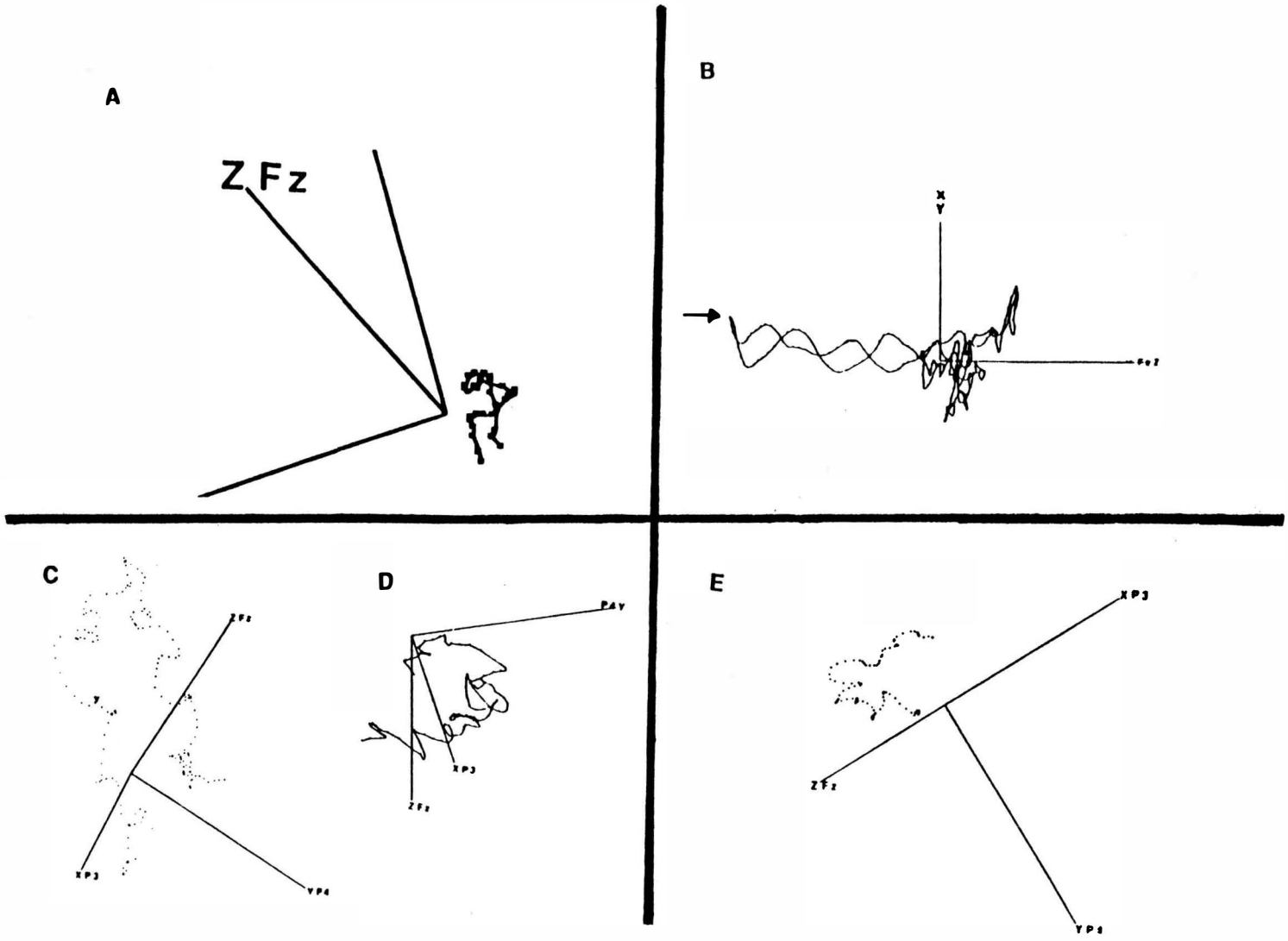

Figure 21 : Assigning Peaks to Variations in Displayed (graphic) Data.

Figure 22 : 'Lighthouse Effect'

A. This Graphic representation of a P100 shows a looping progression, with no discernable peak in the VVEP method. However, when expressed in a conventional evoked potential recording, a peak would be generated with the apiece being at the point where the arrow is drawn up from Oz, because this is the point closest to the recording electrode. This is termed the "light house effect" because in conventional recording a continuous activity will make a peak only when directly confronting the recording electrode. Thus while an activity is isoelectric, as in this example, a peak is factiously assigned in a conventional response when the activity gets nearest an electrode, i.e. a light house is always shinning, but you only see the light at the time it is pointing at you. In this vector plot the peak would be assigned to the midpoint, with the time designated as 114ms. (Bold arrow). The small arrow shows the progression of activity.

B. Conventional Plots of the Same P100. These plots represent the Queen's square method of conventional VEP electrode recording. These single channel recordings are located at Oz -Fz (midline) and just to the left (Q1 - Fz) and

right (Q2 - Fz) of midline posteriorly (see figure 1). The time generated by Oz pair is labeled in the figure as 103ms. These time differences show how using single recording channels, can cause great variation in the evoked response.

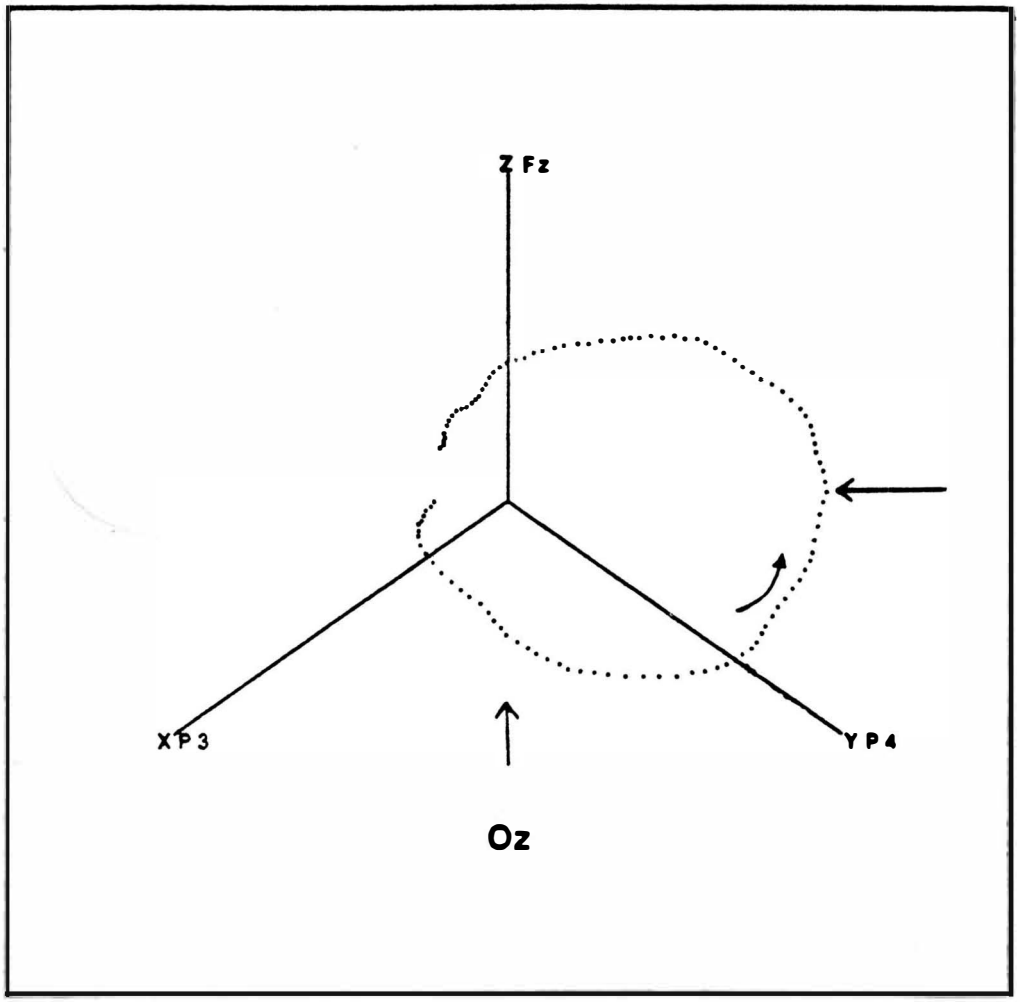

Figure 22a : "Lighthouse Effect"

	ms/div	uV/div
X1 X2 X3 X8 X4 X5 X6	25.000	5.00
X7	25.000	2.50

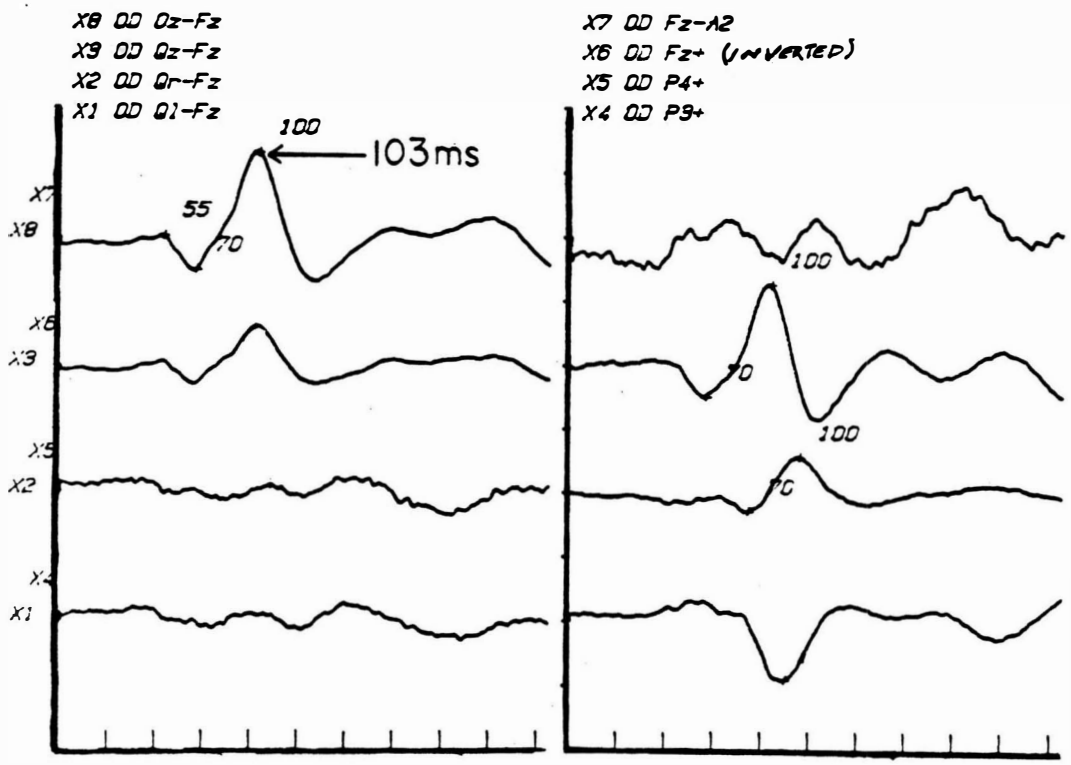

Figure 22 b : "Lighthouse Effect"

Figure 23 : The Best Way to Describe a Peak.

(See the text for discussion). Three entirely different peaks would have the same polar co-ordinates as defined by the MacSpin® program. (Figure **A, B, C**). Likewise, two very similar peaks would have very different polar co-ordinates because they lie on different sides of the axis. (Figure **D. E**). A method to describe the direction of a peak by its inherent shape uses a vector from the bisection of a line connecting the inflection points to the peak apiece. (Figure **F, G**). While the mathematical formulation for such a procedure is not given here, it is believed that this method would give the most accurate description of an event, by its inherent direction.

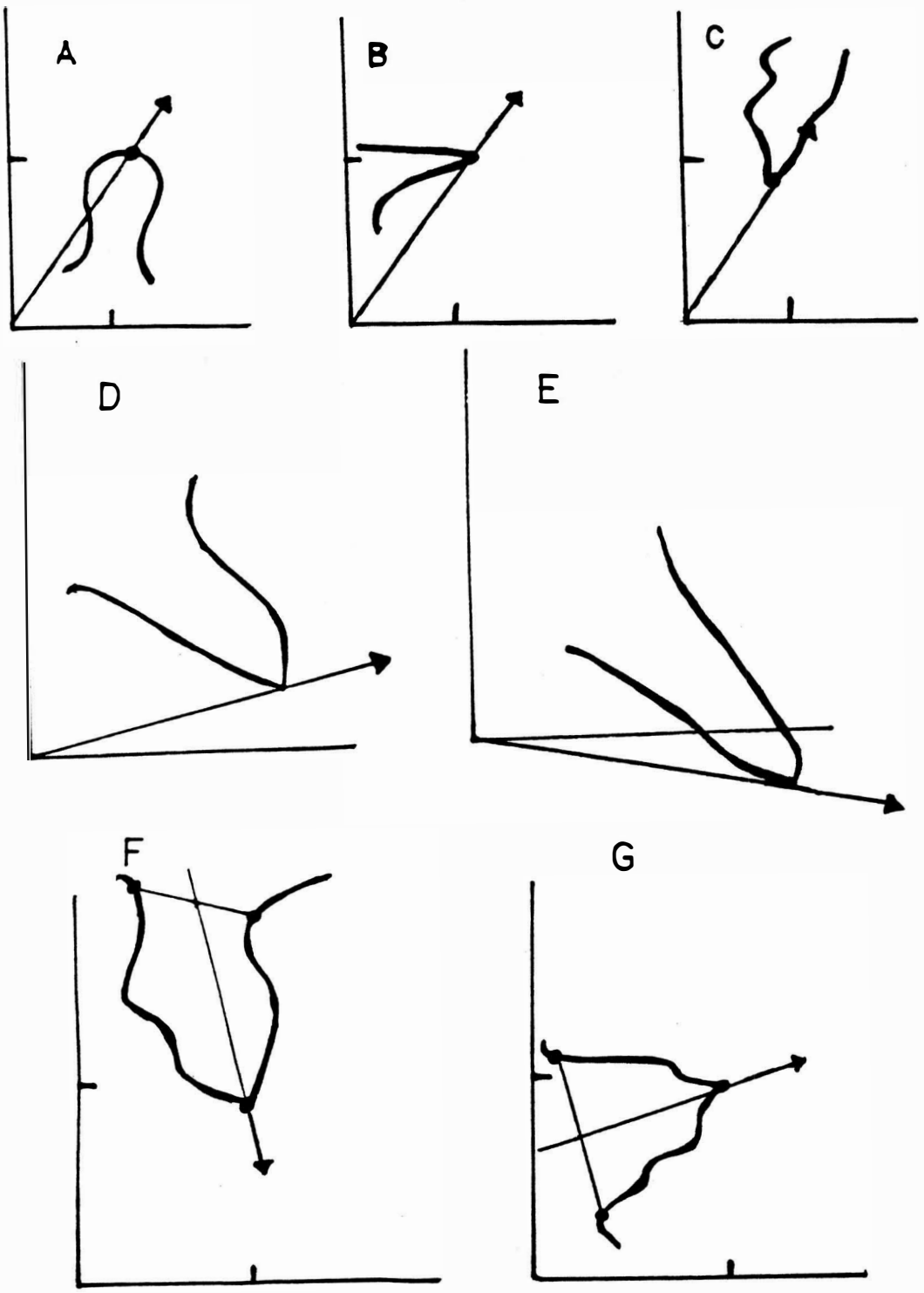

Figure 23 : The Best Way to Describe a Peak.

Figure 24 : Side by Side Comparison of Full Field VVEP of the Left and Right Eye at 60 min of Arc.

(subject G). The corresponding plot of the left versus right eye VVEP is shown in segments (b. - q.). Although a hint of symmetry is present at early times (<50ms) full symmetry is present in the later activity (post 50ms).

The epoch breakdown is as follows:

a : A posterior vertex oblique view rotated to show similarity of the left and right full field stimulation (0 -250ms). Right eye VVEP is connected by a line.

b, c : Vertex views of OS, OD, respectively, (0-250ms).

d, e : OS and OD respectively : 1-15ms

f, g : " " : 15-30ms

h, i : " " : 30-55ms

j, k : " " : 55-95ms

l, m : " " : 95-160ms

n, o : " " : 160-215ms

p, q : " " : 215-250ms

Arrows showing progression are seen in the figures beginning with j and k.

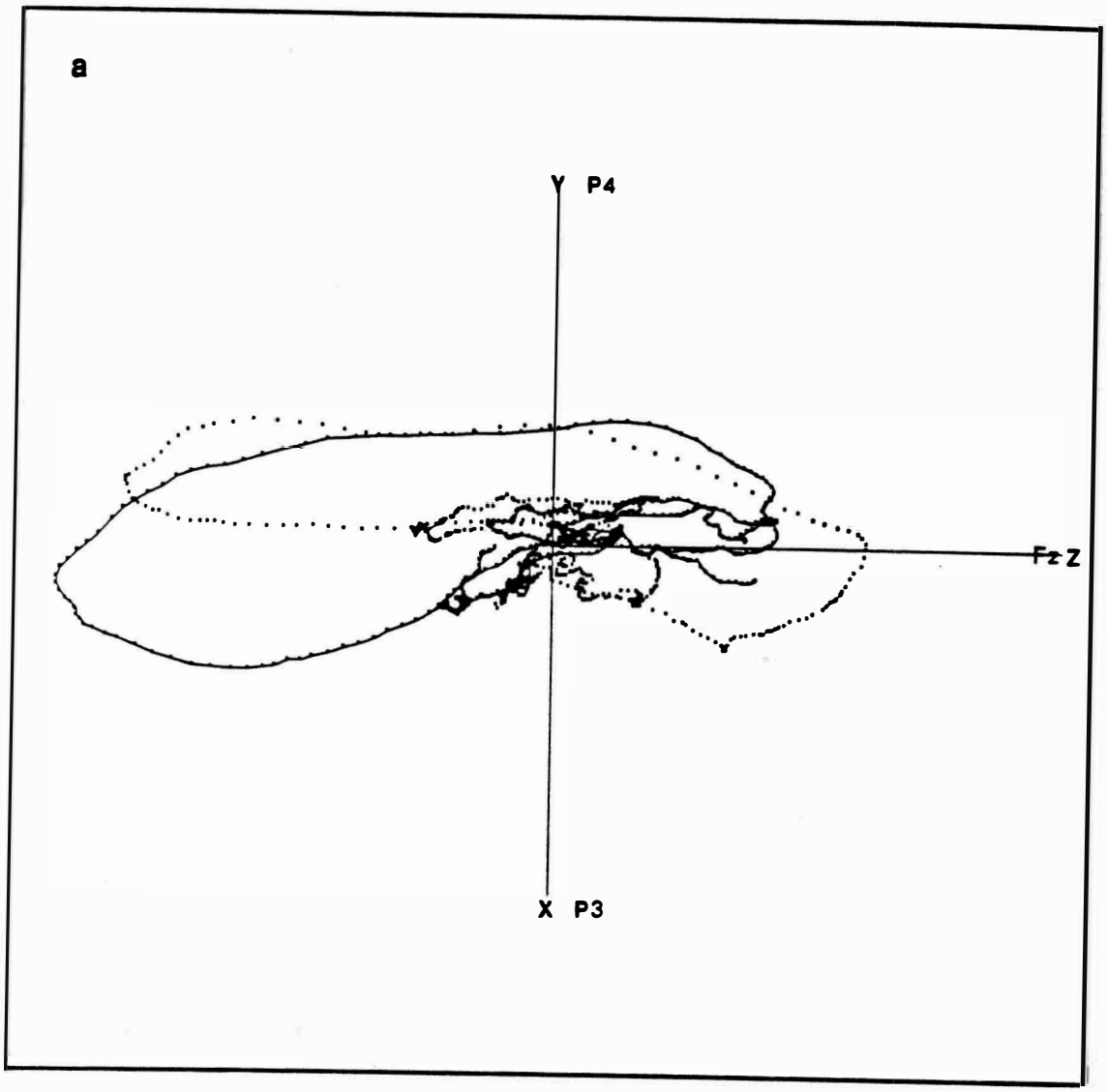

Figure 24 : Side by Side Comparison of Full Field VVEP of the Left and Right Eye at 60 min of Arc.

(right eye connected by solid line)

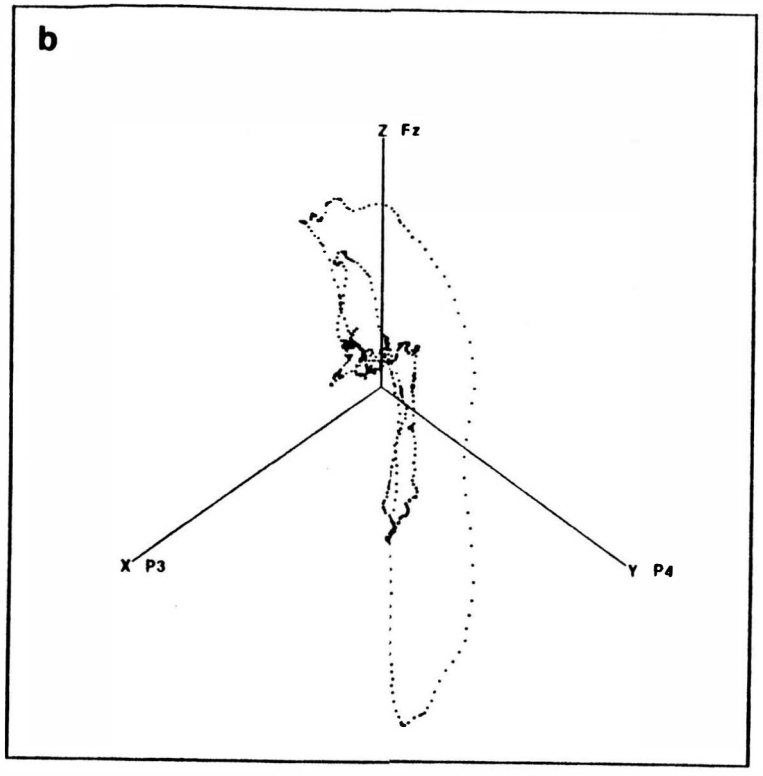

OS

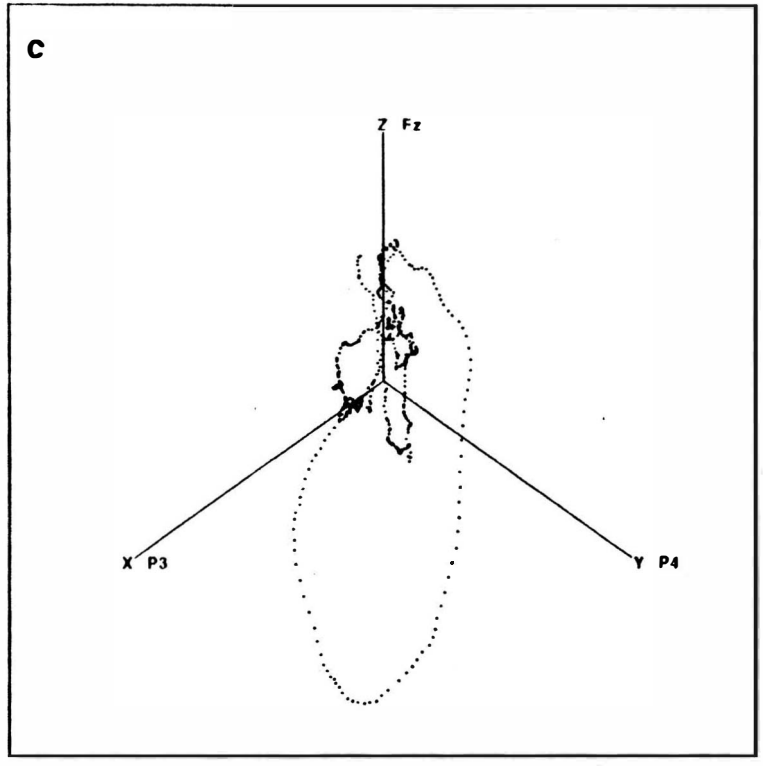

OD

Figure 24 0 - 250 ms

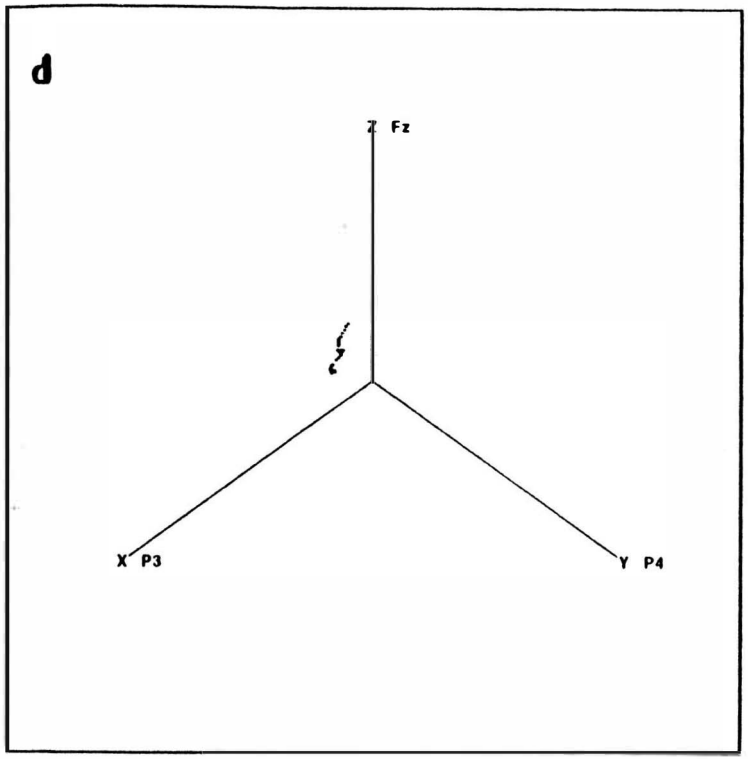

OS

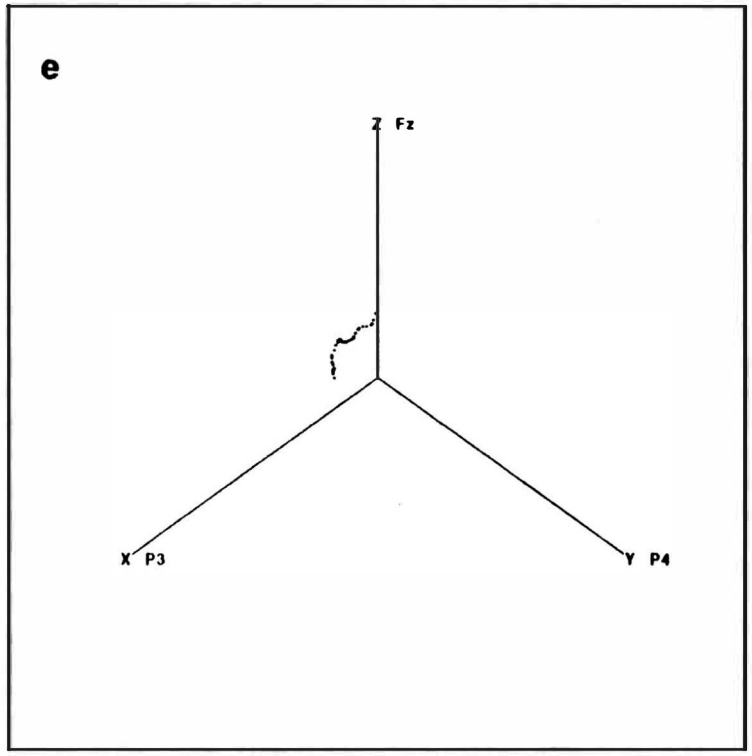

OD

Figure 24 1 - 15 ms

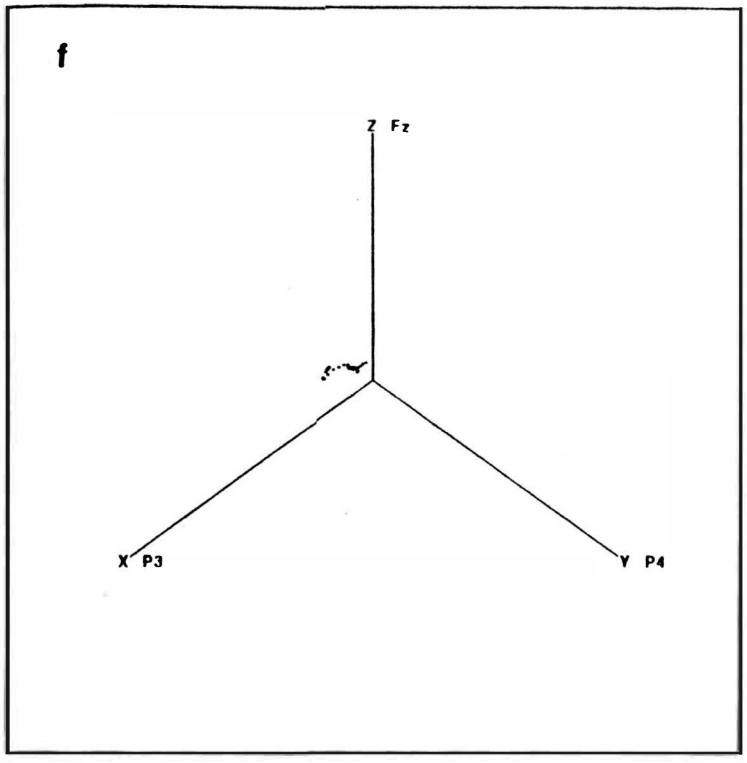

OS

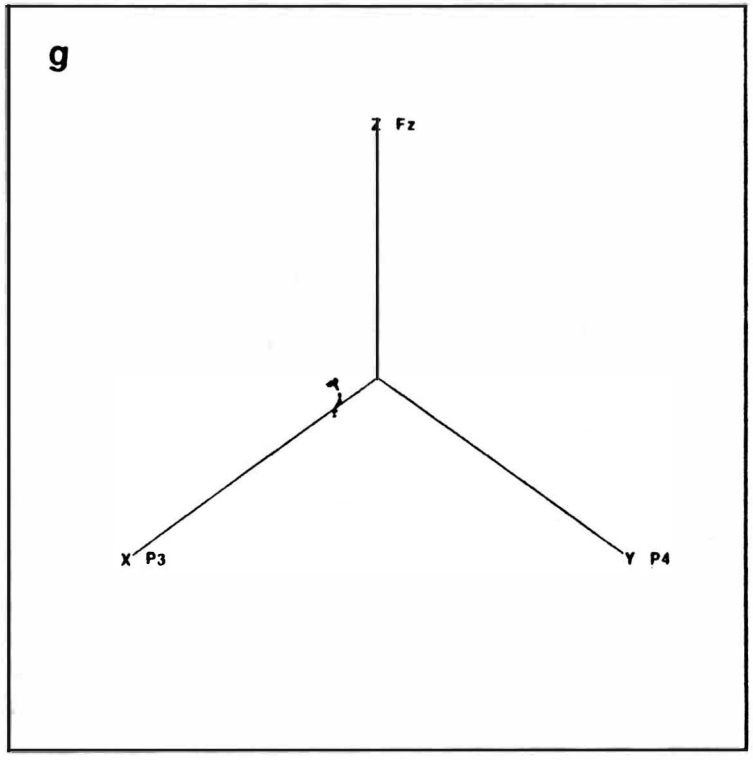

OD

Figure 24 15 - 30 ms

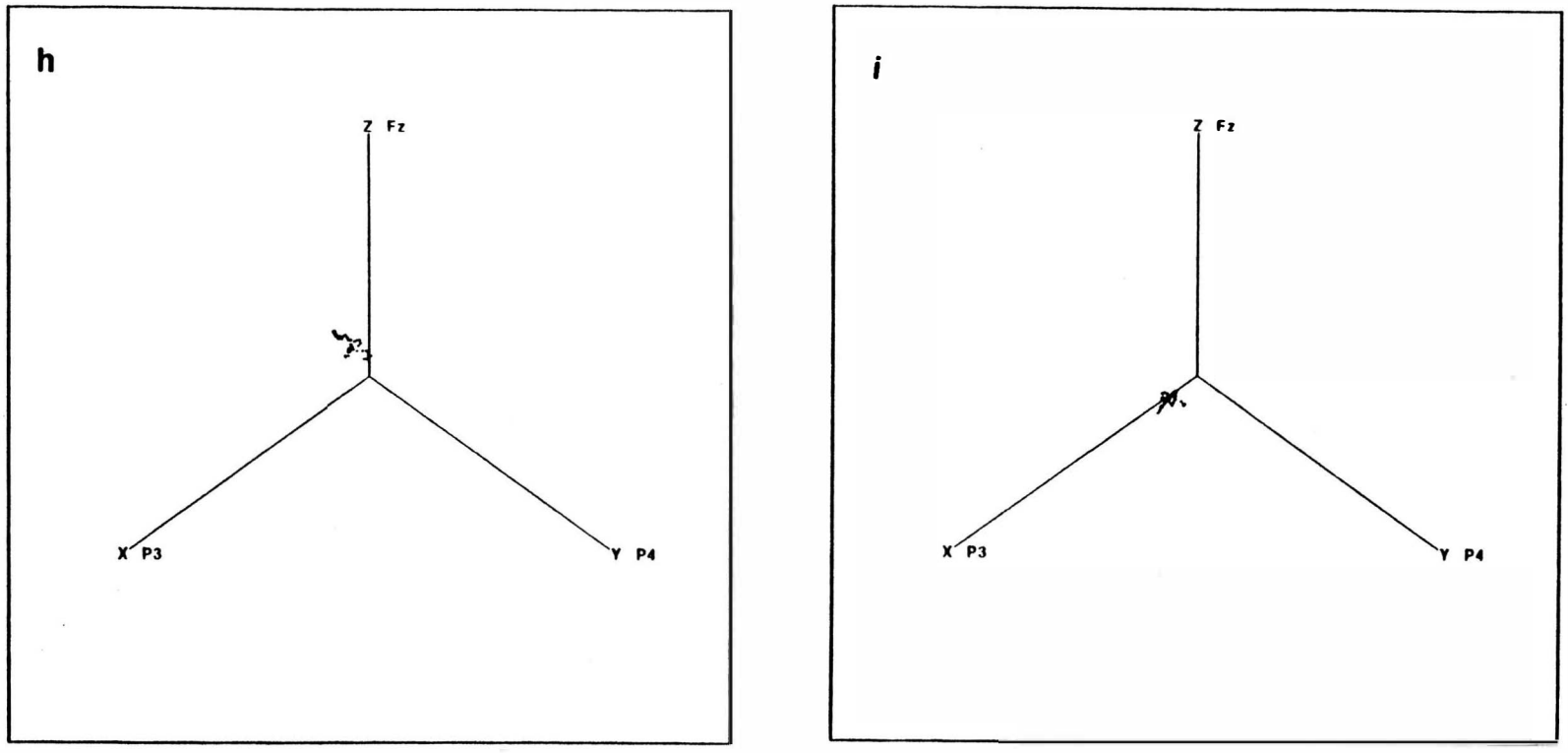

OS OD

Figure 24 30 - 55 ms

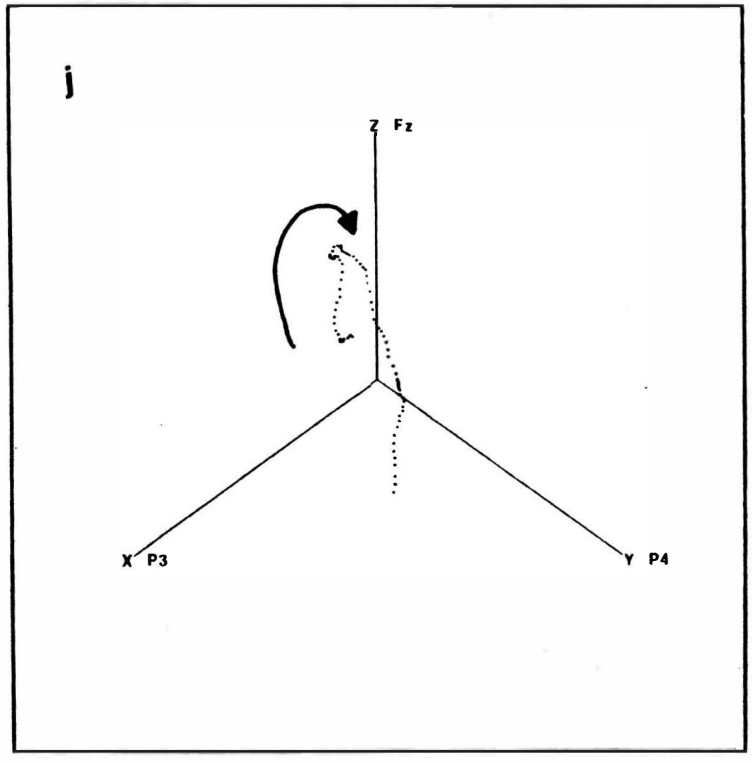

OS

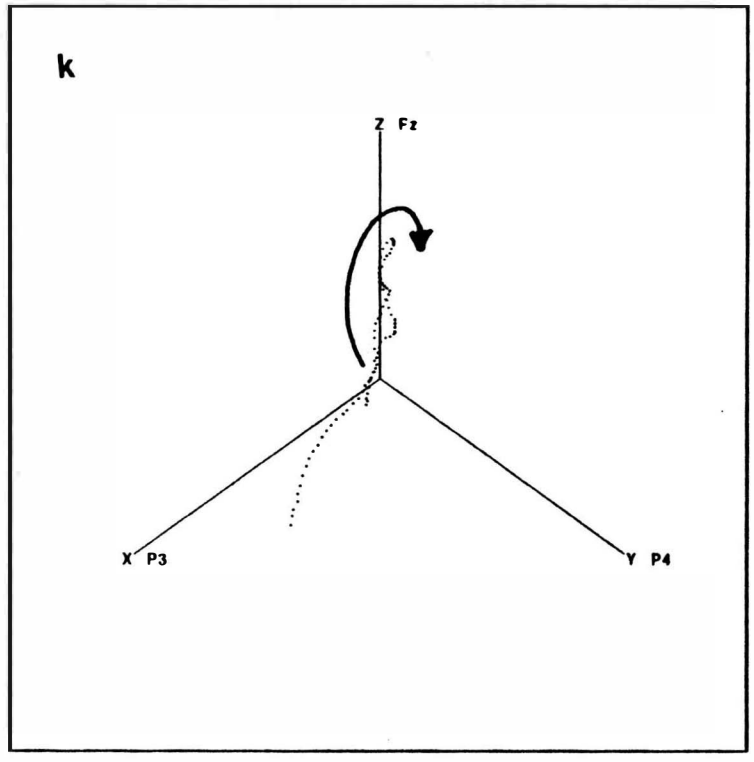

OD

Figure 24 55 - 95 ms

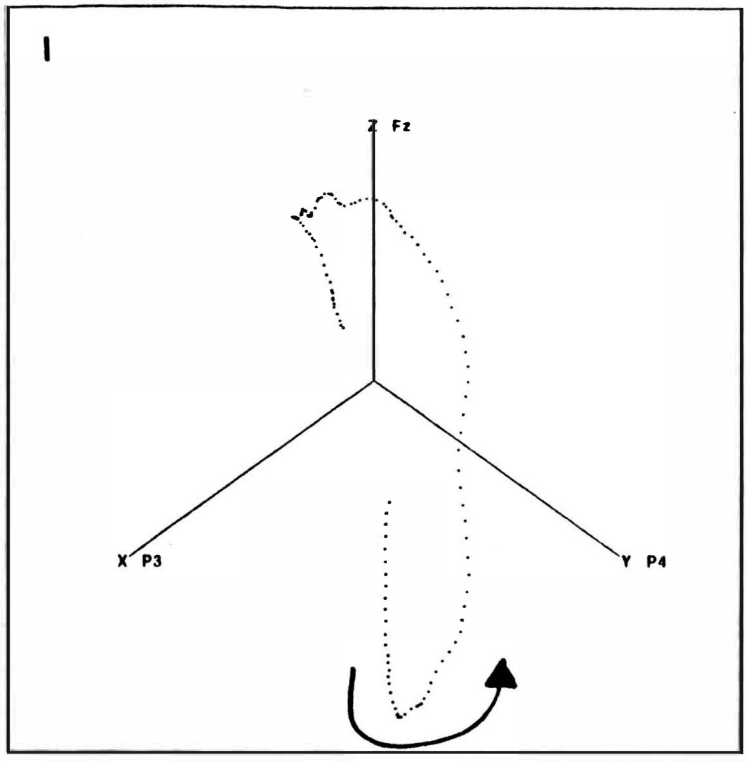

OS

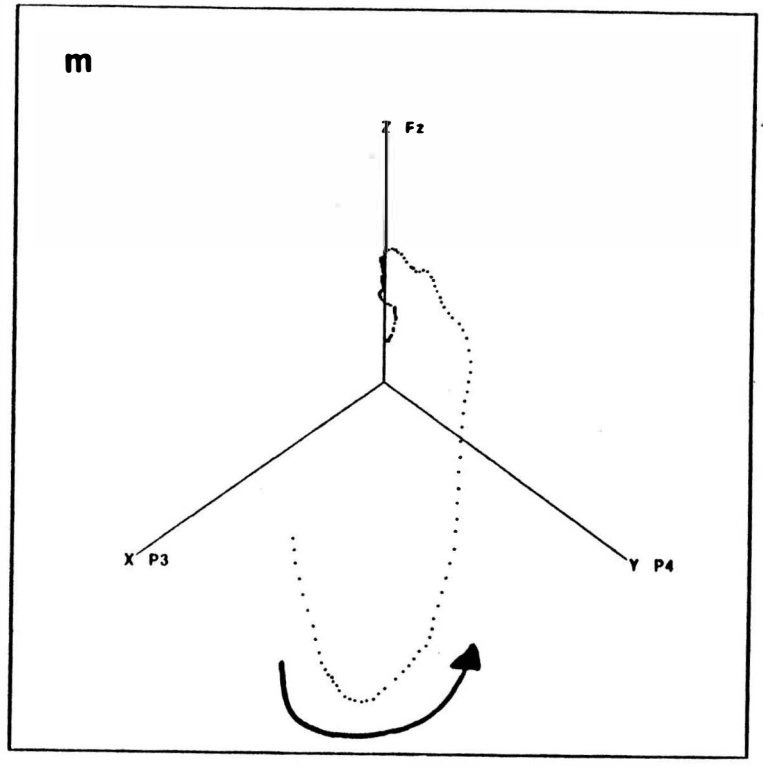

OD

Figure 24 95 - 160 ms

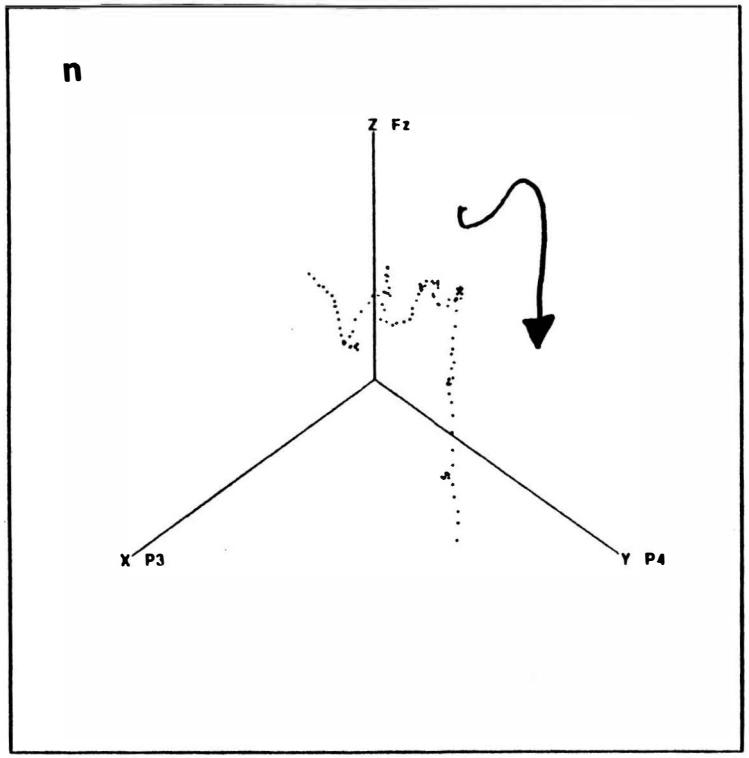

OS

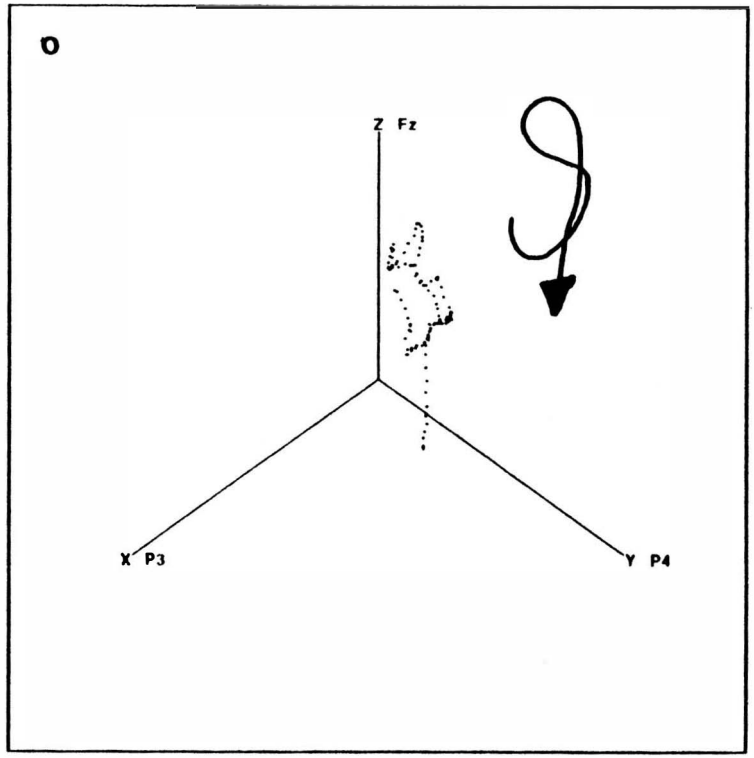

OD

Figure 24

160 - 215 ms

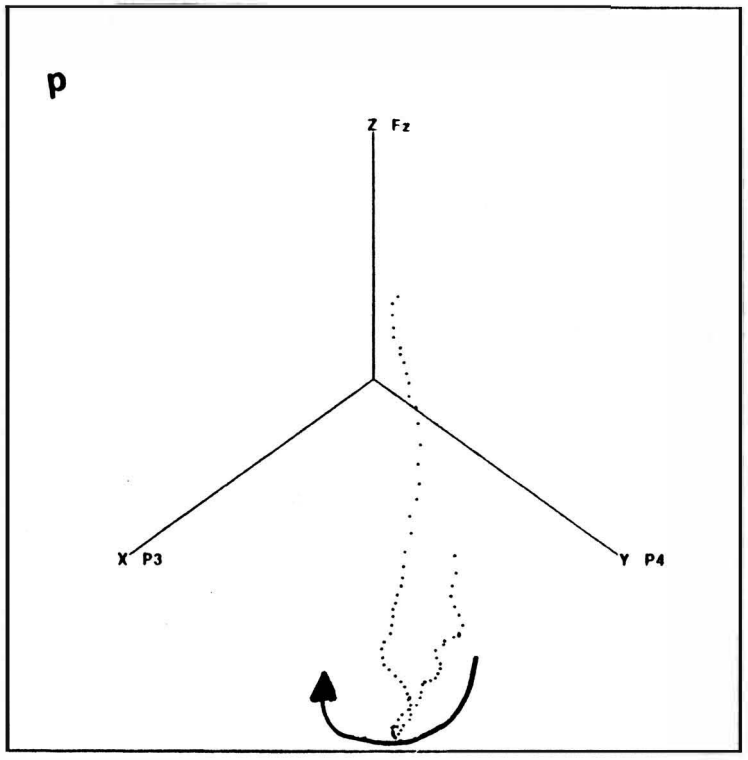

OS

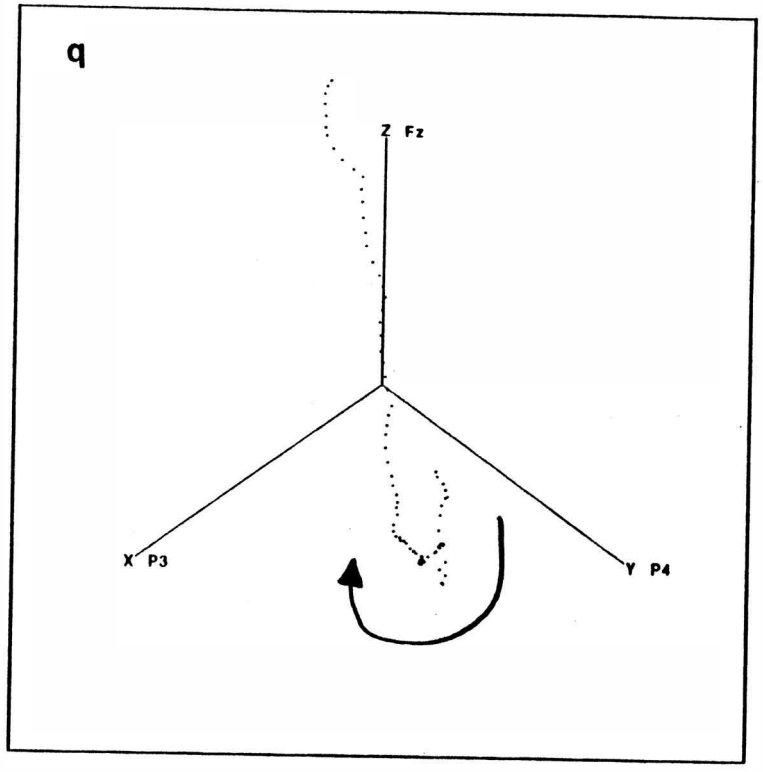

OD

Figure 24 215 - 250 ms

Figure 25 : The Neuroanatomical Correlates of the PERG and VVEP. Nominal peak times are given. (See text for discussion)

Figure 25 : The Neuroanatomical Correlates of the PERG and VVEP

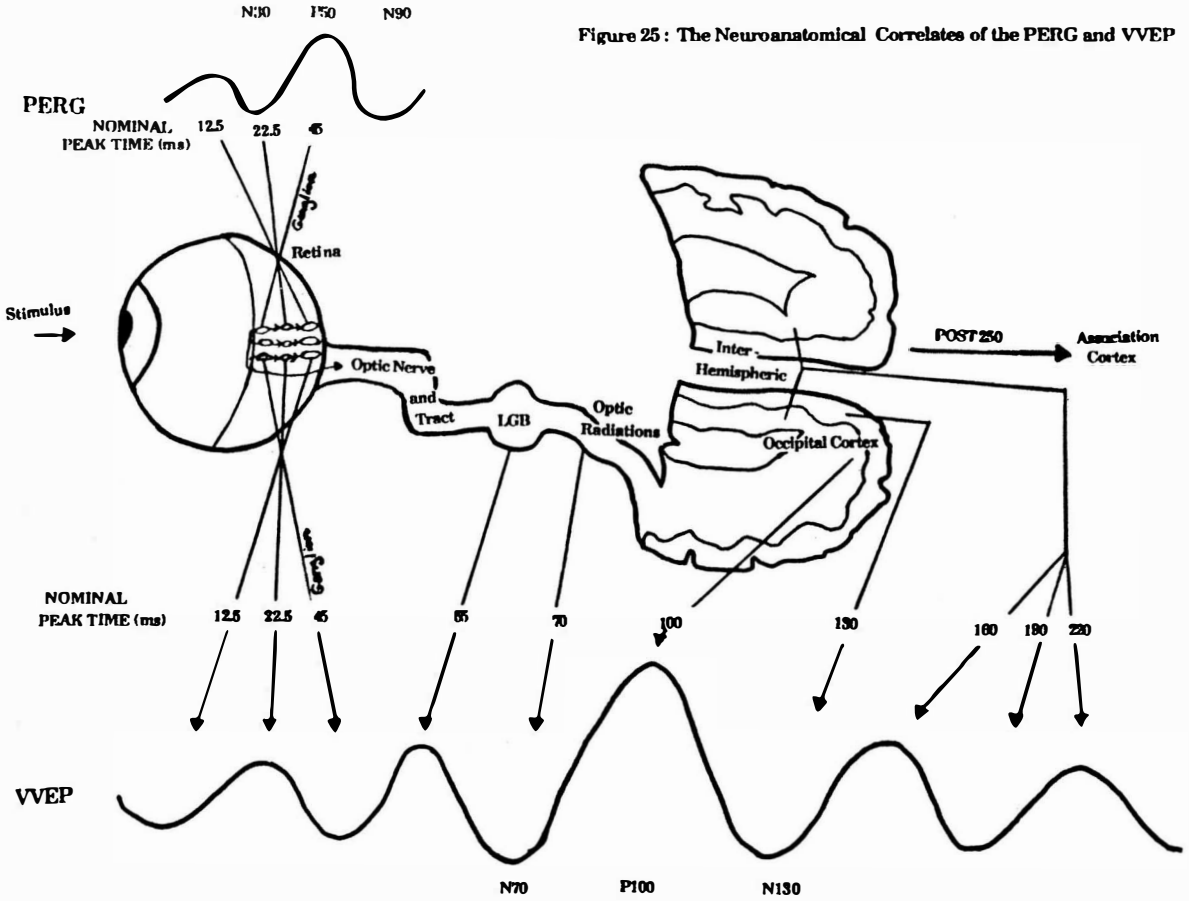

REFERENCES

REFERENCES

AEEGS (American Electroencephalographic Society) Evoked Potential Guidelines. Recommended Standards for the Clinical Practice of Evoked Potentials. J. Clin. Neurophys., 1 (1984). pp. 7-31.

Arden G.B., Vaegan, Hogg C.R., Clinical and Experimental Evidence that the Pattern Electroretinogram (PERG) is Generated in More Proximal Retinal Layers than the Focal Electroretinogram (FERG). Ann. of New York Acad. of Sci., (1982). pp. 581-601.

Bertram E.H., Lee S.I., Voluntary alteration of Pattern Reversal Visual Evoked Potentials (PRVEP's): Can It Be Prevented?. EEG Clin. Neurophys., 64 (Society Proceedings), (1986). p. 83P.

Blumenhardt C.D., Halliday A.M. Hemisphere Contribution to the Composition of the Pattern Evoked Potential Wave Form. Exp. Brain Res., 36 (1979). pp. 53-69.

Blumhardt C.D., Barrett G., Halliday A.M., Kriss A., The Effect Experimental "Scotomata" on the Ipsilateral and Contralateral Response to a Pattern Reversal in One Half-Field. EEG Clin. Neurophys., 45 (1978). pp. 376-392.

Bodis-Wollner I.,Recovery from Cerebral Blindness: Evoked Potential and Psychophysical measurements. EEG Clin. Neurophys., 42 (1977). pp. 178-184.

Celesia, G.G., Evoked Potential Techniques in the Evaluation of Visual Function. J. Clin. Neurophys., 1(1984). pp. 55-76.

Celesia G.G., Archer C. R., Kuroiwa Y., Goldfader P.R., Visual Function of the Extrageniculo-calcarine System in Man: Relationship to Cortical Blindness. Arch. Neurol., 37 (1980). pp. 704-706.

Chimento T.C., Williston J.S., Jewett D.L., Gardi J.N., The Three Channel Lissajous' Trajectory of the Auditory Brain Stem Response. VII. Isolated Frog Sciatic Nerve in a Volume Conductor., EEG Clin. Neurophys., 68 (1987). pp. 380-385.

Ciga'nek L., Variability of the Human VEP: Normative Data. EEG Clin. Neurophys., 55 (1968). pp. 35-42.

Cobb W.A., Morton H.B., Ettlinger G., Cerebral Potentials Evoked by Pattern Reversal and Their Suppression in Visual Rivalry. Nature., 216 (1967) pp. 1123 - 1125.

Ducati A., Fava E., Motti E.D.F., Neuronal Generators of the Visual Evoked Potentials: Intracerebral Recording in Awake Humans. EEG Clin. Neurophys.,71 (1988). pp. 89-99.

Epstein C.M., Reznick B.R., Three Dimensional Display of BAER's. EEG Clin. Neurophys., 64 (Society Proceedings), (1986). p. 69P.

Halliday A.M., Mc Donald W.I., Mushin J., Delayed Visual Evoked Response in Optic Neuritis. The Lancet., May 6 (1972). pp. 982-985.

Halliday A.M., Halliday E., Kriss A., Mc Donald W.I., Mushin J., The Pattern Evoked Potential in Compression of the Anatomical Visual Pathway. Brain., 99 (1976). pp. 357-374.

Halliday A.M., Mc Donald W.I., Mushin J., Visual Evoked Response in the Diagnosis of Multiple Sclerosis. Brit. Med. J., 4 (1973). pp. 661-664.

Herna'ndez Peo'n R., Scherrer H., Jouvet M., Modification of Electrical Activity in Cochlear Nucleus During "Attention" in Unanesthetized Cats. Science., 123 (1956). pp. 331-332.

Holder G.E., Pattern Electroretinography in Patients with Delayed Pattern Visual Evoked Potentials Due to Distal Anterior Visual Pathway Dysfunction. J. Neurol., Neruosurg., Psych., 52 (1989). pp. 1364-1368.

Jeffreys D.A., Axford J.G., Source Locations of Pattern-Specific Components of Human Visual Evoked Potentials. I. component of Striate Cortical Origin. Exp. Brain Res., 16 (1972a). pp. 1-21.

Jeffreys D.A., Axford J.G., Source Locations of Pattern-Specific Components of Human Visual Evoked Potentials. II. Component of Extrastriate Cortical Origin. Exp. Brain Res., 16 (1972b). pp. 22-40.

Jewett D.L., Willinston J.S., Auditory Evoked Far Fields Averaged from the Scalp of Humans., Brain., 94 (1971). pp. 681-696.

Jewett D.L., Martin W.H., Sininger Y.S., Gardi J.N., The 3-Channel Lissajous' Trajectory of the Auditory Brain-Stem Response. I. Introduction and overview. EEG Clin. Neurophys., 68 (1987). pp. 323-326.

Jewett D.L., The 3-Channel Lissajous' Trajectory of the Auditory Brain-Stem Response. IX. Theoretical Aspects., Electroencephalography and Clinical Neurophysiology., 68 (1987). pp. 386-408.

Lorente de No' R., A Study of Nerve Physiology. Stud. Rockefeller Instit., 132 (1947) Chp. 16.

Maffei L., Fiorentini A., Electroretinographic Response to Alternating Gratings Before and After Section of Optic Nerve. Science., Vol. 211, 27 Feb. (1981). pp. 933-935.

Marsters J.B., Good P.A., Mortimer M.J., A Diagnostic Test for Migraine Using the Visual Evoked Potential. Headache., September (1988). pp. 526-530.

Martin W.H., Sininger Y.S., Jewett D.L., Gardi J.N., Morris J.H., The 3-Channel Lissajous' Trajectory of the Auditory Brain-Stem Response. II. Methodology., EEG Clin. Neurophys., 68 (1987). pp. 327-332.

Martin W.H., Jewett D.L., Williston J.S., Gardi J.N. The 3-Channel Lissajous' Trajectory of the Auditory Brain-Stem Response. III. Formation, Analysis, and Reliability of Planar Segments in the Cat., EEG Clin. Neurophys., 68 (1987). pp. 333-340.

Martin W.H., Jewett D.L., Randolph M.G. ,Williston J.S., Gardi J.N. The 3-Channel Lissajous' Trajectory of the Auditory Brain-Stem Response. IV. Effects of Electrode Position in the Cat.,EEG Clin. Neurophys., 68 (1987). pp. 341-348.

Martin W.H., Gardi J.N., Jewett D.L., The 3-Channel Lissajous' Trajectory of the Auditory Brain-Stem Response. V. Effects of Stimulus Intensity in the Cat., EEG Clin. Neurophys., 68 (1987). pp. 349-359.

Mc Donald, W.I., Conduction of the Optic Nerve., Trans. Ophthal. Soc. U.K., 96 (1976). pp. 353-354.

Novak G.P., Wiznitzer M., Kurtzberg D., Giesser B.S., Vaughan H.G., The Utility of visual Evoked Potentials Using Hemifield Stimulation and Several Check Sizes in the Evaluation of Suspected Multiple Sclerosis. EEG Clin. Neurophys.,71 (1988). pp. 1-9.

Pratt H., Har'El Z., Golos E., Geometric Analysis of Human Three Channel Lissajous' Trajectory of Auditory Brainstem Evoked Potentials. EEG Clin. Neurophys., 55 (1984). pp. 83-88.

Pratt H., Bleich N., Berliner E., Short Latency Visual Evoked Potentials in Man. EEG Clin. Neurophys., 54 (1982). pp. 55-62.

Pratt H., Bleich N., Sussel Z., Three-Channel Lissajous Trajectories of Auditory Brainstem-Evoked Potentials in Patients With Neurological Lesions Affecting the Brainstem: Preliminary Impressions. Audiology., 26 (1987). pp. 247-256.

Pratt H., Martin W.H., Bleich N., Kaminer M., Har'El Z., Application of the Three-Channel Lissajous Trajectory of Auditory Brainstem-Evoked Potentials to the Question of Generators., Audiology., 26 (1987). pp. 188-196.

Pratt H., Bleich N., Martin W.H., Three-Channel Lissajous' Trajectory of Human Auditory Brain-Stem Evoked Potentials. I. Normative Measures. EEG Clin. Neurophys., 61 (1985). pp. 530-538.

Pratt H., Bleich N., Har'el A., Golos E., Three-Channel Lissajous' Trajectory of the Human Short Latency Visual Evoked Potentials. Int. J. Bio-Med. Comput., 18 (1986). pp. 249-259.

Radtke R.A., Bohan T.P., Lewis D.V., Erwin C.W., Isolated Absence of wave III in Brain-Stem Auditory Evoked Potentials: Argument for Parallel pathways of wave form generation. EEG Clin. Neurophys., 64 (Society Proceedings), (1986). p. 69P.

Raudino F., Visual Evoked Potentials in Patents with Migraine. Headache., September (1988). pp. 531-532.

Rautaharju P.M., A Hundred Years of Progress in Electrocardiography 2: The Rise and Decline of Vectorcardiography. The Can. J. Cardiol., 4(2) (1988). pp. 60-71.

Sininger Y. S., Gardi J.N., Morris J.H., Martin W.H., Jewett D.L., The 3-Channel Lissajous' Trajectory of the Auditory Brain-Stem Response. VII. Planar Segments in Humans. EEG Clin. Neurophys., 68 (1987). pp. 368-379.

Standard EEG Montages as Proposed by The American EEG Society Guidelines 1980, No. 7. Grass Instruments Inc., Quincy Mass. USA.

Stockard J.J., Stockard J.E., Sharbrough F.W., Detection and Localization of Occult Lesions with Brainstem Auditory Responses. Mayo Clin. Proc., 52 (1977). pp. 761-769.

Towle V.L., Munson R., Spire J.P., Ivanovic L., A Three-Dimensional View of Electrophysiologic Wave Forms. II. Normal Variability of the Pattern VEP. EEG Clin. Neurophys., 64 (Society Proceedings), (1986). p. 83P.

Watanabe Y., Watanabe M., Takigawa M., Lissajous Figures of the Visual Evoked Potential. No. To. Shinkei., 38(3)(1986). pp. 272-279.

Whittaker S.G., Siegfried J. B., Origin of Wavelets in the VEP. EEG Clin. Neurophys., 55 (1983). pp. 91-101.

Wiggins R.C., Guller G.N., Dafny N., Propagation of Photic Evoked Responses Recorded from the Retina, Optic Chiasm, Lateral Geniculate Body, and Visual Cortex of the Nutritionally Rehabilitated Rat Visual System., Exp. Neuro., 77 (1982). pp. 644-653.

Williston J.S., Jewett D.L., Martin W.H., Planar Curve Analysis of Three-Channel Auditory Brain Stem Response: a Preliminary Report. Brain Res., 23 (1981). pp.181-184.

Zahn J.R., Matthews P., An Early Peak of the Pattern Reversal Evoked Potential. Assoc. for Res. in Vision and Ophthal. (ARVO)., 6, June (1983). pp. 793-795.

VITA